ICSuSaT-2024

7th International Conference on Sustainable Sciences and Technology

Proceedings
of
ICSuSaT-2024

EDITORS

Prof.Dr. İskender AKKURT
Dr. Kadir GÜNOĞLU

icsusat2024@gmail.com

www.icsusat.net

Istanbul-TURKEY
12-14 July 2024

Proceeding

of

ICSUSAT-2024

Editors:
Prof.Dr. İskender AKKURT
Dr. Kadir GÜNOĞLU

i

Proceedings of ICSuSaT-2024

7th International Conference on Sustainable Science and Technology **(ICSuSaT-2024)**

12-14 July 2024, Istanbul-TURKEY

Editors:
Prof. Dr. İskender AKKURT
Dr. Kadir GÜNOĞLU

Published : 19 December 2024
ISBN: 978-605-71495-1-0

TABLE OF CONTENTS

FOREWORD

Dear Colleagues,
It is a great honor for me to host you all in **"7th International Conference on Sustainable Science and Technology (ICSuSaT-2024)"** was taken place at Kaya Hotel in Istanbul-TURKEY in the period of 12-14 July 2024.

We are also happy to publish the proceeding of **ICSuSaT-2024**. All papers have been reviewed by two reviewers.

Prof. Dr. İskender AKKURT

Chair for ICSuSaT-2024
Editor for Proceedings of ICSuSaT-2024

ORGANISATION COMMITTEE

Prof.Dr. İskender AKKURT (Chair)	Süleyman Demirel University,Isparta-Turkey
Dr. Kadir GÜNOĞLU	Isparta University of Applied Sciences, Isparta-Turkey
Dr. Osman GÜNAY	YTÜ, Istanbul-Turkey
Dr. Feride KULALI	Üsküdar University,Istanbul-Turkey
Dr. Sabiha Anas BOUSSAA	ALGERIA
Dr. Abdelmadjid RECIOUI	ALGERIA

SCIENTIFIC COMMITTEE

Prof.Dr. Ahmad UMAR (chair)	**SAUDI ARABIA**
Prof.Dr. Şemsettin ALTUNDAL	TURKEY
Prof.Dr. Dilek ALTAŞ	TURKEY
Prof.Dr. Mouloud CHALLAL	ALGERIA
Prof.Dr. Osman SAGDIÇ	TURKEY
Prof.Dr. Amir HUSSAIN	SCOTLAND
Prof.Dr. Abdelkrim KHIREDDINE	ALGERIA
Prof.Dr. Eugtenijus NORKUS	LITIUNIA
Prof.Dr. Ileana RAU	LITIUANIA
Prof.Dr. Nuggehalli M. RAVINDRA	USA
Prof.Dr. Miljko SATARIC	SERBIA
Prof. Jin YANG	CHINA
Dr. Robina AHMAD	OMMAN
Dr. M. I. Abu Al SAYYED	SAUDI ARABIA
Dr. Hakan AKYILDIRIM	TURKEY
Dr. Sabiha Boussaa ANAS	ALGERIA
Dr. Ahmet BEYCİOĞLU	TURKEY
Dr. Ahmed BOUTEJDAR	GERMANY
Dr. Khalida BOUTEMAK	ALGERIA
Dr. Yusuf CEYLAN	TURKEY
Dr. Nilgün DEMİR	TURKEY
Dr. Nurdan Karpuz DEMİR	TURKEY
Dr. Iridia MARKJA	ALBANIA
Dr. Özge Kozguş GÜLDÜ	TURKEY
Dr. Zehra Nur KULUÖZTÜRK	TURKEY
Dr. M.Fatih KULUÖZTÜRK	TURKEY
Dr. Sophia METALLAOI	ALGERIA
Dr. Abdelmadjid RECIOUI	ALGERIA
Dr. Menekşe VAROL	TURKEY

INVITED SPEAKERS

	Dr. Roya Boodaghi Malidarreh Ural Federal University, Ekaterinburg-Russia **Title:** FLASH Radiation therapy: An innovative modality for cancer treatment
	Dr. Aftab Alam Khan Dhaka University Present: UGC Professor BSMR Maritime University, Dhaka, Bangladesh **Title:** Opportunities and Challenges in Maritime Domain for Blue Economy: Role of Geological Oceanography
	Dr. Khedidja BENAROUS University of Laghouat-ALGERIA **Title:** In Silico Leishmaniasis Drug Discovery: A Promising Path towards Novel Therapeutics
	Dr. Ionel MANGALGIU Alexandru Ioan Cuza University of Iasi, Romania **Title:** Five and six member ring azaheterocycles with antimicrobial and anticancer activity
	Prof. Dr. Amir HUSSAIN Centre of AI and Robotics, Edinburgh Napier University, Scotland, UK **Title:** Trustworthy AI-enabled Sustainable Technologies: Applications in Assistive Healthcare, Challenges and Opportunities

Development of a Waste Heat Energy Recovery System for the Production of Power and Heating; An Energy and Exergy a Analysis

Fatih YILMAZ [1*]

[1] Assoc. Prof., Isparta University of Applied Sciences, Faculty of Technology, Mechatronics Engineering, Isparta, Turkiye
*: fatiyilmaz7@gmail.com

ABSTRACT

Waste heat energy recovery systems have gained much more significance day by day in combating environmental problems. Especially, the exhausted gases from industry that come from fossil-based fuels that are released into the atmosphere lead to many environmental problems, such as global warming, etc. For this reason, the developed combined plant deals with the thermodynamic analysis of the energy recovery system, integrating the exhausted gases with the steam Rankine cycle and organic Rankine cycle for power and hot water production. Comprehensive thermodynamic analysis with energy and exergy efficiency methods is fulfilled to define the system performance change. Moreover, the combined system is motivated by exhausted gases at 400 °C. The ORC system works with the isobutane refrigerant. The results show that the developed plant net power and hot water generation loads are computed as 14143 kW and 11294 kW, respectively. Additionally, the energy and exergy efficiency of the suggested plant are 37.4% and 36.71%, respectively.

KEYWORDS: Energy, exergy, waste heat, isobutane, steam, power

1 INTRODUCTION

Due to the limited availability of fossil fuels and their negative effects such as global warming, the use of more efficient power plants has become a critical necessity [1]. Struggling with environmental problems is as important as developing more efficient systems, as well as carbon-free energy sources. At this point, combined cycles come to the fore. Additionally, another important parameter is waste heat management. More optimum systems can be obtained by reusing the thermal energy of the waste heat that combines systems. A combined plant presents many advantages which are better performance, higher efficiency, more suitability, more power lowest environmental impact, and low maintenance cost, etc.,[2].

The literature survey indicated that the combined energy generation plant is one of the most important working issues for improving system efficiency. Yilmaz et al. [3] proposed an innovative combined plant that generates different beneficial products. Their developed plant is motivated by biomass energy and they computed that overall energy efficiency is 44.50%. Moharram et al. [4] examined and analyzed a novel multigeneration plant that integrated with desalination. Their modeled cycle had 0.38 $/m^3 of levelized cost. Dincer and Meke [5] evaluated the design and assessment of the solar energy-based combined plant for producing beneficial products. They conducted a comprehensive

7

thermodynamic analysis according to energetic and energetic performance indicators. In case study 2, the overall energy and exergy performance indicators are determined to be 20.685 and 16.87%, respectively.

Temiz and Dincer [6] suggested the development of a solar energy-based combined plant for beneficial commodities. They united that floating and bifacial PV in the combined plant. Their plant even efficiencies are to be 41.04% and 46.88% for energetic and energetic indicators. Choudhary et al. [7] proposed a newly designed combined plant that united ORC for using waste heat, based on thermodynamic performance. Their analysis finding indicate that the ORC system can generate 2.3 MW of electrical power with 12.48% energetic efficiency. Yang et al. [8] developed a combined plant that provides heat recovery for heating. The system is powered by industrial waste heat. 271.2 million tons of DW and 91.5 million GJ of heat are provided to the system annually.

As a result of the brief literature research above, combined systems are among the important and current issues. Therefore, this study focuses on the thermodynamic analysis of a waste heat combined Steam Rankine and ORC system. Here, to obtain net electrical power and heating, a parametric analysis is conducted.

2 SYSTEM DEFINATION

The developed combined plant is designed for producing power and heating proposed as shown in Figure 1.
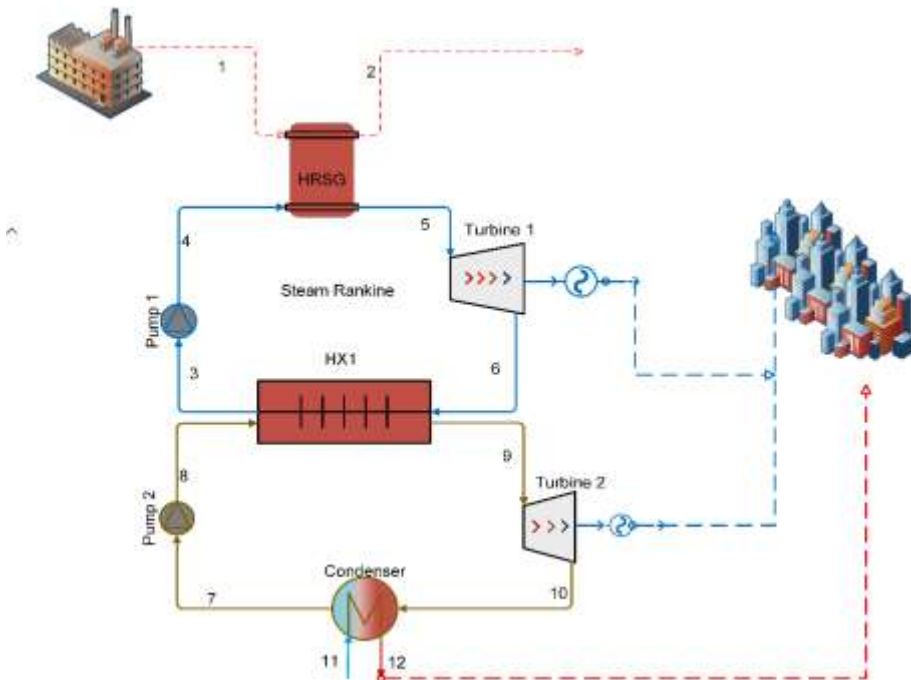
Figure 1 Combined plant with integrated steam Rankine cycle and ORC

The system embraces a waste heat energy cycle, a steam Rankine cycle (SRC) (points between 3-6) and an Organic Rankine cycle (points between 7-10). At point 1, the waste heat at 350 ℃ goes into heat recovery generator (HRSG) unit and then the thermal energy transferred into sRC. ın the sRC, points 5 and 6 in which the turbine, the power generation is occurs. After that, at point 6, the exhausted vapor-water mixture inlet in the heat exchanger 1. This unit meets the thermal energy required for ORC by integrating sRC and ORC power generation systems. In the ORC system, power production occurs in the turbine between points 9-10. Hot water can be produced with the waste heat in the condenser and used for heating purposes.

3 ANALYSES

To perform the assessment and investigation of the waste heat-based combined plant, a comprehensive thermodynamic analysis method is used in terms of energetic and exergetic efficiency. For the analysis methods, the assumptions and input values are given in Table 1. Moreover, the system has been modeled and analyzed based on steady-state conditions. The kinetic and potential energy changes are disregarded. The system heat loss between components and the environment is overlooked.

Table 1. The design assumptions and indicators for the proposed system

Parameters	Value	Unit
Waste heat temperature	400	℃
Waste heat pressure	101.325	kPa
Pump 1 input temperature	99.61	℃
Pump 1 input pressure	100	kPa
Turbine 1 inlet pressure	5000	kPa
ORC working fluid	Isobutane	-
Pump 2 inlet pressure	600	kPa
Pump 2 inlet temperature	44.74	℃
Turbine 2 inlet pressure	1200	kPa
HEX effectiveness	80	%
Reference temperature	25	℃
Reference pressure	101.325	kPa

9

To conduct the thermodynamic mathematical formulation, four balance equations which are mass, energy, entropy, and exergy, should be taken into account [9-11];

$$\sum \dot{m}_{in} = \sum \dot{m}_{out} \tag{1}$$

$$\sum \dot{m}_{in} h_{in} + \sum \dot{Q}_{in} + \sum \dot{W}_{in} = \sum \dot{m}_{out} h_{out} + \sum \dot{Q}_{out} + \sum \dot{W}_{out} \tag{2}$$

$$\sum \dot{m}_{in} s_{in} \sum \left(\frac{\dot{Q}}{T}\right) + \dot{S}_{gen} = \sum \dot{m}_{out} s_{out} \tag{3}$$

$$\sum \dot{m}_{in} ex_{in} + \dot{Ex}_{in}^{\dot{Q}} + \dot{Ex}_{in}^{\dot{W}} = \sum \dot{m}_{out} ex_{out} + \dot{Ex}_{out}^{\dot{Q}} + \dot{Ex}_{out}^{\dot{W}} + \dot{Ex}_{dest} \tag{4}$$

By applying the general energy Eq. (2) to each component, the net work rates obtained or consumed by the system are formulated as follows

$$\dot{W}_{P1} = \dot{m}_3 (h_4 - h_3) \tag{5}$$

$$\dot{W}_{P2} = \dot{m}_8 (h_8 - h_7) \tag{6}$$

$$\dot{W}_{T1} = \dot{m}_5 (h_5 - h_6) \tag{7}$$

$$\dot{W}_{T2} = \dot{m}_9 (h_9 - h_{10}) \tag{8}$$

Overall, the energy and exergy efficiency of the developed plant can be modeled as;

$$\eta_{sys} = \frac{\dot{W}_{net}}{\dot{Q}_{in}} \tag{9}$$

$$\psi_{sys} = \frac{\dot{W}_{net}}{\dot{Ex}_{,Qin}} \tag{10}$$

$$\dot{W}_{net} = \dot{W}_{T1} + \dot{W}_{T2} - \dot{W}_{P1} - \dot{W}_{P2} \tag{11}$$

4 RESULTS AND DISCUSSION

After a comprehensive thermodynamic modeling of the proposed plant, the results are presented in Table 2. The results indicated that the developed plant's net electrical and heating generation loads are 14143 kW and 11294 kW, respectively. If the system works single generation mode, only electrical, the system has 19.31% energy efficiency and 34.65% exergy efficiency. However, the system is designed for a cogeneration model and it had 37.40% energetic and 36.71% exergy efficiency.

Table 2. Thermodynamic modeling results of the developed plant

Parameters	Results
Net power generation rate	14143 kW
Hot water generation rate	11294 kW

10

η_{SG}	19.31 %
ψ_{SG}	34.65 %
η_{sRC}	24.14 %
ψ_{sRC}	43.32 %
η_{ORC}	6.873 %
ψ_{ORC}	34.27 %
η_{ov}	37.40 %
ψ_{ov}	36.71 %

Energy and exergy efficiency for SG and the entire system are calculated and depicted in Figure 2. Here it is clearly seen that energy efficiency is higher when the entire system operates in cogeneration mode. The energy and exergy efficiency of the entire system is determined as 37.4% and 36.71%.
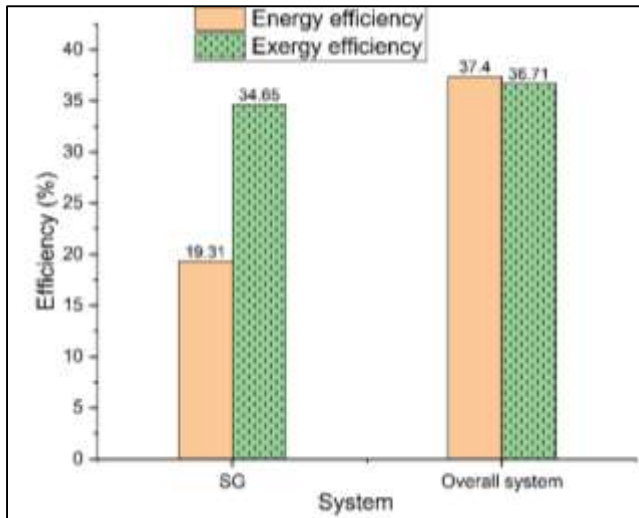
Fig. 2 Energy and exergy efficiency of the SG and overall system

To investigate the how effect of the waste heat temperature on the system's products and efficiency, a parametric analysis is performed and charted in Figure 3 (a-b). As indicated in this chart, by increasing the waste heat between 3000 to 600 ℃, the generated net electrical load increases from 5000 kW to 28000 kW(blue line in Figure 3a). Looking at another perspective, with this increment temperature of waste heat, the system energy efficiency increases from 30 to 40%, and also exergy efficiency is increases between 26 and 35%, respectively.

11
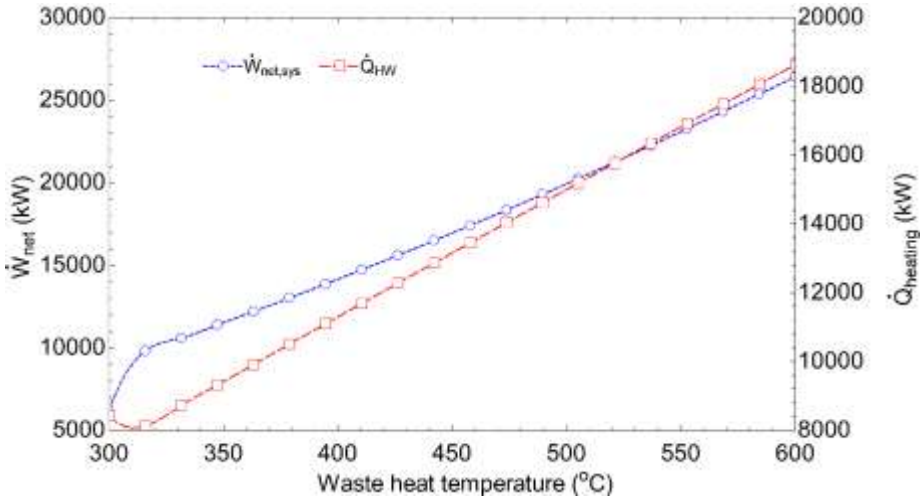
(a)
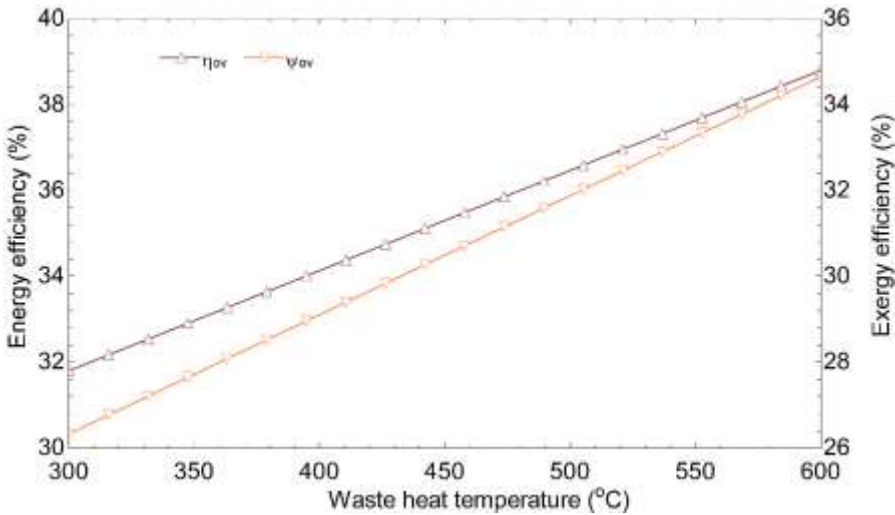
(b)

Figure 3. Effect of the waste heat on the system products (a) and on the system efficiency (b)

The effect of turbine 1 inlet pressure (P_5) on system outputs and efficiency was investigated and presented in Figure 4. Here, with the increase of P_5 pressure, both the amount of electricity produced from the system and the system efficiency showed a positive change. The reason for the decrease in the heating load is that the mass flow rate required for cooling decreases as the temperature and pressure increase.

12
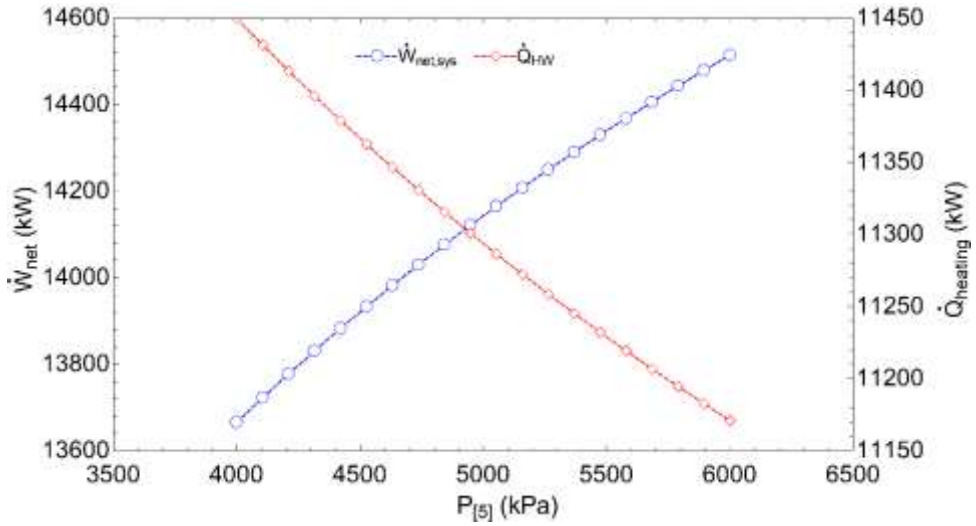
(a)
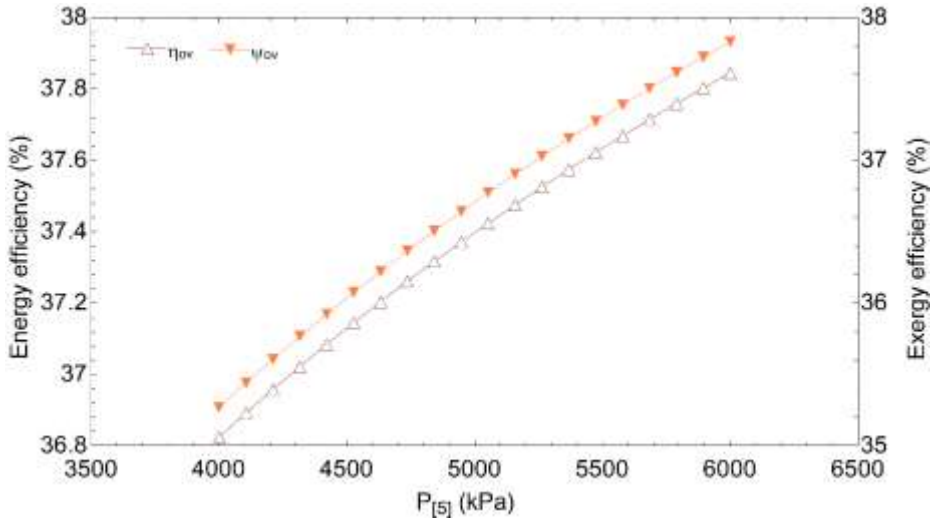
(b)

Figure 4. Effect of turbine 1 inlet pressure on system outputs (a) and efficiency(b)

A heat exchanger thermally connects the subsystems. Therefore, the heat exchanger efficiency value is an important indicator. By increasing the heat exchanger efficiency from 0.6 to 0.9, the system energy efficiency increases from 20% to 45%. Additionally, as seen in Figure 5, exergy efficiency also increases. It is worth noting that HEX efficiency means high efficiency of the system.

13
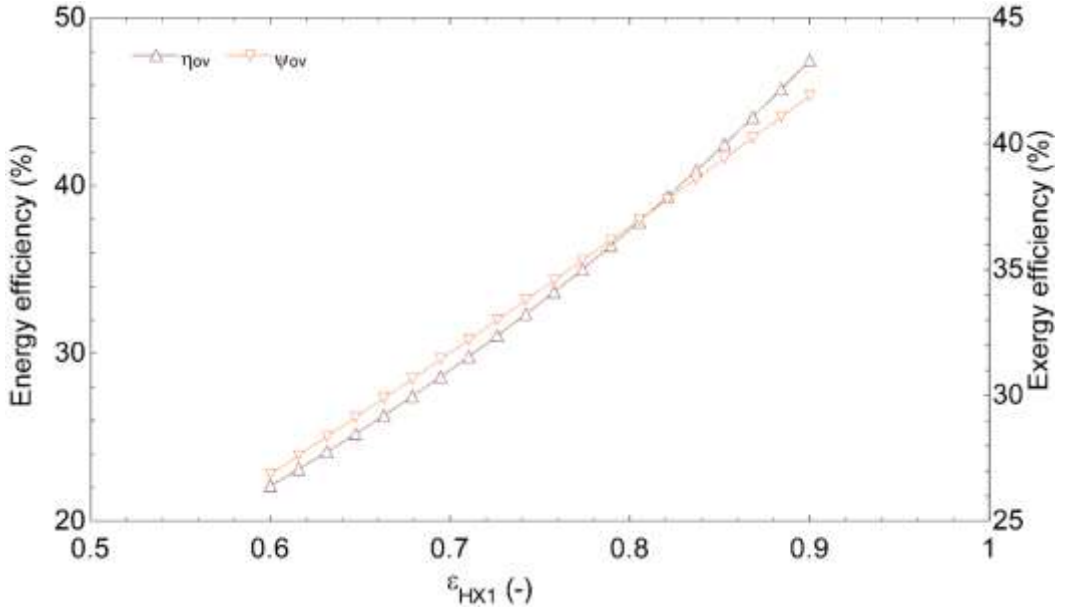
Figure 5 The relationship between HEX effectiveness and system efficiency

5 CONCLUSIONS

The present study focuses on waste heat recovery for a more efficient system design. For this reason, a detailed thermodynamic analysis is conducted for power and heating generation on the developed plant. The system mainly consists of a steam Rankine cycle, ORC, and waste heat recovery unit. The results show that the electrical and power generation capacity of this model is favorable. More results can be drawn as below;

- The system's net electrical and heating generation capacity are found to be 14143 kW and 11294 kW, respectively.
- The sub-systems; ORC has 6.8% of energy efficiency and 34.27% of exergetic efficiency, and sRC has 24.14% energy efficiency and 43.32% exergy efficiency.
- For the entire plant, the energy and exergy efficiency indicators are 37.40% and 36.71%, respectively.
- The parametric analysis results show that an increment in the waste heat temperature leads to rise in the system products as well efficiency

To sum up, the waste heat energy recovery systems are much more important for a clean and sustainable future. It should be concluded that the developed system is favorable in terms of commodities and efficiency**.**

14

REFERENCES

[1] Al-Sulaiman, F. A., Dincer, I., & Hamdullahpur, F. (2010). Energy analysis of a trigeneration plant based on solid oxide fuel cell and organic Rankine cycle. *International Journal of Hydrogen Energy*, *35*(10), 5104-5113.

[2] Ozturk, M., & Dincer, I. (2013). Thermodynamic analysis of a solar-based multi-generation system with hydrogen production. *Applied Thermal Engineering*, *51*(1-2), 1235-1244.

[3] Yilmaz, F., Ozturk, M., & Selbas, R. (2024). Design and performance evaluation of a biomass-based multigeneration plant with supercritical CO2 brayton cycle for sustainable communities. *International Journal of Hydrogen Energy*, *59*, 1540-1554.

[4] Moharram, N. A., Konsowa, A. H., Shehata, A. I., & El-Maghlany, W. M. (2024). Advances in zero liquid discharge multigeneration plants: A novel approach for integrated power generation, supercritical desalination, and salt production. *Energy Conversion and Management*, *307*, 118352.

[5] Meke, A. S., & Dincer, I. (2024). Design and assessment of a novel solar-based sustainable energy system with energy storage. *Journal of Energy Storage*, *88*, 111556.

[6] Temiz, M., & Dincer, I. (2024). Development of a hybridized small modular reactor and solar-based energy system for useful commodities required for sustainable cities. *Energy*, *286*, 129562.

[7] Choudhary, N. K., Deep, A. P., & Karmakar, S. (2024). Thermodynamic Analysis of Integrated Gasification Combined Cycle Integrated with Organic Rankine Cycle for Waste Heat Utilization. *Waste and Biomass Valorization*, 1-19.

[8] Yang, X., Kong, Y., Zhou, Y., Liu, D., & Xia, J. (2024). Case study on combined heat and water system for district heating in Beijing through recovery of industrial waste heat in Tangshan. *Energy*, 131316.

[9] Bejan A, George T, Moran MJ. Thermal design and optimization. Wiley; 1995.

[10] Cengel YA, Boles MA. Thermodynamics : an engineering approach. 8th ed. Mc. New York: McGraw-Hil;2015; 2015.

[11] Dincer I. Thermodynamics: A Smart Approach. USA: John Wiley & Sons Ltd; 2020

Green Hydrogen Production Potential for Isparta; An Evaluation and Thermodynamic Analysis

Fatih YILMAZ [1]

[1] Assoc. Prof., Isparta University of Applied Sciences, Faculty of Technology, Mechatronics Engineering, Isparta, Turkiye
E-mail: fatiyilmaz7@gmail.com

ABSTRACT

Renewable energy sources have great potential in overcoming global warming and environmental problems. Using renewable energy sources offers many environmental advantages. and is a clean energy source. Wind energy has an important position in terms of the potential of clean energy resources. In this study, clean and sustainable power and hydrogen energy production with a wind turbine in Isparta conditions is examined. This developed study is designed according to Isparta wind data and its hydrogen production capacity is examined from a thermodynamic perspective. Additionally, this system consists of a series of wind turbines and alkaline electrolysis units. The energy and exergy efficiency of the designed system is investigated and its potential to produce hydrogen is examined according to the months of the year. The capacity to produce hydrogen with the wind turbine and available wind energy under Isparta conditions is investigated. According to the analysis results, this system developed in 6.38 m/s wind produces 4.5 MW net electricity. Additionally, this system can produce a total of 0.01263 kg/s of green hydrogen. It is concluded that depending on the change in wind speed, both electricity production and hydrogen production may be suitable for Isparta conditions.

Keywords: Energy, Hydrogen, wind energy, thermodynamic

1 INTRODUCTION

Global warming and environmental problems are increasing day by day due to reasons such as population growth and globalization. A more sustainable and carbon-free future is important and indispensable for the future of humanity. Therefore, the trend towards carbon-free energy sources is important. At this point, renewable energy sources are a factor that attracts attention. Also, another important parameter is hydrogen.

Renewable energy sources, carriers, and systems can potentially solve all global environmental problems by reducing dependence on fossil fuel reserves and reducing environmentally damaging emissions. Hydrogen is a sustainable energy carrier and can be used as a fuel in sustainable energy systems due to its zero or negligible end-use emissions and the endless possibilities of producing hydrogen from continuously renewed energy and material sources [1]. An alternative to fossil fuels is 'green' hydrogen, which can be generated through water electrolysis using an electric current to split water into hydrogen and oxygen without greenhouse gas emissions, provided the electricity used to power the process is entirely from renewable sources [2]. Green hydrogen will play a vital role in decarbonizing the economy and industry. Moreover, the analysis of green

16

hydrogen integrated systems is expected to be highly meaningful [3]. There are many articles in the literature on green hydrogen production using wind turbines. Gado et al. [4] examined the potential of green hydrogen generation by solar and wind power for Middle East and North Africa countries. They used a Matlab/Simulink model for calculation and validation. Their analysis results indicate that the hydrogen generation cost for Hurghada is 4.4$/kg.

Kareyel et al. [5] investigated the green hydrogen generation potential for Turkiye with onshore and offshore wind power. They concluded that The Turkiye total hydrogen generation potential is estimated to be 248.56 million tons. In another study, authors [6] considered two-stage model predictive control for a hydrogen-based storage system coupled with a wind farm for green hydrogen production for fuel cell electric vehicles. Yilmaz [7] developed a wind-hydro-based green hydrogen generation system. The author has examined this system based on energy and exergy efficiency methods and found that the overall system had 61.29% energy efficiency. Here also some newly published papers in 2024 can be summarized [8-10].

As can be seen from the above literature research, green hydrogen is an important and promising technology for a sustainable future. In this study, the potential to produce green hydrogen with wind power under Isparta conditions is discussed. A detailed thermodynamic analysis is carried out for hydrogen production from a wind turbine-assisted system.

2 SYSTEM DESCRIPTION AND ANALYSIS

This system focuses on clean and sustainable green hydrogen production. A schematic representation of the developed system is given in Figure 1. Here, it consists of wind turbines, PEM electrolysis and water heater. Pure water at point 1 enters the heater at 25 ℃. and then PEM enters at the required temperature for PEM, approximately 80 ℃. The electrical energy required by the PEM unit is met by wind turbines. The system is designed and analyzed for the purpose of producing both hydrogen and electricity.
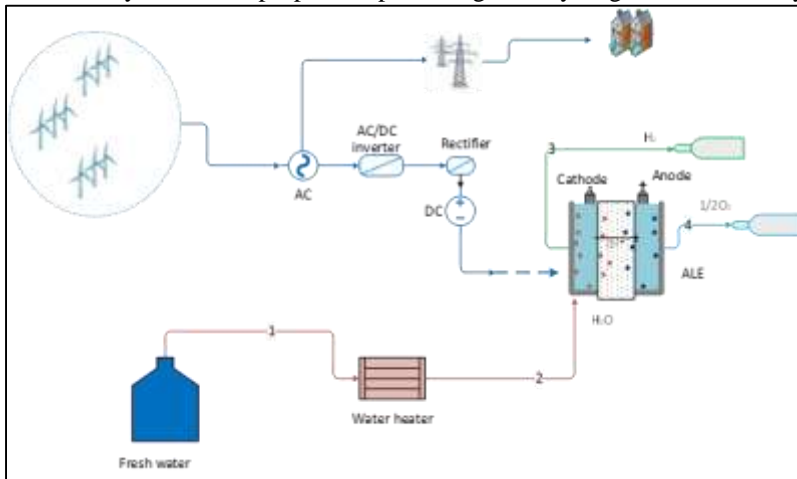
Figure 1. Wind turbine based developed system flow chart

17

In this part of the study, the analysis method is discussed according to thermodynamic performance examination. Accepted values for system design are given in Table 1.

Table 1. Design parameters and inputs of the developed system

Parameters	Value
Wind speed	6.38 m/s
Diameter	47.9, m
Performance ecoefficiency	0.55
Turbine-generator efficiency	90.25,%
ALE inlet temperature	85, ℃
ALE inlet pressure	101.3, kPa
ELE efficiency	66.10,%
Reference temperature	25 ℃
Reference pressure	101.3 kPa

Accompanied by the assumptions in Table 1, the energy and exergy efficiency of this system are examined thermodynamically. For this purpose, the four thermodynamic general equilibrium equations, mass, energy, entropy, and exergy relations, were analyzed separately for each component with the EES program. These four balance equations can be generalized and formulated as follows [11-12];

$$\dot{m}_{in} = \dot{m}_{out} \tag{1}$$

$$\dot{Q}_{in} + \dot{W}_{in} + \sum \dot{m}_{in}h_{in} = \dot{Q}_{out} + \dot{W}_{out} + \sum \dot{m}_{out}h_{out} \tag{2}$$

$$\sum \left(\frac{\dot{Q}}{T}\right)_{in} + \sum \dot{m}_{in}s_{in} + \dot{S}_{gen} = \sum \left(\frac{\dot{Q}}{T}\right)_{out} + \sum \dot{m}_{out}s_{out} \tag{3}$$

$$\dot{Ex}^{\dot{Q}_{in}} + \dot{Ex}^{\dot{W}_{in}} + \sum \dot{m}_{in}ex_{in} = \dot{Ex}^{\dot{Q}_{out}} + \dot{Ex}^{\dot{W}_{out}} + \sum \dot{m}_{out}ex_{out} + \dot{Ex}_{des} \tag{4}$$

Wind turbine calculations can be formulated as follows;

$$\dot{W}_T = 1/2\eta_{wt}\rho_{air}A_{wt}V^3 \tag{5}$$

$$\dot{W}_{in} = 1/2\rho_{air}A_{wt}V^3 \tag{6}$$

$$\dot{Ex}_{wt} = 1/2\rho_{air}A_{wt}V^3 \tag{7}$$

18

Finally, the overall system energy and exergy efficiency can be written as;

$$\eta_{sys} = \frac{\dot{W}_{net} + (\dot{m}_{H2}LHV_{H2})}{\dot{E}_{in}}$$
(8)

$$\psi_{sys} = \frac{\dot{W}_{net} + (\dot{m}_{H2}ex_{H2})}{\dot{Ex}_{in}}$$
(9)

3 RESULTS AND DISCUSSION

To determine the system performance, power, and hydrogen generation based on wind power for Isparta, a case study and parametric analysis are conducted. The calculation results are presented in Table 2. The wind turbine can generate 6878 kW of power. The generated net green hydrogen rate is computed to be 0.01263kg/s. Also, the system had 44.03% energy efficiency and also 1.779 sustainability index value.

Table 2 Thermodynamic analysis results of the developed system

Indicators	Value
Wind turbine power rate	6878, kW
Net power rate	4585, kW
ALE power rate	2293, kW
Hydrogen rate	0.01263, kg/s
Oxygen rate	0.1002, kg/s
System energy efficiency	44.03, %
System exergy efficiency	43.78, %
SI	1.779

Figure 2 shows the wind speed and average air temperature for Isparta City where the case study is conducted here. The wind speed is about 20 m/s in January 2021 while the lowest value is 6 m/s in Jun 2021. this city has nearly good potential based on the wind speed at 50 m.
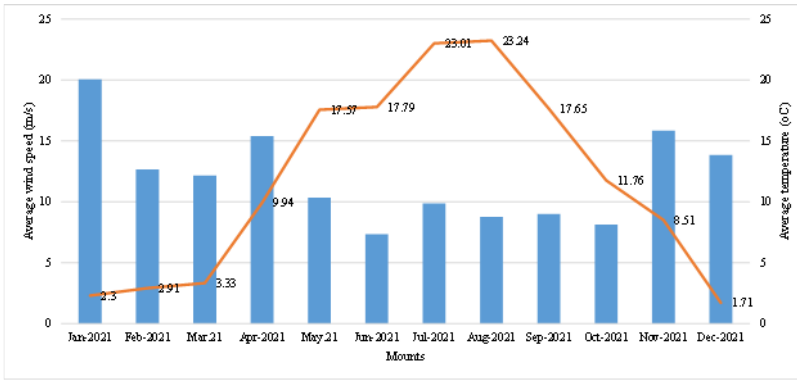
Figure 2 Average wind speed and reference temperature for Isparta city

 Figure 2 and Figure 3 show the increase in net electrical power, hydrogen, and system efficiency that will be achieved by increasing the wind speed from 1 to 20 m/s. Here, (Figure 3), depending on the increase in wind speed, the net electrical power obtained from the entire system increases from 0 to approximately 150 MW. Additionally, according to this increase, Figure 4 indicates that the energy efficiency of the entire system increases from 42% to 47% and the exergy efficiency increases from 40% to 48%.
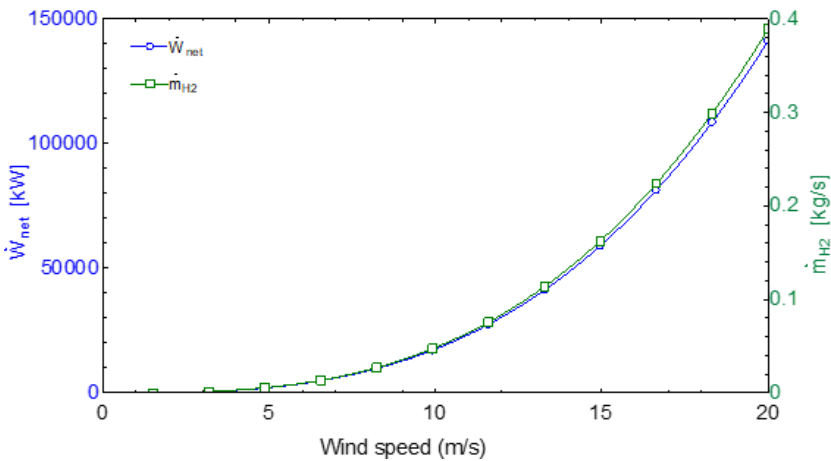
Figure 3 effect of the wind speed on the net power and hydrogen generation rate

20
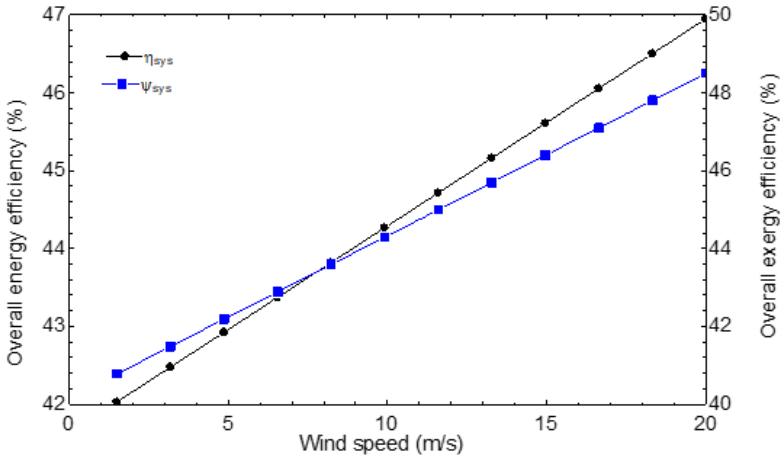
Figure 4 Impact of the wind speed on the overall system performance

It is a known fact that systems with renewable energy sources are more sustainable. Thus, the linear increase relationship between the increase in wind speed and the sustainability index is depicted in Figure 5. This SI value increased from approximately 1.5 to 2.1 with increasing wind speed. This shows that it is positive in terms of sustainability.
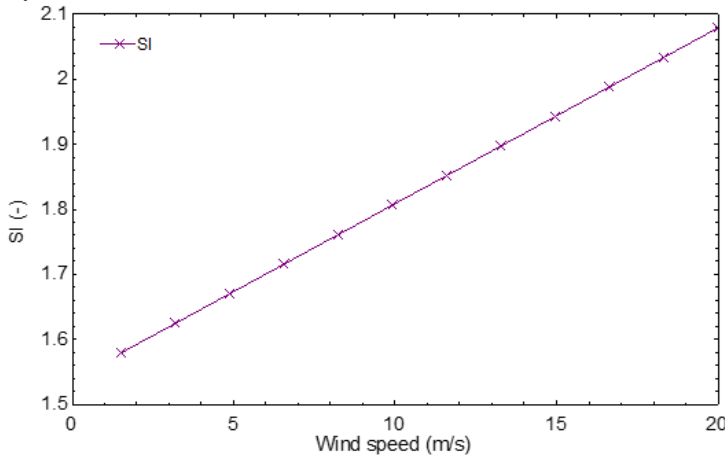
Figure 5 The relationship between wind speed and SI

Since the density of air is an effective parameter in wind turbine calculations, as seen in the equation above, the net work to be obtained in the system and the change in the amount of hydrogen as the environmental temperature increases are analyzed and presented in Figure 6. The situation that arises here is that as the environmental temperature increases, the density of the air decreases and the useful outputs obtained also decrease. It seems that the density of the air is an effective parameter.

21
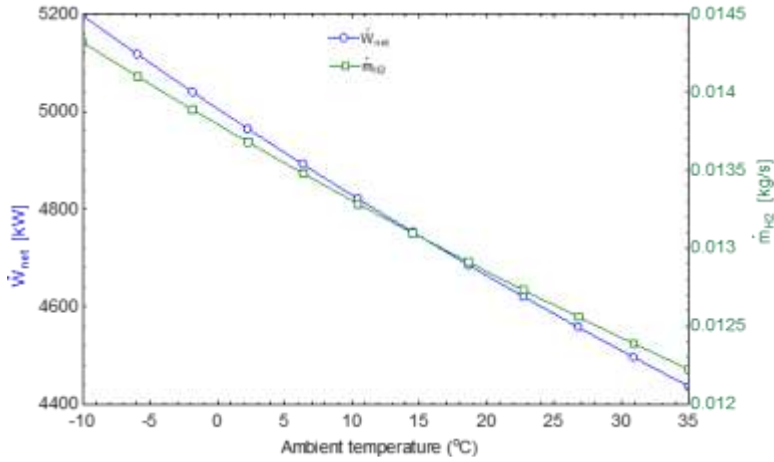
Figure 6 The association between ambient temperature and SI

Accompanied by the values given in Figure 2, the dynamic analysis results of hydrogen and net electrical power production for Isparta province are discussed and illustrated in Figure 7. Here, the maximum amount of electrical power and also the amount of hydrogen was obtained in January 2021, when the wind speed was highest. Since the electricity produced from wind turbines is intended to be sent proportionally to PEM electrolysis, there is a linear relationship between the electrical power produced and the amount of hydrogen. The current potential of Isparta province in terms of wind turbine-supported systems can be interpreted as good.
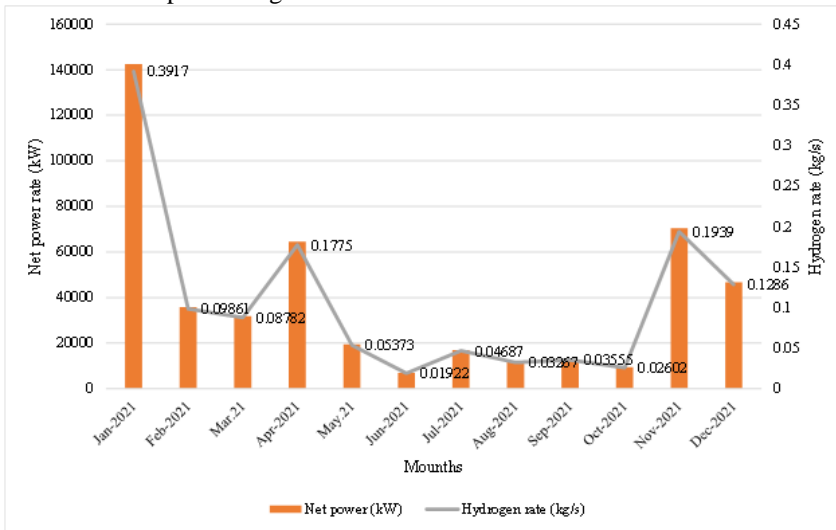
Figure 7 A dynamic analysis results of the power and hydrogen generation rate for Isparta

22

4 CONSLUSION

In this study, the analysis of electrical power and hydrogen production according to real wind data for Isparta province is discussed. This system generally consists of a PEM electrolysis system and a series of wind turbines. For analysis, a comprehensive thermodynamic evaluation is considered according to energy and exergy efficiencies. Some important results obtained can be summarized as follows;

- The thermodynamic analysis results show that: The wind turbines can generate a of total 6878 kW power, the net electrical power rate is computed as 4585 kW, and the net green hydrogen rate is determined to be 0.01263 kg/s, respectively. Also, the system SI value is 1.779. For the entire plant, the energy and exergy efficiency is computed as 44.03% and 43.78%, respectively.
- For parametric analysis results, when the rise in wind speeds the net power and hydrogen rate also upsurged. Moreover, the system has run higher performance. However, the rise in the ambient temperature leads to a negative effect on the beneficial products.

Overall, to reach carbon-free energy conversion systems, the renewable energy-based combined plant and hydrogen generation methods are much more important shortly.

REFERENCES

[1] Dincer, I., & Acar, C. (2017). Innovation in hydrogen production. *International Journal of Hydrogen Energy*, *42*(22), 14843-14864.

[2] Oliveira, A. M., Beswick, R. R., & Yan, Y. (2021). A green hydrogen economy for a renewable energy society. *Current Opinion in Chemical Engineering*, *33*, 100701.

[3] Pagani, G., Hajimolana, Y., & Acar, C. (2024). Green hydrogen for ammonia production–A case for the Netherlands. *International Journal of Hydrogen Energy*, *52*, 418-432.

[4] Gado, M. G., & Hassan, H. (2023). Potential of prospective plans in MENA countries for green hydrogen generation driven by solar and wind power sources. *Solar Energy*, *263*, 111942.

[5] Karayel, G. K., Javani, N., & Dincer, I. (2023). Green hydrogen production potential in Turkey with wind power. *International Journal of Green Energy*, *20*(2), 129-138.

[6] Abdelghany, M. B., Shehzad, M. F., Mariani, V., Liuzza, D., & Glielmo, L. (2022). Two-stage model predictive control for a hydrogen-based storage system paired to a wind farm towards green hydrogen production for fuel cell electric vehicles. *International Journal of Hydrogen Energy*, *47*(75), 32202-32222.

[7] Yilmaz, F. (2024). Design and performance analysis of hydro and wind-based power and hydrogen generation system for sustainable development. *Sustainable Energy Technologies and Assessments*, *64*, 103742.

[8] Hassan, Q., Algburi, S., Sameen, A. Z., & Salman, H. M. (2024). Assessment of industrial-scale green hydrogen production using renewable energy. *Proceedings of the Institution of Mechanical Engineers, Part A: Journal of Power and Energy*, *238*(3), 569-587.

[9] Ramakrishnan, S., Delpisheh, M., Convery, C., Niblett, D., Vinothkannan, M., & Mamlouk, M. (2024). Offshore green hydrogen production from wind energy: Critical review and perspective. *Renewable and Sustainable Energy Reviews*, *195*, 114320.

[10] Karayel, G. K., & Dincer, I. (2024). A study on green hydrogen production potential of Canada with onshore and offshore wind power. *Journal of Cleaner Production*, *437*, 140660.

[11] Cengel, Y. A., Boles, M. A., & Kanoğlu, M. (2015). *Thermodynamics: an engineering approach* (Vol. 5, p. 445). New York: McGraw-hill.

[12] Dinçer, İ. (2020). *Thermodynamics: a smart approach*. John Wiley & Sons.

Analysis of Electronic Cross Section (ECS) in Complex Borate Glass Containing CaO

Osman GÜNAY[1✉],

[1] *Yıldız Technical University, Faculty of Electrical and Electronics Engineering, Department of Biomedical Engineering, Istanbul, TURKEY*

✉ *Email : ogunay@yildiz.edu.tr*

ABSTRACT

The use of glass in radiation environments, such as medical imaging facilities and nuclear reactors, is critical for ensuring both operational safety and human health. These environments emit high levels of ionizing radiation, which can pose significant risks to individuals and sensitive equipment if not adequately shielded. Radiation shielding glasses are specifically engineered to mitigate these risks by incorporating materials that absorb or deflect ionizing radiation. These glasses undergo rigorous manufacturing processes that enhance their ability to attenuate radiation while maintaining optical clarity, essential for effective visual monitoring and equipment operation within these high-risk environments. By effectively reducing radiation exposure, these glasses contribute significantly to maintaining a safe working environment and minimizing health hazards associated with prolonged radiation exposure. The development and deployment of radiation shielding glasses involve a multidisciplinary approach integrating materials science, optics, and engineering. Specialized glass compositions and coatings are tailored to optimize radiation attenuation properties without compromising transparency or mechanical strength. Advanced manufacturing techniques, such as ion implantation and chemical vapor deposition, are utilized to enhance the glass's resistance to radiation damage and ensure long-term reliability in challenging operational conditions. These glasses are essential not only for protecting personnel but also for safeguarding critical equipment and infrastructure in industries where radiation exposure is a constant concern. Through continuous innovation and stringent quality control measures, radiation shielding glasses play a crucial role in mitigating the health and safety risks associated with ionizing radiation in various industrial and medical applications. In this study, the electronic cross-sectional area of a complex borate glass incorporating CaO has been analyzed across a range of energy levels.

Keywords: Glass, electronic cross section, Borat

1   INTRODUCTION

The application of glass in radiation environments, such as medical imaging facilities and nuclear reactors, is paramount for ensuring both operational safety and the protection of human health. Ionizing radiation, which is prevalent in these settings, presents substantial risks to personnel and sensitive equipment if effective shielding measures are not employed. Radiation shielding glasses are specifically designed to address these challenges by incorporating materials that absorb or deflect ionizing radiation, thereby mitigating its harmful effects.

Radiation shielding glasses are engineered through advanced manufacturing processes to optimize radiation attenuation while preserving optical clarity. This balance is crucial for visual monitoring and the efficient operation of equipment in radiation-prone environments. By effectively reducing radiation exposure, these glasses play a vital role in minimizing health hazards associated with prolonged exposure and maintaining safe working conditions.

The development and deployment of radiation shielding glasses involve an interdisciplinary approach that integrates materials science, optics, and engineering. Specialized glass compositions, including tailored additives and coatings, are designed to enhance radiation attenuation properties without compromising transparency or mechanical integrity. Advanced fabrication techniques, such as ion implantation and chemical vapor deposition, further improve the glass's resistance to radiation damage, ensuring long-term durability in demanding operational environments.

In addition to personnel protection, radiation shielding glasses are instrumental in safeguarding critical infrastructure and equipment, which are essential for the continuity of operations in radiation-intensive industries. Continuous innovation in material composition and manufacturing techniques, coupled with rigorous quality control, has enabled the development of high-performance shielding solutions that meet the growing demands of medical, nuclear, and industrial applications. Numerous studies have investigated various parameters related to radiation shielding[1-8].

This study focuses on analyzing the electronic cross-sectional area of a complex borate glass incorporating calcium oxide (CaO) across various energy levels. By investigating the interaction of ionizing radiation with borate-based glass systems, this work aims to contribute to the optimization of glass compositions for improved shielding performance and reliability in radiation environments.

2   MATERIAL AND METHODS

26

In this study, the electronic cross-sectional area of a complex borate glass system incorporating calcium oxide (CaO) was analyzed using the phy-X simulation program. The phy-X[9] software is a widely used tool for evaluating the radiation shielding properties of various materials, including attenuation coefficients, effective atomic numbers, and energy absorption coefficients. The borate glass sample analyzed in this study was composed of boron oxide (B_2O_3) as the base material with calcium oxide (CaO) as an additive. The inclusion of CaO was aimed at enhancing the glass's radiation attenuation properties. The glass composition was selected based on its potential to optimize shielding performance at different photon energy levels.

The radiation shielding parameters of the glass system were simulated using the phy-X program. The following steps were carried out:

1. **Input Parameters**: The chemical composition and density of the glass sample were input into the phy-X software.
2. **Energy Range**: Simulations were conducted across a broad range of photon energies, typically spanning from 0.01 MeV to 10 MeV, to evaluate the material's attenuation capabilities at low, medium, and high energy levels.
3. **Output Parameters**: The software calculated Electronic Cross Section

The obtained results from the phy-X simulations were analyzed to assess the glass's performance in attenuating ionizing radiation..

By leveraging the capabilities of the phy-X simulation program, this study provides detailed insights into the radiation shielding behavior of borate glasses, contributing to the development of more effective and reliable shielding materials for radiation environments.

3   RESULTS AND DISCUSSION

The electronic cross-section (ECS) values are presented in Table 1. Generally, ECS values tend to decrease with increasing energy. However, slight increases are observed at certain energy values, such as 10^{-2} and 10^{-1} MeV. These fluctuations may be attributed to photoelectric effects. Beyond 100 MeV, no significant changes are observed. The highest ECS value is $1.17 \times 10{-}20$, corresponding to gamma rays with an energy of 10^{-3} MeV.

27

Table 1. Electronic Cross Section (ECS)

Energy (MeV)	ECS (cm²/g)		Energy (MeV)	ECS (cm²/g)
1,00E-03	1,17E-20		1,60E+01	6,41E-26
1,50E-03	4,64E-21		1,80E+01	6,29E-26
2,00E-03	2,30E-21		2,00E+01	6,21E-26
3,00E-03	7,49E-22		2,20E+01	6,15E-26
4,00E-03	3,32E-22		2,40E+01	6,11E-26
5,00E-03	1,96E-22		2,60E+01	6,08E-26
6,00E-03	1,95E-22		2,80E+01	6,07E-26
8,00E-03	8,91E-23		3,00E+01	6,06E-26
1,00E-02	4,82E-23		4,00E+01	6,06E-26
1,50E-02	1,59E-23		5,00E+01	6,13E-26
2,00E-02	7,39E-24		6,00E+01	6,20E-26
3,00E-02	2,76E-24		8,00E+01	6,35E-26
4,00E-02	4,45E-24		1,00E+02	6,49E-26
5,00E-02	2,71E-24		1,50E+02	6,76E-26
6,00E-02	1,86E-24		2,00E+02	6,95E-26
8,00E-02	1,12E-24		3,00E+02	7,20E-26
1,00E-01	8,19E-25		4,00E+02	7,35E-26
1,50E-01	5,50E-25		5,00E+02	7,46E-26
2,00E-01	4,55E-25		6,00E+02	7,54E-26
3,00E-01	3,70E-25		8,00E+02	7,64E-26
4,00E-01	3,25E-25		1,00E+03	7,72E-26
5,00E-01	2,94E-25		1,50E+03	7,82E-26
6,00E-01	2,71E-25		2,00E+03	7,88E-26

28

8,00E-01	2,37E-25		3,00E+03	7,95E-26
1,00E+00	2,12E-25		4,00E+03	7,99E-26
1,50E+00	1,73E-25		5,00E+03	8,01E-26
2,00E+00	1,49E-25		6,00E+03	8,03E-26
3,00E+00	1,20E-25		8,00E+03	8,05E-26
4,00E+00	1,04E-25		1,00E+04	8,06E-26
5,00E+00	9,36E-26		1,50E+04	8,08E-26
6,00E+00	8,64E-26		2,00E+04	8,09E-26
7,00E+00	8,11E-26		3,00E+04	8,11E-26
8,00E+00	7,71E-26		4,00E+04	8,11E-26
9,00E+00	7,41E-26		5,00E+04	8,12E-26
1,00E+01	7,17E-26		6,00E+04	8,12E-26
1,10E+01	6,97E-26		8,00E+04	8,12E-26
1,20E+01	6,81E-26		1,00E+05	8,12E-26
1,30E+01	6,68E-26			
1,40E+01	6,58E-26			
1,50E+01	6,49E-26			

4 CONSLUSION

This study analyzed the electronic cross-sectional area of a borate glass system incorporating calcium oxide (CaO) across a range of photon energy levels. The findings highlight the glass's effective radiation shielding performance, particularly its ability to attenuate ionizing radiation at lower energy levels, with minimal variation observed beyond 100 MeV. These results contribute to optimizing borate glass compositions for enhanced reliability and safety in radiation-intensive environments.

REFERENCES

[1] Sivasailanathan V, Kumar P, Sagadevan S (2017) Investigation of Attenuation Parameters for Concrete Shielding Using Simulations through Iterative Approach and Meausurement. Sci. Res. Essays 12(7):69-76

[2] Gupta N, Viyas VK, Mandal A (2021) Studies of Substitution Effect of B2O3 on Structure and Properties of 1393 Bioactive Glass. Oriental Journal of Chemistry 37(6):1409-1414

[3] Akkurt, ˙I., Emikonel, S., Akarslan, F., Gunoglu, K., Kilincarslan, S., Uncu, I.S., 2015. Barite effect on radiation shielding properties of cotton-polyester fabric. Acta Phys. Pol., A 128. B-53.

[4] Almisned, G., Bilal, G., Baykal, D.S., Ali, F.T., Kilic, G.¨ O.K.H.A.N., Tekin, H.O., 2023. Bismuth (III) oxide and boron (III) oxide substitution in bismuth-boro-zinc glasses: a focusing in nuclear radiation shielding properties. Optik 272, 170214.

[5] AlMisned, G., Ghaida, B., Sen Baykal, D., Ali, F.T., Kilic, G., Tekin, H.O., 2023. Bismuth (III) oxide and boron(III) oxide substitution in bismuth-boro-zinc glasses: a focusing in nuclear radiation shielding properties. Optik 272, 170214.

[6] Rashad, M., Hanafy, T.A., Issa, S.A.M., 2020. Structural, electrical andradiation shielding properties of polyvinyl alcohol doped with different nanoparticles. J. Mater. Sci. Mater. Electron. 31, 15192–15197.

[7]Saddeek, Y.B., Issa, S.A., Alharbi, T., Elsaman, R., AbdElfadeel, G.S., Mostafa, A.M.A., Aly, K.A., Ahmed, M., 2020. Synthesis and characterization of leadborate glasses comprising cement kiln dust and Bi2O3 forradiation shielding protection. Mater. Chem. Phys. 242, 122510.

[8] Şakar E, Özpolat ÖF, Alım B, Sayyed MI, Kurudirek M (2020) Phy-X/PSD: Development of a user friendly online software for calculation of parameters relevant to radiation shielding and dosimetry. Radiation physics and chemistry. 166:108496

[9] Şakar, E., Özpolat, Ö. F., Alım, B., Sayyed, M. I., & Kurudirek, M. (2020). Phy-X/PSD: development of a user friendly online software for calculation of parameters relevant to radiation shielding and dosimetry. Radiation Physics and Chemistry, 166, 108496.

Assessment of the Mass Attenuation Coefficient in Boron-Enhanced Glass Systems

Kadir GÜNOĞLU[1*] Osman GÜNAY[2], İskender AKKURT[3]

[1]Isparta University of Applied Sciences, Technical Vocational School, Isparta-TURKEY*

[2]Yıldız Technical University, Faculty of Electrical and Electronics Engineering, Department of Biomedical Engineering, Istanbul, TURKEY
[3]Suleyman Demirel University, Science Faculty,Physics Department, Isparta-TURKEY

✉ *Corresponding Author Email   : kadirgunoglu@isparta.edu.tr*

ABSTRACT

Radiation shielding glasses play a pivotal role in facilities exposed to high-energy radiation sources such as X-rays and gamma rays, prevalent in sectors like nuclear energy and medical diagnostics. These glasses are specifically designed to provide effective protection against ionizing radiation, which can cause biological harm and damage to electronic components if not adequately mitigated. The development of radiation shielding glasses involves a meticulous selection of materials known for their high radiation attenuation properties, such as leaded glass or borosilicate compositions infused with heavy metals. These materials are strategically integrated into glass formulations using advanced manufacturing techniques to ensure optimal performance under varying radiation intensities. In addition to their material composition, radiation shielding glasses undergo rigorous testing and certification processes to validate their effectiveness and reliability in real-world radiation environments. These glasses are engineered to maintain optical clarity and mechanical integrity while effectively reducing the penetration of ionizing radiation. Their deployment is critical for protecting the health and safety of personnel working in proximity to radiation sources and for safeguarding sensitive equipment from potential damage. By employing radiation shielding glasses, industries can adhere to stringent safety regulations and standards, ensuring sustainable operational practices that prioritize both human welfare and environmental protection. In this study, the mass attenuation coefficient of boron-enhanced glass systems has been assessed across different energy levels.

Keywords: Glass, Mass Attenuation, Boron

1 INTRODUCTION

Radiation shielding glasses play a crucial role in environments where high-energy radiation, such as X-rays and gamma rays, is prevalent. These environments include key sectors like nuclear energy facilities and medical diagnostic centers, where exposure to ionizing radiation poses significant risks to human health and electronic equipment. To

mitigate these risks, radiation shielding glasses are specifically engineered to attenuate radiation effectively while maintaining critical properties such as optical clarity and mechanical durability.

The development of radiation shielding glasses relies on the strategic incorporation of materials with superior radiation attenuation capabilities, such as leaded glass or borosilicate glass infused with heavy metals. These specialized materials are integrated into glass compositions through advanced manufacturing processes, enabling the glasses to perform reliably across various radiation intensities. Furthermore, rigorous testing and certification processes are essential to validate the shielding effectiveness of these glasses under real-world operational conditions.

In addition to protecting personnel from harmful radiation exposure, shielding glasses safeguard sensitive equipment and support compliance with stringent safety regulations. Their implementation ensures that industries maintain sustainable and safe operational practices while prioritizing health, safety, and environmental protection. This study investigates the mass attenuation coefficient of boron-enhanced glass systems across different photon energy levels to evaluate their suitability for radiation shielding applications.

2   MATERIALS AND METHODS

In this study, boron-enhanced glass systems were analyzed to determine their mass attenuation coefficients across a range of photon energy levels. The Simulation procedures were designed to assess the glass's radiation shielding capabilities. The boron-enhanced glass systems were prepared using a combination of boron oxide (B_2O_3) as the base material, enhanced with heavy metal oxides to improve radiation attenuation properties. A wide range of parameters concerning radiation shielding has been analyzed in several studies [1-10].

To evaluate the shielding performance of the boron-enhanced glass, the mass attenuation coefficient (μ/ρ) was assessed across a wide energy range. Simulations and calculations were performed for photon energies ranging from 0.001 MeV to 10000 MeV, which are typical for X-ray and gamma-ray applications. The analysis was conducted using the phy-X [11] simulation software, a validated computational tool for determining radiation shielding parameters, including the mass attenuation coefficient and effective atomic number. The chemical composition, density, and energy range of the glass samples were entered into the phy-X software to simulate the interaction of photons with the glass systems.

3   RESULTS

The mass attenuation coefficient as a function of energy is presented in Table 1. Generally, the mass attenuation coefficient tends to decrease with increasing energy. However, a slight increase is observed around 1 MeV, after which it stabilizes. A minor rise in the mass attenuation coefficient is noted at 4×10^{-2}. Figure 1 illustrates the variation of the mass attenuation coefficient with photon energy.

32

Table 1. Mass Attenuation Coefficient

Energy (*MeV)*	MAC (*cm²/g)*
1,00E-03	4680,236
2,00E-03	1109,773
4,00E-03	180,316
8,00E-03	96,769
1,00E-02	53,515
2,00E-02	8,348
3,00E-02	2,865
4,00E-02	6,383
5,00E-02	3,629
6,00E-02	2,283
8,00E-02	1,120
1,00E-01	0,666
4,00E-01	0,102
5,00E-01	0,089
6,00E-01	0,080
8,00E-01	0,069
1,00E+00	0,061
4,00E+00	0,032
8,00E+00	0,026
9,00E+00	0,026
1,00E+01	0,026
1,10E+01	0,025
3,00E+01	0,026
4,00E+01	0,027
1,00E+02	0,031
5,00E+02	0,037
1,00E+04	0,040
1,00E+05	0,040

33
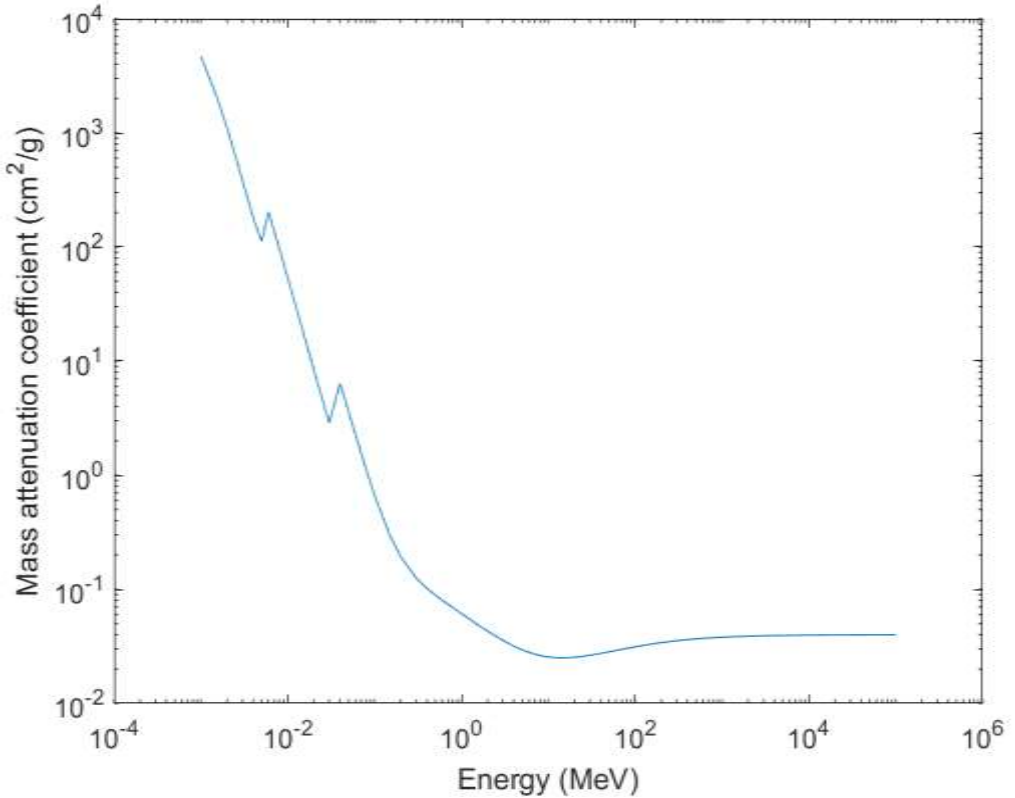
Figure 1. The mass attenuation coefficient with respect to energy variation.

4   CONSLUSION

This study evaluated the mass attenuation coefficient of boron-enhanced glass systems across a wide range of photon energy levels. The results revealed that the mass attenuation coefficient generally decreases with increasing energy, stabilizing beyond 1 MeV, with a slight rise observed around 4×10^{-2} MeV. These findings highlight the effectiveness of boron-enhanced glass in attenuating ionizing radiation, particularly at lower energy levels, making it a suitable candidate for radiation shielding applications. The integration of advanced materials and simulation techniques provides valuable insights into optimizing glass compositions for improved performance in radiation-prone environments

REFERENCES

[1] Abuslroos NJ, Yaacob KA, Zainon R (2023) Radiation attenuation effectiveness of polymer-based radiation shielding materials for gamma radiation. Radiat. Phys. Chem. 212:111070

[2] Şahin MC, Manisa K (2023) Evaluation of X-Ray Shielding Ability of Tungsten Rubber: A GAMOS Monte Carlo Study. Süleyman Demirel University Faculty of Arts and Sciences Journal of Science 18(1):1-9

[3] Agar O (2018) Study on Gamma Ray Shielding Performance of Concretes Doped with Natural Sepiolite Mineral. Radichim. Acta 106:1009-1016

[4] Kumar A, Gaikwad DK, Obaid SS, Tekin HO, Agar O, Sayyed MI (2020) Experimental Studies and Monte Carlo Simulations on Gamma Ray Shielding Competence of $(30+x)$ PbO-10WO$_3$-10Na$_2$O-10MgO-$(40-x)$B$_2$O$_3$ Glasses. Prog. Nucl. Energy. 119:103047

[5]Altunsoy, E.E., Tekin, H.O., Mesbahi, A., Akkurt, I., 2020. MCNPX simulation for radiation dose absorption of anatomical regions and some organs. Acta Phys. Pol., A 137, 561–565.

[6]Henaish, A.M.A., Mostafa, M., Salem, B.I., Zakaly, H.M.H., Issa, S.A.M., Weinstein, I.A., Hemeda, O.M., 2020. Spectral, electrical, magnetic and radiation shielding studies of Mg-doped Ni–Cu–Zn nanoferrites. J. Mater. Sci. Mater. Electron. 22, 1–13.

[7]Jawad, A.A., Demirkol, N., Gunoglu, K., Akkurt, I., 2019. Radiation shielding properties of some ceramic wasted samples. Int. J. Environ. Sci. Technol. 16, 5039–5042.Kulali, F., 2020. Simulation studies on radiological parameters for marble concrete. Emerg. Mater. Res. 9, 1341–1347.

[8] Bashter II. Calculation of radiation attenuation coefficients for shielding concretes.Ann Nucl Energy 1997;24:1389–401. https://doi.org/10.1016/s0306-4549(97)00003-0.

[9] Ilik E, Kavaz E, Kilic G, Issa SAM, Ghada ALMisned, H.O. Tekin, Synthesis and characterization of vanadium(V) oxide reinforced calcium-borate glasses:Experimental assessments on Al2O3, BaO2, ZnO contributions, Journal of NonCrystalline Solids, Volume 580,. 121397. ISSN 2022;0022–3093. https://doi.org/10.1016/j.jnoncrysol.2022.121397.

[10]Akkurt, I., Tekin, H.O., 2020. Radiological parameters for bismuth oxide glasses using phy-X/PSD software. Emerg. Mater. Res. 9, 1020–1027.

[11] Şakar, E., Özpolat, Ö. F., Alım, B., Sayyed, M. I., & Kurudirek, M. (2020). Phy-X/PSD: development of a user friendly online software for calculation of parameters relevant to radiation shielding and dosimetry. Radiation Physics and Chemistry, 166, 108496.

Covid-19 Vaccines in Preventing Thromboembolic and Cardiovascular Complications in Post-Covid

Arslan SAY[1] ✉, Taina AVRAMESCU[2], Daniela NEAGOE[3], Yanislav ZHELEV[4], Joanna KOMOREK[5]

Amasya University, Sabuncuoğlu Şerefeddin Vocational School of Health Services, Department of Medical Services and Techniques, Amasya, TURKEY
[2]University of Craiova, Craiova, Romania
[3]University of Medicine and Pharmacy of Craiova, Craiova, Romania
[4]Free Burgas University, Burgas, Bulgaria
[5]College of Business and Health Sciences, Łódź, Poland
✉:*arslan.say@amasya.edu.tr*

ABSTRACT

In this research article, we aimed to conduct a literature review examining the association between COVID-19 vaccination and the risk of cardiac and thromboembolic complications after COVID-19. The articles we reviewed pooled outcomes between 0.17 million vaccinated and 10.39 million unvaccinated people. This information showed a reduced risk of heart failure, venous thromboembolism, and arterial thrombosis/thromboembolism in post-Covid cases 30 days after vaccination.

Keywords: Post-Covid, Vaccination, Cardiac and thromboembolic complications

1. INTRODUCTION

The Covid-19 pandemic has raised numerous health concerns, some of which extend beyond the acute phase of infection. Ongoing concerns include the potential risks of thromboembolic and cardiovascular complications in post-Covid individuals. As the world grapples with the aftermath of the pandemic, the role of Covid-19 vaccines in preventing these complications is becoming increasingly important. As the world continues to struggle with the ongoing COVID-19 pandemic, the importance of vaccines in preventing the spread of the virus and reducing the severity of the disease cannot be overstated. In recent months, there has been growing concern about the potential long-term health impact of COVID-19, including the risk of cardiovascular and thromboembolic complications in survivors [1]. This article examines the risks of thromboembolic and cardiovascular complications in post-COVID individuals, the protective effects of vaccines in reducing these risks, and strategies to address concerns and promote vaccination for a healthier post-pandemic future [2].

2. COVID-19 VACCINATION

On December 8, 2020, emergency use authorization was granted for the NT162b2 messenger RNA (mRNA) vaccine (Pfizer-BioNTech) in the UK and around the world,

36

with the necessary approvals from institutions, and the UK became the first country to launch a COVID-19 vaccination program [3].

COVID-19 vaccines have since been approved and in use. Subsequently, the Oxford-AstraZeneca adenovirus vector vaccine, ChAdOx1 nCOV-19 2, and later the mRNA-based COVID-19 vaccine (mRNA-1273) developed by Moderna were approved and started to be used [4,5].

3. COVID-19 AND THROMBOSIS

There is a direct association between COVID-19 and thrombosis and thus cardiovascular disease. A history of cardiovascular disease prior to the Covid pandemic may result in higher rates of adverse outcomes in COVID-19 in direct proportion to the severity, extent or symptoms of coronary lesions [6]. Thrombosis is a common symptom during COVID-19. Cardiovascular diseases caused by thrombosis would then be inevitable. It is also normal to see more cardiovascular diseases in more severe Covid-19 cases. In contrast, in COVID-19, and among patients hospitalized with serious conditions in general, the incidence of very different acute cardiac diseases such as arrhythmias, fulminant myocarditis, acute heart failure, cardiogenic shock, pulmonary embolism (PE) or acute coronary syndromes (ACS) is very high. These diseases stand out as both symptoms of Covid-19 and symptoms that can be seen in post-Covid cases [7, 8, 9]. From the beginning of the pandemic to the present day, the incidence of thrombo-embolic events is higher in the literature sources we reviewed and can be seen in 14% of patients hospitalized in wards and 17% to 50% of patients hospitalized in the intensive care unit [10]. In a study involving 533 patients hospitalized with thrombotic events, it was described that acute myocardial infarction (AMI) occurred in more than half of the cases [11]. This picture has very dangerous implications for the consequences of Covid-19 symptoms. It has also been explained that the increased risk of ACS from COVID-19 may be excessive, as oxygen starvation as a result of respiratory depression and increased oxygen demand in response to infections may lead to a mismatch between oxygen supply and demand. Local inflammation and hemodynamic differences have also been found to increase the risk of atherosclerotic plaque rupture [12, 13, 14].

Covid-19, the hemodynamic stress of the acute critical illness picture, inflammation (up to the typical hyper-reactive immune response manifested by a cytokine storm) and fever can often trigger a prothrombotic state and inhibit the ability to dissolve thrombi, leading to early or late instability and rupture and thrombosis of coronary plaques. This can lead to a more fatal and riskier outcome. At present, the fact that the symptoms of Covid-19 disease are very mild and, in some patients, not present at all has no effect on the outcome. We see this especially in post-Covid cases [15].

4. COVID-19 VACCINES AND THE EFFECTS OF THROMBOEMBOLIC AND CARDIOVASCULAR COMPLICATIONS

The approval of Coronavirus vaccinations in the context of an emergency authorization in December 2020 and their high efficacy towards SARS-CoV-2 infection resulted in a reduction in Covid-19-related hospitalizations and deaths. However, spontaneous reports of an increase in unusual thromboembolic diseases after vaccination have led to a

situation of association of vaccines and symptoms [16]. More recently, the disclosure that mRNA-based vaccines carry a risk of rare post-vaccination myocarditis events has highlighted the need for further observational studies of vaccines [17].

Several studies suggest that COVID-19 vaccines may play an important role in reducing the risk of virus-induced complications in previously infected individuals. A recent literature review examined data from more than 10 million unvaccinated individuals and 0.17 million vaccinated individuals and highlighted a significant reduction in the incidence of heart failure, venous thromboembolism, and arterial thrombosis/thromboembolism in those vaccinated against COVID-19 [18, 19, 20].

Studies have shown that SARS-CoV-2 infection triggers cardiac and thromboembolic complications [21]. Studies have shown that the risk of serious complications remains high up to one year after infection, with these symptoms slowly decreasing over time [22]. While acute and post-acute cardiac and thromboembolic complications after COVID-19 are not common, they pose a significant health challenge for affected patients and the absolute number of cases can be significant when considered globally. These findings are particularly encouraging for individuals who have already experienced COVID-19 and may be at high risk of developing cardiovascular or thromboembolic complications as a result. It has been shown that these individuals may be able to mitigate some of the potential long-term health effects of the virus and reduce their risk of serious illness by receiving COVID-19 vaccination [23, 24].

Therefore, the development of vaccines and the expansion of vaccination in the wake of the global COVID-19 pandemic has been an important component not only for the fight against the virus, but also for the reduction of post-Covid symptoms. In this sense, the role of COVID-19 vaccines in preventing thromboembolic and cardiovascular complications in survivors of COVID-19 infection is undeniable. Studies have shown a reduced risk of heart failure, venous thromboembolism and arterial thrombosis/thromboembolism in individuals vaccinated against COVID-19 [25, 26]. These benefits were observed as early as 30 days after vaccination, suggesting that vaccines may also have a protective effect on the cardiovascular system in individuals recovering from COVID-19 [27].

5. RESULTS

While more research is needed to fully understand the mechanisms behind these findings, the results of this literature review offer hope for individuals who have faced the challenging aftermath of a COVID-19 infection. By receiving a COVID-19 vaccine, individuals may not only protect themselves from future infections but also reduce the risk of developing serious cardiovascular and thromboembolic complications. Regretfully, a part of society is still hesitant to recognize the dangers associated with SARS-CoV-2. Today, vaccine hesitancy today risks delaying the treatment of infectious diseases. In this situation, appearing indifferent should not be an option, as it would result in failing to help a large group of people in danger.

In conclusion, COVID-19 vaccines have shown potential in preventing thromboembolic and cardiovascular complications in individuals post-COVID-19. Further studies are

warranted to explore the long-term benefits of vaccination in this population and to inform public health strategies moving forward. With continued research and widespread vaccination efforts, we can work towards a healthier and safer future for all.

REFERENCES
[1] Pritchard, E., Matthews, P. C., Stoesser, N., Eyre, D. W., Gethings, O., Vihta, K. D., ... & Pouwels, K. B. (2021). Impact of vaccination on new SARS-CoV-2 infections in the United Kingdom. Nature medicine, 27(8), 1370-1378.
[2] Burn, E., Roel, E., Pistillo, A., Fernández-Bertolín, S., Aragón, M., Raventós, B., ... & Duarte-Salles, T. (2022). Thrombosis and thrombocytopenia after vaccination against and infection with SARS-CoV-2 in Catalonia, Spain. Nature communications, 13(1), 7169.
[3] Leav, B., Straus, W., White, P., Leav, A., Gaines, T., Maggiacomo, G., ... & Chen, R. T. (2022). A Brighton Collaboration standardized template with key considerations for a benefit/risk assessment for the Moderna COVID-19 Vaccine (mRNA-1273). Vaccine, 40(35), 5275-5293.
[4] Saad-Roy, C. M., Morris, S. E., Metcalf, C. J. E., Mina, M. J., Baker, R. E., Farrar, J., ... & Wagner, C. E. (2021). Epidemiological and evolutionary considerations of SARS-CoV-2 vaccine dosing regimens. Science, 372(6540), 363-370.
[5] Polack, F. P., Thomas, S. J., Kitchin, N., Absalon, J., Gurtman, A., Lockhart, S., ... & Gruber, W. C. (2020). Safety and efficacy of the BNT162b2 mRNA Covid-19 vaccine. New England journal of medicine, 383(27), 2603-2615.
[6] Chen, R., Liang, W., Jiang, M., Guan, W., Zhan, C., Wang, T., ... & for COVID, M. T. E. G. (2020). Risk factors of fatal outcome in hospitalized subjects with coronavirus disease 2019 from a nationwide analysis in China. Chest, 158(1), 97-105.
[7] Khawaja, S. A., Mohan, P., Jabbour, R., Bampouri, T., Bowsher, G., Hassan, A. M., ... & Mikhail, G. W. (2021). COVID-19 and its impact on the cardiovascular system. Open heart, 8(1), e001472.
[8] Schiavone, M., Gobbi, C., Biondi-Zoccai, G., D'Ascenzo, F., Palazzuoli, A., Gasperetti, A., ... & Forleo, G. B. (2020). Acute coronary syndromes and Covid-19: exploring the uncertainties. Journal of clinical medicine, 9(6), 1683.
[9] Stefanini, G. G., Montorfano, M., Trabattoni, D., Andreini, D., Ferrante, G., Ancona, M., ... & Chieffo, A. (2020). ST-elevation myocardial infarction in patients with COVID-19: clinical and angiographic outcomes. Circulation, 141(25), 2113-2116.
[10] Middeldorp, S., Coppens, M., van Haaps, T. F., Foppen, M., Vlaar, A. P., Müller, M. C., ... & van Es, N. (2020). Incidence of venous thromboembolism in hospitalized patients with COVID- 19. Journal of Thrombosis and Haemostasis, 18(8), 1995-2002.
[11] Bilaloglu, S., Aphinyanaphongs, Y., Jones, S., Iturrate, E., Hochman, J., & Berger, J. S. (2020). Thrombosis in hospitalized patients with COVID-19 in a New York City health system. Jama, 324(8), 799-801.
[12] Bugert, C. L., Kwiat, V., Valera, I. C., Bugert, J. J., & Parvatiyar, M. S. (2021). Cardiovascular injury due to SARS-CoV-2. Current clinical microbiology reports, 1-11.

[13] Luo, J., Zhu, X., Jian, J., Chen, X., & Yin, K. (2021). Cardiovascular disease in patients with COVID-19: evidence from cardiovascular pathology to treatment. Acta biochimica et biophysica Sinica, 53(3), 273-282.
[14] Magadum, A., & Kishore, R. (2020). Cardiovascular manifestations of COVID-19 infection. Cells, 9(11), 2508.

[15] Soumya, R. S., Unni, T. G., & Raghu, K. G. (2021). Impact of COVID-19 on the cardiovascular system: a review of available reports. Cardiovascular drugs and therapy, 35, 411-425.

[16] Li, X., Burn, E., Duarte-Salles, T., Yin, C., Reich, C., Delmestri, A., ... & Prieto-Alhambra, D. (2022). Comparative risk of thrombosis with thrombocytopenia syndrome or thromboembolic events associated with different covid-19 vaccines: international network cohort study from five European countries and the US. bmj, 379.

[17] Mercadé-Besora, N., Li, X., Kolde, R., Trinh, N. T., Sanchez-Santos, M. T., Man, W. Y., ... & Català, M. (2024). The role of COVID-19 vaccines in preventing post-COVID-19 thromboembolic and cardiovascular complications. Heart, 110(9), 635-643.

[18] Husby, A., Hansen, J. V., Fosbøl, E., Thiesson, E. M., Madsen, M., Thomsen, R. W., ... & Hviid, A. (2021). SARS-CoV-2 vaccination and myocarditis or myopericarditis: population-based cohort study. bmj, 375.

[19] Simone A, Herald J, Chen A, et al. Acute myocarditis following COVID-19 mRNA vaccination in adults aged 18 years or older. JAMA Intern Med 2021; 181:1668–70.

[20] Montgomery, J., Ryan, M., Engler, R., Hoffman, D., McClenathan, B., Collins, L., ... & Cooper, L. T. (2021). Myocarditis following immunization with mRNA COVID-19 vaccines in members of the US military. JAMA cardiology, 6(10), 1202-1206.

[21] Burn, E., Duarte-Salles, T., Fernandez-Bertolin, S., Reyes, C., Kostka, K., Delmestri, A., ... & Prieto-Alhambra, D. (2022). Venous or arterial thrombosis and deaths among COVID-19 cases: a European network cohort study. The Lancet Infectious Diseases, 22(8), 1142-1152.

[22] Xie, Y., Xu, E., Bowe, B., & Al-Aly, Z. (2022). Long-term cardiovascular outcomes of COVID-19. Nature medicine, 28(3), 583-590.

[23] Xie, J., Prats-Uribe, A., Feng, Q., Wang, Y., Gill, D., Paredes, R., & Prieto-Alhambra, D. (2022). Clinical and genetic risk factors for acute incident venous thromboembolism in ambulatory patients with COVID-19. JAMA internal medicine, 182(10), 1063-1070.

[24] Al-Aly, Z., Bowe, B., & Xie, Y. (2022). Long COVID after breakthrough SARS-CoV-2 infection. Nature medicine, 28(7), 1461-1467.

[25] Houghton, D. E., Wysokinski, W., Casanegra, A. I., Padrnos, L. J., Shah, S., Wysokinska, E., ... & Padmanabhan, A. (2022). Risk of venous thromboembolism after COVID- 19 vaccination. Journal of Thrombosis and Haemostasis, 20(7), 1638-1644.

[26] Katsoularis, I., Fonseca-Rodríguez, O., Farrington, P., Jerndal, H., Lundevaller, E. H., Sund, M., ... & Connolly, A. M. F. (2022). Risks of deep vein thrombosis, pulmonary embolism, and bleeding after covid-19: nationwide self-controlled cases series and matched cohort study. bmj, 377.

[27] Byambasuren, O., Stehlik, P., Clark, J., Alcorn, K., & Glasziou, P. (2023). Effect of covid-19 vaccination on long covid: systematic review. BMJ medicine, 2(1).

Face-to-face/Online Education in the Field of Health Sciences: Blended Education

Arslan SAY[1] ✉, Taina AVRAMESCU[2], Daniela NEAGOE[3], Yanislav ZHELEV[4], Joanna KOMOREK[5]

[1]Amasya University, Sabuncuoğlu Şerefeddin Vocational School of Health Services, Department of Medical Services and Techniques, Amasya, TURKEY
[2]University of Craiova, Craiova, Romania
[3]University of Medicine and Pharmacy of Craiova, Craiova, Romania
[4]Free Burgas University, Burgas, Bulgaria
[5]College of Business and Health Sciences, Łódź, Poland
✉:*arslan.say@amasya.edu.tr*

ABSTRACT

Blended learning, defined as the combination of traditional face-to-face learning and synchronous or asynchronous e-learning, has grown rapidly and is now widely used in education. In this article, we aimed to evaluate the effectiveness of blended learning for health professional students in comparison with non-intervention and blended learning in the literature. The results of our study show that blended learning has a consistent positive effect compared to no intervention and is more effective or at least as effective as non-blended teaching in terms of knowledge acquisition in health professions.

Keywords: Blended learning, Health students, Effectiveness

1. INTRODUCTION

Health science education is constantly evolving with new technologies and teaching methods revolutionizing the way students learn and prepare for their careers. In the rapidly evolving field of health sciences, education plays a crucial role in preparing future healthcare professionals for the challenges they will face in their careers. One of the most popular trends in education today is blended learning, which combines traditional face-to-face education with online learning platforms [1, 2]. In the field of health sciences, this approach is proving to be extremely beneficial for students who want to develop their knowledge and skills in a flexible and convenient way. With advances in technology, the traditional face-to-face education model is being augmented by the integration of online learning, resulting in what is commonly known as blended learning [3].

2. MIXED EDUCATION, BLENDED LEARING

Blended learning combines the best of both worlds, enabling students to benefit from the interactive and collaborative nature of face-to-face education while also enjoying the flexibility and accessibility offered by online platforms. This approach has gained popularity in recent years and many institutions have incorporated blended learning into their curricula [4].

Blended learning in health sciences allows students to engage with course material both face-to-face and online, offering a more dynamic and interactive learning experience. This combination of traditional and digital learning resources offers students the opportunity to learn at their own pace, review information as needed, and interact with multimedia content to enhance their understanding of complex concepts [5].

Research has shown that blended learning is highly effective for health profession students and leads to greater knowledge acquisition and retention compared to traditional face-to-face instruction alone. In fact, studies have shown that blended learning is at least as effective, if not more effective, than non-blended teaching methods in terms of improving student outcomes in health sciences [6]. A study comparing the effectiveness of blended learning with traditional face-to-face instruction found that students in the blended learning group had higher levels of knowledge acquisition and retention [7]. This highlights the potential of blended learning to enhance the learning experience for health science students [8, 9].

One of the most important benefits of blended learning in health sciences education is the ability to adapt education to meet the different needs of students. In this model, it can offer students a more personalized learning experience [10]. With online resources and interactive tools, instructors can provide personalized feedback, track students' progress and offer additional support when needed. Online modules can be tailored to meet individual needs, allowing students to progress at their own pace and focus on areas where they may need additional support [11]. This level of individualized instruction can greatly benefit students who have different learning styles or need extra help in certain areas of study [12].

Furthermore, blended learning allows students to interact with course materials beyond the traditional classroom boundaries, offering flexibility and convenience for those with busy schedules or other commitments. By providing access to online lectures, discussion forums and virtual simulations, students can deepen their understanding of complex topics and apply their knowledge in real-world scenarios.

Simulation exercises and virtual patient encounters can help students develop their clinical skills and decision-making abilities by providing valuable hands-on experience in a safe and controlled environment [13]. Furthermore, blended learning in health sciences fosters collaboration and communication between students and faculty. Utilizing online platforms for group discussions, collaborative projects and virtual simulations, students can engage in interactive learning experiences that mirror real-world healthcare settings [14].

Despite its many advantages, blended learning in health sciences brings its own challenges. One of these challenges is to ensure that the online components of the curriculum are engaging and interactive to promote active learning. Furthermore, to maximize the benefits of blended learning, educators need to be trained to effectively integrate technology into teaching practices [15].

3. RESULTS

In conclusion, blended learning is a valuable approach to education in the health sciences, offering a flexible and dynamic learning experience for students. Specifically, blended

learning in health sciences offers a unique and effective approach to prepare students for careers in healthcare. Blended learning in health sciences has proven to be a valuable tool in enhancing the learning experience for students. By combining traditional face-to-face instruction with online resources, students can develop their knowledge and skills in a way that is both effective and engaging. As technology continues to advance, blended learning will undoubtedly play a crucial role in shaping the future of health sciences education.

REFERANCES

[1] Liu, Q., Peng, W., Zhang, F., Hu, R., Li, Y., & Yan, W. (2016). The effectiveness of blended learning in health professions: systematic review and meta-analysis. Journal of medical Internet research, 18(1), e2.

[2] Valiathan, P. (2002). Blended learning models. Learning circuits, 3(8), 50-59.

[3] Graham, C. R. (2009). Blended learning models. In Encyclopedia of Information Science and Technology, Second Edition (pp. 375-382). IGI Global.

[4] Lam, J. (2014). The context of blended learning: The TIPS blended learning model. In Hybrid Learning. Theory and Practice: 7th International Conference, ICHL 2014, Shanghai, China, August 8-10, 2014. Proceedings 7 (pp. 80-92). Springer International Publishing.

[5] Bryan, A., & Volchenkova, K. N. (2016). Blended learning: definition, models, implications for higher education. Вестник Южно-Уральского государственного университета. Серия: Образование. Педагогические науки, 8(2), 24-30.

[6] Arifin, M., & Abduh, M. (2021). Peningkatan motivasi belajar model pembelajaran blended learning. Jurnal Basicedu, 5(4), 2339-2347.

[7] AlAbdulkarim, L., & Albarrak, A. (2015, October). Students' attitudes and satisfaction towards blended learning in the health sciences. In International Conference on Advances in Education and Social Sciences (Vol. 423, p. 434).

[8] Alabdulkarim, L. (2021). University health sciences students rating for a blended learning course framework. Saudi Journal of Biological Sciences, 28(9), 5379-5385.

[9] Milic, N., Masic, S., Bjegovic-Mikanovic, V., Trajkovic, G., Marinkovic, J., Milin-Lazovic, J., ... & Stanisavljevic, D. (2018). Blended learning is an effective strategy for acquiring competence in public health biostatistics. International journal of public health, 63, 421-428.

[10] Booth, A., Carroll, C., Papaioannou, D., Sutton, A., & Wong, R. (2009). Applying findings from a systematic review of workplace- based e- learning: implications for health information professionals. Health Information & Libraries Journal, 26(1), 4-21.

[11] Carroll, C., Booth, A., Papaioannou, D., Sutton, A., & Wong, R. (2009). UK health-care professionals' experience of on- line learning techniques: A systematic review of qualitative data. Journal of Continuing Education in the Health professions, 29(4), 235-241.

[12] McDonald, P. L., & Picciano, A. G. (2014). Introduction to the special issue on blended learning in the health sciences. Online Learning, 18(4), 7-11.

[13] Beckem, J. M., & Watkins, M. (2012). Bringing life to learning: Immersive experiential learning simulations for online and blended courses. Journal of Asynchronous Learning Networks, 16(5), 61-70.

[14] Mirmoghtadaie, Z., Kohan, N., & Rasouli, D. (2020). Determination and comparison of the factors related to effective blended learning in medical sciences from the viewpoints of instructors and learners. Advances in medical education and practice, 205-214.

[15] Moskal, P., Dziuban, C., & Hartman, J. (2013). Blended learning: A dangerous idea?. The internet and higher education, 18, 15-23.

Effect of Nano TiC and Process Control Agent Additions on the Synthesis of Cu-TiC Composite Powder

Serkan BIYIK[1]*, Aykut ÇANAKÇI[2]

[1]Karadeniz Technical University, Abdullah Kanca Vocational School, Department of Machinery and Metal Technologies, Trabzon, Turkey
[2]Karadeniz Technical University, Department of Metallurgical and Materials Engineering, Trabzon, Turkey

* serkanbiyik@ktu.edu.tr

ABSTRACT

This study investigated the effect of titanium carbide (TiC) and process control agent (PCA) additions on particle size and morphology of nano TiC reinforced copper (Cu) based composite powder. For this aim, powder mixtures having Cu and TiC were prepared at the amounts of 99 and 1wt.%, respectively. Two different types of PCAs, namely stearic acid and methanol were used to observe the evolution of powder characteristics including powder morphology and particle size throughout specified milling durations. A two stationary planetary-type ball-mill was used for milling experiments. Scanning electron microscopy (SEM) and laser diffraction analysis (Mastersizer) techniques were carried out to observe starting and milled powder morphologies and to determine powder particle sizes, respectively. It was found that the type of PCA significantly affected powder morphologies. Besides, particle size reduction was apparently improved for powder specimens having methanol as a PCA.

KEYWORDS- *Ball-milling, composites, copper, methanol, powder technology, stearic acid, titanium carbide.*

1. INTRODUCTION

Copper (Cu) metal is used to produce electrical contact materials due to its favourable material properties, such as high electrical and thermal conductivities, low cost and high formability [1]. However, to further improve its physical and mechanical properties, some minor doped elements such as oxides, carbides and refractory metals are frequently used with Cu [2-5]. Therefore, titanium carbide (TiC) is chosen to reinforce Cu matrix for enhancing material properties by composite production. Production of composite materials by conventional powder metallurgy (PM) combined with mechanical alloying (MA) or ball-milling technique involves a number of process parameters. Among these, powder preparation methods, powder compaction, sintering regime and secondary operations affect physical, mechanical and thermal properties of composites [6-9].

MA method is used to obtain homogenous structures with grain refinement. However, it has several processing parameters to be optimized, such as milling speed, nature and amount of process control agent (PCA), ball-to-powder weight ratio (BPR) and milling time [10-13]. In this study, stearic acid and methanol are chosen as PCAs to investigate their effects on powder shape, morphology and homogenization.

45

Since the performance of materials is directly related to the material properties, microstructural examinations are crucial to obtain high quality products. In this regard, fine grained materials are advantageous as compared to coarse grained materials. Therefore, the aim of this study is to investigate the synergetic effect of type of PCA and TiC reinforcement on the synthesis of Cu/TiC composite powder.

2. EXPERIMENTAL PROCEDURES

In this study, Cu powder was used as the matrix material whereas TiC as the reinforcement. Morphology of as-received powders was investigated by means of scanning electron microscopy (SEM) on a Zeiss Evo LS 10 model (Fig. 1). Table 1 lists the properties of as-received powders used for ball-milling experiments. Two different powder specimens were prepared with the proper amounts (wt.%) as described in Table 2. Further, these prepared powder mixtures were milled for 15 hours in a two stationary planetary-type ball mill (Fritsch Pulverisette 7). Milling parameters were selected as a milling speed of 300 rpm and a BPR of 10:1. By the way, stearic acid and methanol were also separately added to prepared powder mixtures as PCAs at the amounts of 6 wt.% for each vial. All milling parameters were listed in Table 3. To compensate overheating of the grinding medium, milling experiments were paused at specified milling cycles until the room temperature attained. Powder characterization was achieved using a laser diffractometer (Malvern Instruments Mastersizer 2000). In addition, the relationship between average particle size (APS, (d_{50})) and milling duration was investigated using SEM.

(a)　　　　　　　　　　　　　　(b)
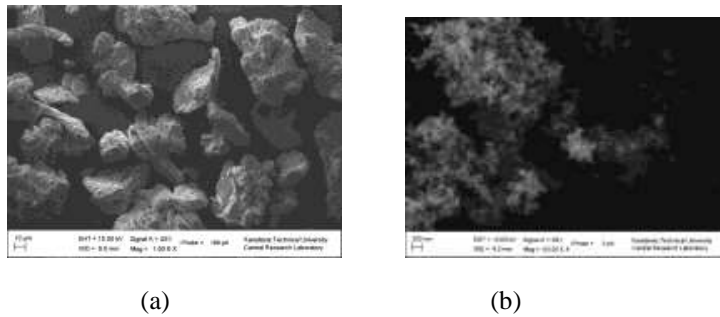
Figure 1. Morphology of as-received a) Cu and b) nano TiC powders.

Table 1. Type, particle size and purity of as-received powders used for ball-milling experiments.

Type of powder	Particle size (microns)	Purity (%)
Cu	max. 44 μm	99%
TiC	40 nm	98.8%

46

Table 2. Chemical compositions of the prepared powder specimens.

No	Cu (wt.%)	TiC (wt.%)	PCA (wt.%)
P1	99%	1%	6% stearic acid
P2	99%	1%	6% methanol

Table 3. Milling parameters used to investigate the effect of different PCAs on milling behavior of Cu/TiC powder.

Chemical composition	Cu/TiC
Type and amount of process control agent (PCA)	6% stearic acid; 6% methanol
Ball-to-powder weight ratio (BPR)	10:1
Milling speed	300 rpm
Grinding mode	2 min grinding, 1 min pause cycles / reverse mode active
Diameter and material of the grinding balls	10 mm, Tungsten carbide (WC)
Type of ball-mill	Fritsch Pulverisette 7 / 80 ml vials
Milling duration	3, 6, 9, 12 and 15 hours

3. RESULTS AND DISCUSSION

In this study, two different process control agent (PCA) contents, namely stearic acid and methanol were comparatively studied to synthesize Cu-TiC composite powder. It can be seen from Fig. 1 that, from a morphological point of view, Cu powder particles have an irregular shape (Fig. 1a) and TiC powder particles have an angular and irregular shape (Fig. 1b). APS values of all powder specimens obtained after Mastersizer results for each milling period were given in Table 4.

47

Table 4. Average particle size values of Cu/TiC powder mixtures as functions of PCA and milling duration.

Chemical composition	Milling time (h) and average particle size (APS, µm)					
	0	3	6	9	12	15
Cu/TiC - 6% stearic acid	28.895	29.551	27.454	18.157	12.098	8.195
Cu/TiC - 6% methanol	28.895	26.673	23.009	14.145	9.452	6.794

Particle size variation of Cu/TiC powder mixtures as a function of milling duration was shown in Fig. 2. It can be seen from this figure that APS was generally decreased for both composition.
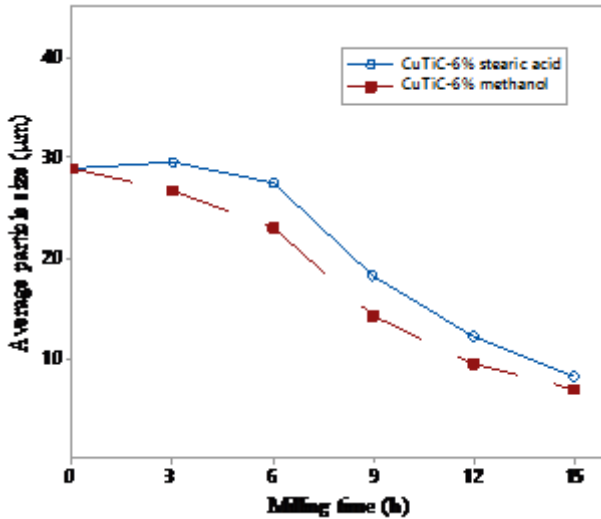
Figure 2. Particle size variation of Cu/TiC powder mixtures as a function of milling duration.

Fig. 3 shows the morphological evolution of Cu/TiC composite powders obtained after milling for 3, 6 and 9 h with PCA contents of 6% stearic acid and 6% methanol. Accordingly, particle size values were shown decreasing trends for both composition, although some fluctuations were observed at first 3 hours of milling process for the specimen milled with stearic acid addition (Fig. 3a). Flaky particles are dominant at first 6 h of milling (Figs. 3a-b and Figs. 3d-e) due to plastic deformation and cold welding effects. With further milling, fracturing trails are observed (Figs. 3c and f).
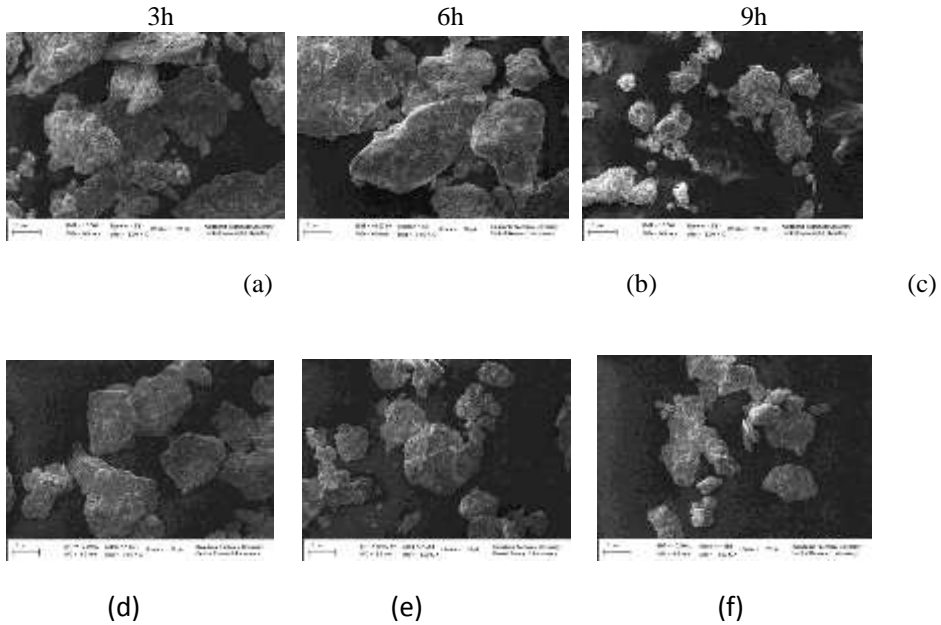
48

3h   6h   9h

(a)   (b)   (c)

(d)   (e)   (f)

Figure 3. Morphology of the Cu-TiC having 6% stearic acid after milled for a) 3 h, b) 6 h and c) 9 h; and Cu-TiC having 6% methanol after milled for d) 3 h, e) 6 h and f) 9 h.

The morphological evolution of Cu/TiC composite powders, obtained after milling for 12 and 15 h with PCA contents of 6% stearic acid and 6% methanol, is given in Fig. 4. Methanol addition was exhibited better milling behavior (Figs. 4c and d) as compared to stearic acid (Figs. 4a and b) for the whole milling process, namely up to 15 hours. Average particles size values at the end of milling cycles were recorded to be 8.195 and 6.794 μm for stearic acid and methanol usages, respectively. Considering SEM pictures and particle size values obtained after milling, it was found that 6% of methanol content was determined to be optimum condition to synthesize Cu-TiC composite powder.

49

12h   15h

(a)   (b)

(c)   (d)
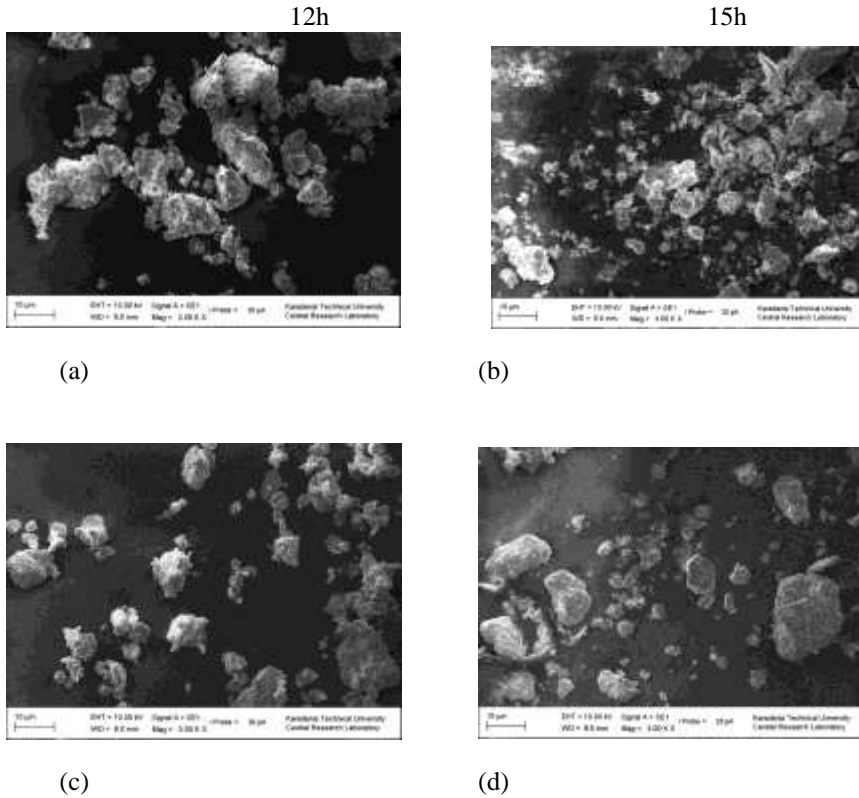
Figure 4. Morphology of the Cu-TiC having 6% stearic acid after milled for a) 12 h and b) 15 h; and Cu-TiC having 6% methanol after milled for c) 12 h and d) 15 h.

4. CONCLUSIONS

In this study, two different process control agent (PCA) contents, namely stearic acid and methanol were comparatively studied to synthesize Cu-TiC composite powder. Accordingly, particle size values were shown decreasing trends for both composition, although some fluctuations were observed at first 3 hours of milling process for the specimen milled with stearic acid addition. Methanol addition was exhibited better milling behavior as compared to stearic acid for the whole milling process, namely up to 15 hours. Average particles size values at the end of milling cycles were recorded to be 8.195 and 6.794 µm for stearic acid and methanol usages, respectively. Considering SEM pictures and particle size values obtained after milling, it was found that 6% of methanol content was determined to be optimum condition to synthesize Cu-TiC composite powder.

50

REFERENCES

[1] P. G. Slade, Electrical Contacts: Principles and Applications, CRC, Boca Raton, FL, 2014.

[2] O. Guler, T. Varol, U. Alver, S. Biyik, The wear and arc erosion behavior of novel copper based functionally graded electrical contact materials fabricated by hot pressing assisted electroless plating, Adv. Powder Technol. 32 (2021) 2873-2890. https://doi.org/10.1016/j.apt.2021.05.053

[3] S. C. Shu, Q. Zhang, J. Ihde, Q. L. Yuan, W. Dai, M. L. Wu, D. Dai, K. Yang, B. Wang, C. Xue, H. B. Ma, X. Zhang, J. M. Han, X. Y. Chen, C. T. Lin, W. B. Ren, Y. F. Ma, N. Jiang, Surface modification on copper particles toward graphene reinforced copper matrix composites for electrical engineering application, J. Alloy. Compd. 891 (2022) 162058. https://doi.org/10.1016/j.jallcom.2021.162058

[4] A. Canakci, T. Varol, H. Cuvalci, F. Erdemir, S. Ozkaya, Development and characterization of bronze-Cr-Ni composites produced by powder metallurgy, Sci. Eng. Compos. Mater. 22 (2015) 425-432. https://doi.org/10.1515/secm-2013-0262

[5] Y. X. Zhou, Y. L. Xue, K. Zhou, Failure analysis of arc ablated tungsten-copper electrical contacts, Vacuum. 164 (2019) 390-395. https://doi.org/10.1016/j.vacuum.2019.03.052

[6] S. Biyik, F. Arslan, M. Aydin, Arc-erosion behavior of boric oxide-reinforced silver-based electrical contact materials produced by mechanical alloying, Journal of Electronic Materials 44 (2015) 457-466. *DOI:10.1007/s11664-014-3399-4*

[7] J. F. Li, B. Chen, H. Tang, S. Zhang, C. Li, Tribological behaviors of Cu-based composites with $NbSe_2$ and TiB_2, Dig. J. Nanomater. Bios. 12 (2017) 1205-1214.

[8] C. Suryanarayana, A. A. Al-Joubori, Z. Wang, Nanostructured materials and nanocomposites by mechanical alloying: an overview, Met. Mater. Int. 28 (2022) 41-53. https://doi.org/10.1007/s12540-021-00998-5

[9] X. H. Guo, Y. B. Yang, K. X. Song, S. L. Li, F. Jiang, X. Wang, Arc erosion resistance of hybrid copper matrix composites reinforced with CNTs and micro-TiB_2 particles, J. Mater. Res. Technol. 11 (2021) 1469-1479. https://doi.org/10.1016/j.jmrt.2021.01.084

[10] S. A. Tunc, A. Canakci, A. H. Karabacak, M. Celebi, M. Turkmen, Effect of different PCA types on morphology, physical, thermal and mechanical properties of AA2024-B4C composites, Powder Technology 434 (2024) 119373. DOI:10.1016/j.powtec.2024.119373.

[11] S. Biyik, Characterization of nanocrystalline Cu25Mo electrical contact material synthesized via ball milling, Acta Phys. Pol. A 132 (2017) 886-888. https://doi.org/10.12693/APhysPolA.132.886

[12] S. Biyik, M. Aydin, Optimization of mechanical alloying parameters of Cu25W electrical contact material, Acta Phys. Pol. A 132 (2017) 909-912. https://doi.org/10.12693/APhysPolA.132.909

[13] F. Erdemir, T. Varol, A. Canakci, Synthesis of SiC nanoparticles by central composite design response surface methodology directed mechanical milling, Micro Nano Lett. 15 (2020) 187-190. https://doi.org/10.1049/mnl.2019.0468

52

Influence of Nanographene and Methanol Additions on the Mechanical Alloying Behavior of Al-Cu/SiC/NG Composites

Serkan BIYIK[1]*, Aykut ÇANAKÇI[2], Sedat Alperen TUNÇ[2]

[1]Karadeniz Technical University, Abdullah Kanca Vocational School, Department of Machinery and Metal Technologies, Trabzon, Turkey
[2]Karadeniz Technical University, Department of Metallurgical and Materials Engineering, Trabzon, Turkey

* serkanbiyik@ktu.edu.tr

ABSTRACT

This study investigated the effect of nanographene (NG) addition as a reinforcement and methanol addition as a process control agent (PCA) on mechanical alloying behavior of Al-Cu/SiC/NG composites. For this purpose, elemental aluminum (Al) and copper (Cu) powders were used to prepare the matrix. The amount of silicon carbide (SiC) was kept constant whereas various amounts of NG (0.5 and 1 wt.%) were used to reinforce matrix. Prior to ball-milling of these two powder specimens, different amounts of methanol additions (2 and 6 wt.%) were also chosen to observe the evolution of powder characteristics such as powder morphology and particle size distribution during mechanical alloying. These different powder mixtures were then injected to a two stationary planetary-type ball-mill having both tungsten carbide (WC) vials and milling balls as a grinding medium. Scanning electron microscopy (SEM) and laser diffraction analysis (Mastersizer) techniques were carried out to characterize both starting and milled powder morphologies and to determine powder particle sizes after certain periods of ball-milling, respectively. It was found that the increase in methanol addition significantly changed powder morphology. Moreover, lesser amounts of NG promote embedding of powder particles, whereas higher amounts of NG provide fracturing efficiency.

KEYWORDS- *Aluminum, composites, copper, mechanical alloying, nanographene, powder technology, silicon carbide.*

1. INTRODUCTION

Metal matrix composites (MMCs) have been applied in a variety of applications including automotive, aerospace, electrical and electronics industries [1-3]. Among metallic materials, copper (Cu) metal is advantageous to be used as a base material to produce electrical contacts due to its high electrical and thermal conductivities, high formability and low cost. On the other hand, Cu has also some drawbacks such as poor resistance to oxidation and corrosion. Therefore, to further improve its physical and mechanical properties, some minor doped elements such as oxides, carbides and refractory metals are frequently used with Cu [4-6].

53

Composite materials can be produced by powder metallurgy (PM) technique [7-8]. In PM method, powder preparation is one of the most important parameter affecting the homogeneity and final properties of the composites. Therefore, conventional PM method is generally combined with another technique called mechanical alloying (MA) or ball-milling to prepare composite powders, which will be further compacted and sintered [9-10]. MA technique has also several processing parameters such as milling speed, nature and amount of process control agent (PCA), ball-to-powder weight ratio (BPR) and milling time to produce composite powders efficiently [11-13]. Among these, PCA plays a key role to shorten milling times. PCA material may be solid or liquid. Solid PCAs may be stearic acid, polyethylene glycol (PEG) or zinc stearate whereas solid types may be ethanol or methanol.

The performance of materials is directly related to the material parameters such as particle size and homogeneity of the constituent elements. Fine grained materials are advantageous as compared to coarse grained materials. Therefore, the aim of this study is to investigate the combined effect of different amounts of reinforcement (0.5 and 1 wt.% NG) and PCA (2 and 6 wt.% methanol) on the synthesis of Al-Cu/SiC/NG composite powder.

2. EXPERIMENTAL PROCEDURES

In this study, Al and Cu powders were used as the matrix materials whereas SiC and NG as the reinforcements. Morphology of as-received powders was investigated by means of scanning electron microscopy (SEM) on a Zeiss Evo LS 10 model (Fig. 1). Table 1 lists the type, particle size and purity of as-received powders used for ball-milling experiments. Four different powder specimens were prepared with the proper amounts (wt.%) as described in Table 2. Accordingly, these prepared powder mixtures were milled for 6 hours in a two stationary planetary-type ball mill (Retsch PM 200). Milling parameters were selected as a milling speed of 400 rpm and a BPR of 5:1. Methanol was also added to powder mixtures as a PCA at the amounts of 2 and 6 wt.%. All milling parameters were listed in Table 3. To inhibit excessive heating of the grinding medium, milling experiments were paused at specified milling cycles until the room temperature attained. Particle size distribution of the powders after milling process was analyzed using a laser diffractometer (Malvern Instruments Mastersizer 2000). Besides, the interaction between average particle size (APS, (d_{50})) and milling duration was investigated using SEM.

(a)

(b)

(c)

(d)
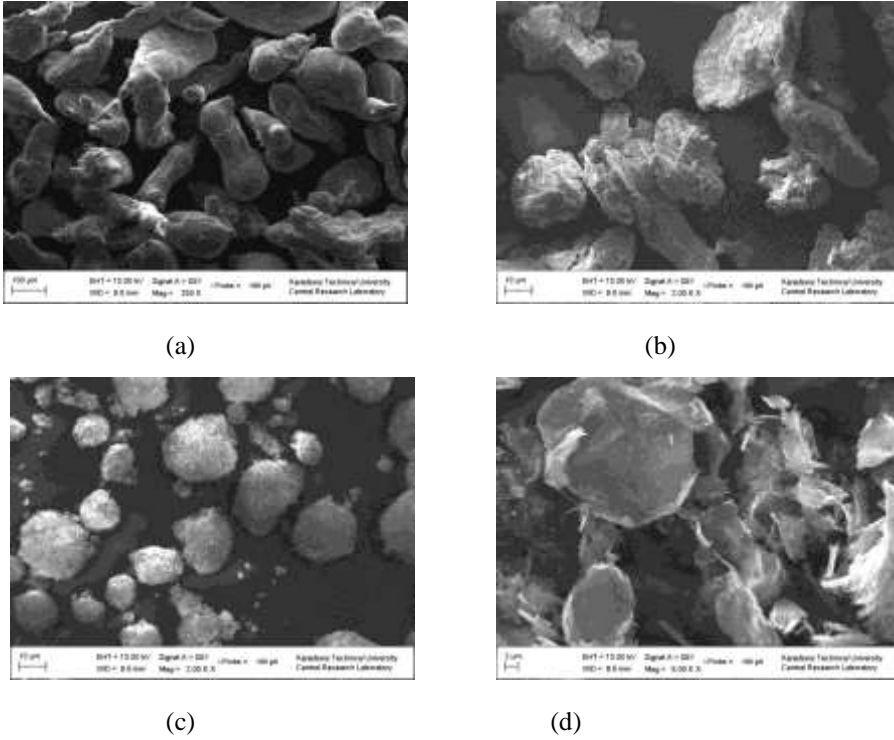
Figure 2. Morphology of as-received a) Al, b) Cu, c) SiC and d) NG powders.

Table 1. Type, particle size and purity of as-received powders used for ball-milling experiments.

Type of powder	Particle size (microns)	Purity (%)
Al	max. 125 µm	99.7%
Cu	max. 44 µm	99%
SiC	40 nm	99.9%
NG	50-100 nm	99%

Table 2. Chemical compositions of the prepared powder specimens.

No	Al (wt.%)	Cu (wt.%)	SiC (wt.%)	NG (wt.%)	PCA (methanol, wt.%)
P1	49.5%	49.5%	0.5%	0.5%	2%

P2	49.5%	49.5%	0.5%	0.5%	6%
P3	49.25%	49.25%	0.5%	1%	2%
P4	49.25%	49.25%	0.5%	1%	6%

Table 3. Milling parameters used to synthesize Al-Cu/SiC/NG composite powders.

Chemical composition	Al-Cu / SiC - 0.5NG; Al-Cu / SiC - 1NG
Type and amount of process control agent (PCA)	Methanol, 2 wt.% and 6 wt.%
Ball-to-powder weight ratio (BPR)	5:1
Milling speed	400 rpm
Grinding mode	2 min grinding, 1 min pause cycles / reverse mode active
Diameter and material of the grinding balls	10 mm, Tungsten carbide (WC)
Type of ball-mill	Retsch PM 200 / 125 ml vials
Milling duration	2, 4 and 6 hours

3. RESULTS AND DISCUSSION

It can be seen from Fig. 1 that, from a morphological point of view, Al powder particles have an irregular shape (Fig. 1a), Cu powder particles have also an irregular shape (Fig. 1b), SiC powder particles have an angular and irregular shape (Fig. 1c) and NG powder particles have a flake morphology (Fig. 1d). Table 4 lists APS values of all powder specimens obtained after Mastersizer results for each milling period. The relationship between particle size and milling time was shown in Fig. 2.

Table 4. APS values of Al-Cu/SiC/NG powder mixtures as a function of milling duration.

Chemical composition	Milling time (h) and average particle size (APS, µm)

56

	0	2	4	6
Al-Cu/SiC/0.5NG - 2% methanol	125	40.265	45.357	22.168
Al-Cu/SiC/0.5NG - 6% methanol	125	52.236	50.594	30.267
Al-Cu/SiC/1NG - 2% methanol	125	40.664	48.326	45.764
Al-Cu/SiC/1NG - 6% methanol	125	32.264	38.652	16.432
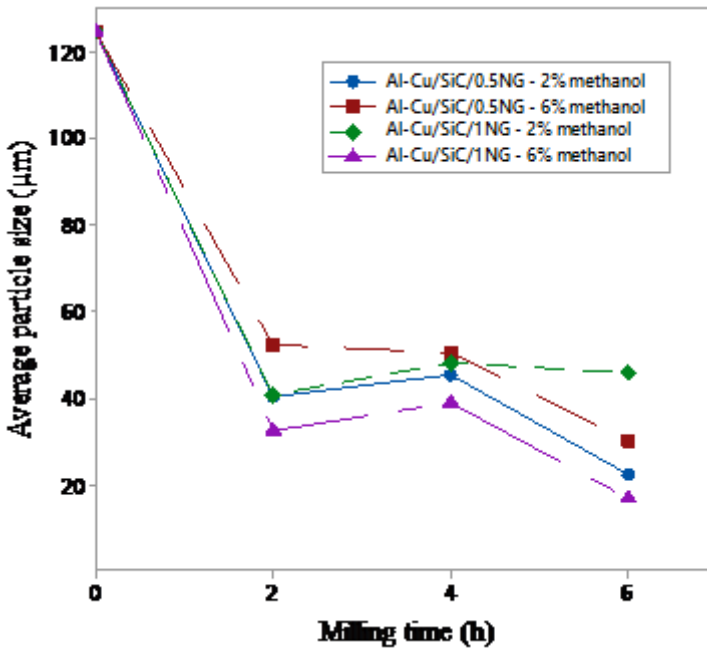
Figure 2. Particle size variation of Al-Cu/SiC/NG powder mixtures as a function of milling duration.

It should be emphasized that some fluctuations in APS occur at milling durations ranging from 2 to 4 hours. Fig. 3 shows the morphological evolution of Al-Cu/SiC/0.5NG composite powders obtained after milling for 2, 4 and 6 h with PCA contents of 2 and 6%

57

methanol. It can be seen from this figure that cold welded flaky particles dominate the milling process, especially those milled with 6% methanol (Figs. 3d and e). Powder particles tend to embed (Fig. 3f) rather than fracturing (Fig. 3c), and consequently APS values changed depending on methanol and NG additions. Higher methanol addition is negatively affected particle size reduction for lower contents of NG (0.5%). Therefore, final particle sizes are determined to be 22.168 and 30.267 μm for P1 and P2 specimens, respectively.
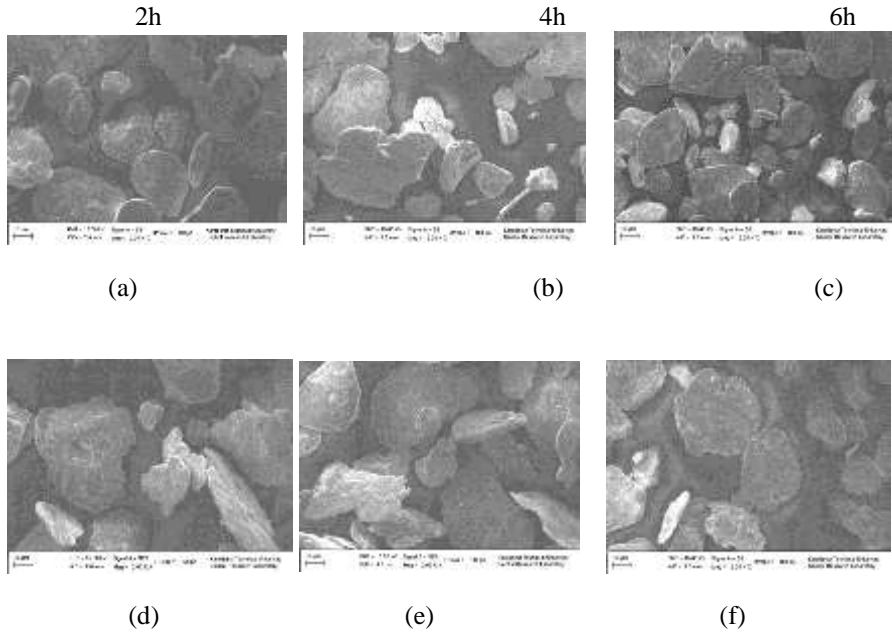
Figure 3. Morphology of the Al-Cu/SiC/0.5NG having 2% methanol after milled for a) 2 h, b) 4 h and c) 6 h; and Al-Cu/SiC/0.5NG having 6% methanol after milled for d) 2 h, e) 4 h and f) 6 h.

The morphological evolution of Al-Cu/SiC/1NG composite powders, obtained after milling for 2, 4 and 6 h with PCA contents of 2 and 6% methanol, is given in Fig. 4. Accordingly, the yield is too low for powders milled with 2% methanol additive (Figs. 4a-c). This may be attributed to the inadequate level of PCA during milling. Besides, the increment in NG content plays a key role in the reflection of this milling behavior. On the other hand, higher methanol addition is positively affected particle size reduction for 1% NG, as can be seen from Figs. 4d-f. Fracturing effect continues to take place (Figs. 4f) throughout the whole milling process. The differences in APS stem from various methanol additives may be clearly seen from Figs. 4c and f. As a result, final particle sizes are quantified to be 45.764 and 16.432 μm for P3 and P4 specimens, respectively.

58

2h   4h   6h

(a)   (b)   (c)

(d)   (e)   (f)
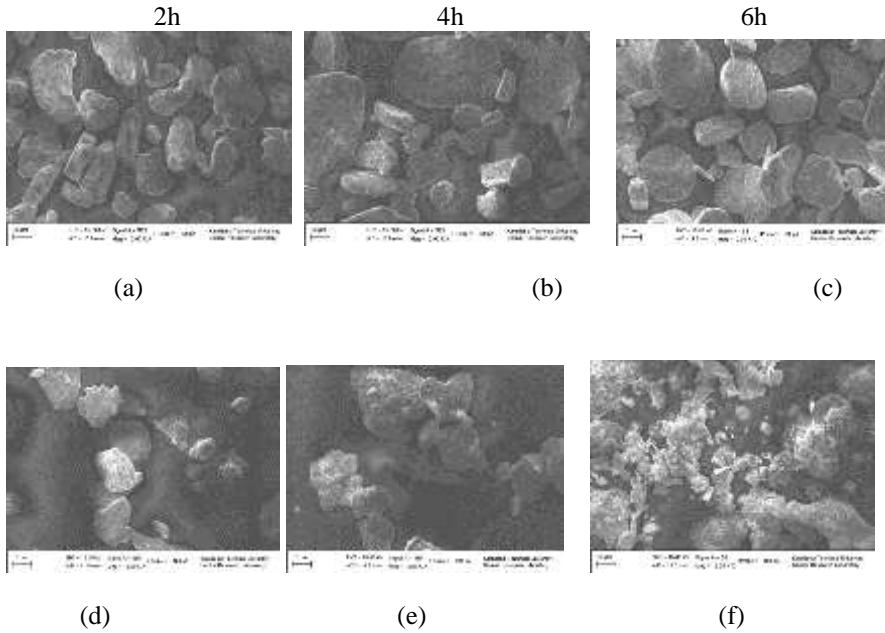
Figure 4. Morphology of the Al-Cu/SiC/1NG having 2% methanol after milled for a) 2 h, b) 4 h and c) 6 h; and Al-Cu/SiC/1NG having 6% methanol after milled for d) 2 h, e) 4 h and f) 6 h.

Taking all these factors into consideration, the optimal particle size reduction is achieved from the P4 specimen. Besides, lesser amounts of NG promote embedding of powder particles, whereas higher amounts of NG provide fracturing efficiency.

4. CONCLUSIONS

Al-Cu/SiC/NG composite powders were successfully synthesized by mechanical alloying technique. Particle size generally decreases with increasing milling duration except for the earlier periods of grinding. It was found that the increase in methanol addition significantly changed powder morphology. Higher amounts of methanol (6 wt.%) caused increment in cold welded flaky particles even after milling for 6 hours for powder specimens having 0.5% NG. On the other hand, in powder specimens having 1% NG as a reinforcement, milling efficiency is considerably improved for 6 wt.% of methanol usage comparing lower content of methanol. Therefore, lesser amounts of NG promote embedding of powder particles, whereas higher amounts of NG provide fracturing efficiency.

59

REFERENCES

[14] P. G. Slade, Electrical Contacts: Principles and Applications, CRC, Boca Raton, FL, 2014.

[15] O. Guler, T. Varol, U. Alver, S. Biyik, The wear and arc erosion behavior of novel copper based functionally graded electrical contact materials fabricated by hot pressing assisted electroless plating, Adv. Powder Technol. 32 (2021) 2873-2890. *DOI:10.1016/j.apt.2021.05.053*

[16] S. C. Shu, Q. Zhang, J. Ihde, Q. L. Yuan, W. Dai, M. L. Wu, D. Dai, K. Yang, B. Wang, C. Xue, H. B. Ma, X. Zhang, J. M. Han, X. Y. Chen, C. T. Lin, W. B. Ren, Y. F. Ma, N. Jiang, Surface modification on copper particles toward graphene reinforced copper matrix composites for electrical engineering application, J. Alloy. Compd. 891 (2022) 162058. *DOI:10.1016/j.jallcom.2021.162058*

[17] X. H. Guo, Y. B. Yang, K. X. Song, S. L. Li, F. Jiang, X. Wang, Arc erosion resistance of hybrid copper matrix composites reinforced with CNTs and micro-TiB_2 particles, J. Mater. Res. Technol. 11 (2021) 1469-1479. *DOI:10.1016/j.jmrt.2021.01.084*

[18] J. F. Li, B. Chen, H. Tang, S. Zhang, C. Li, Tribological behaviors of Cu-based composites with $NbSe_2$ and TiB_2, Dig. J. Nanomater. Bios. 12 (2017) 1205-1214.

[19] Y. X. Zhou, Y. L. Xue, K. Zhou, Failure analysis of arc ablated tungsten-copper electrical contacts, Vacuum. 164 (2019) 390-395. *DOI:10.1016/j.vacuum.2019.03.052*

[20] S. Biyik, F. Arslan, M. Aydin, Arc-erosion behavior of boric oxide-reinforced silver-based electrical contact materials produced by mechanical alloying, Journal of Electronic Materials 44 (2015) 457-466. *DOI:10.1007/s11664-014-3399-4*

[21] A. Canakci, T. Varol, H. Cuvalci, F. Erdemir, S. Ozkaya, Development and characterization of bronze-Cr-Ni composites produced by powder metallurgy, Sci. Eng. Compos. Mater. 22 (2015) 425-432.   *DOI:10.1515/secm-2013-0262*

[22] F. Erdemir, T. Varol, A. Canakci, Synthesis of SiC nanoparticles by central composite design response surface methodology directed mechanical milling, Micro Nano Lett. 15 (2020) 187-190. *DOI:10.1049/mnl.2019.0468*

[23] S. Biyik, Characterization of nanocrystalline Cu25Mo electrical contact material synthesized via ball milling, Acta Phys. Pol. A 132 (2017) 886-888. *DOI:10.12693/APhysPolA.132.886*

[24] S. A. Tunc, A. Canakci, A. H. Karabacak, M. Celebi, M. Turkmen, Effect of different PCA types on morphology, physical, thermal and mechanical properties of AA2024-

60

B4C   composites,   Powder   Technology   434   (2024)   119373. *DOI:10.1016/j.powtec.2024.119373*

[25] S. Biyik, M. Aydin, Optimization of mechanical alloying parameters of Cu25W electrical contact material, Acta Phys. Pol. A 132 (2017) 909-912. *DOI:10.12693/APhysPolA.132.909*

[26] C. Suryanarayana, A. A. Al-Joubori, Z. Wang, Nanostructured materials and nanocomposites by mechanical alloying: an overview, Met. Mater. Int. 28 (2022) 41-53. *DOI:10.1007/s12540-021-00998-5*

61

Effect of Methanol Addition on the Particle Size and Morphology of Al-Cu Composites

Serkan BIYIK[1]*, Aykut ÇANAKÇI[2], Sedat Alperen TUNÇ[2]

[1]Karadeniz Technical University, Abdullah Kanca Vocational School, Department of Machinery and Metal Technologies, Trabzon, Turkey
[2]Karadeniz Technical University, Department of Metallurgical and Materials Engineering, Trabzon, Turkey

*serkanbiyik@ktu.edu.tr

ABSTRACT

In this study, the effect of methanol addition as a process control agent (PCA) on particle size and morphology of Al-Cu matrix composites, was investigated. For this purpose, two different powder specimens were prepared. Accordingly, powder specimens having 2 and 6 wt.% of methanol additions were chosen to observe the evolution of powder characteristics such as powder morphology and particle size distribution during mechanical alloying. These different powder mixtures were then injected to a two stationary planetary-type ball-mill. Scanning electron microscopy (SEM) and laser diffraction analysis (Mastersizer) techniques were carried out to characterize both starting and milled powder morphologies and to determine powder particle sizes after certain periods of ball-milling, respectively. It was found that considerable change in powder morphology occurred depending the increase in methanol addition. Besides, excess amounts of methanol cause detrimental effect on maximal possible efficiency of milling.

KEYWORDS- *Aluminum, composites, copper, mechanical alloying, powder technology.*

1. INTRODUCTION

Powder metallurgy (PM) is a powder processing technique containing compaction of the powder mixtures, sintering of the green compacts and some secondary operations (optional) such as repressing and surface treatments [1-3]. It allows to synthesize composite materials, which find applications in a variety of industries such as aerospace, defense, automotive, electrics and electronics [4-9]. However, to further improve the physical and mechanical properties of the composites, powder preparation methods must be improved. Therefore, another technique called mechanical alloying (MA) or ball-milling is generally applied in conjunction with PM method [10-11].

62

MA is basically used to enhance sufficient compositional homogeneity with refined particle sizes owing to establishment of the balance between cold welding and fracturing. However, to shorten milling durations and to reach the desired morphologies, MA process parameters such as ball-to-powder weight ratio (BPR), milling speed, nature and amount of process control agent (PCA) and milling time must be optimized for a specific composition [12-14]. PCA is a key parameter significantly affecting final powder morphologies. Therefore, it must be used in powder mixtures, especially in compositions having ductile components. Nonetheless, excessive amounts of PCA content lead harmful effects on ball milling process. Thus, the quantity of the PCA additives must be optimized to achieve a particular grain size in a reasonable time.

In this study, the effect a liquid type of PCA called methanol on the particle size and morphology of Al-Cu composite powder was investigated.

2. EXPERIMENTAL PROCEDURES

Elemental Al (max. 125 µm) and Cu (max. 44 µm) powders were used to prepare powder mixtures. Scanning electron microscopy (SEM) pictures showing the morphology of starting powders were presented in Fig. 1. The characteristics of as-received or starting powders were given in Table 1. Morphology of as-received powders was investigated by means of SEM on a Zeiss Evo LS 10 model. Table 2 represents the weight percentages of the specimens having various amounts of methanol addition as a process control agent (PCA). A two stationary planetary-type ball mill (Retsch PM 200) was used to carry out milling experiments of the aforementioned powder specimens. Powder mixtures were grinded with a milling speed of 400 rpm and a ball-to-powder weight ratio (BPR) of 5:1. Various amounts of methanol (2 and 6 wt.%) were also added to powder mixtures as a PCA. Table 3 lists the parameters used to synthesize Al-Cu composite powders. A laser diffractometer (Malvern Instruments Mastersizer 2000) was used to detect average particle size (APS, (d_{50})) values throughout the milling experiments.

(a)   (b)
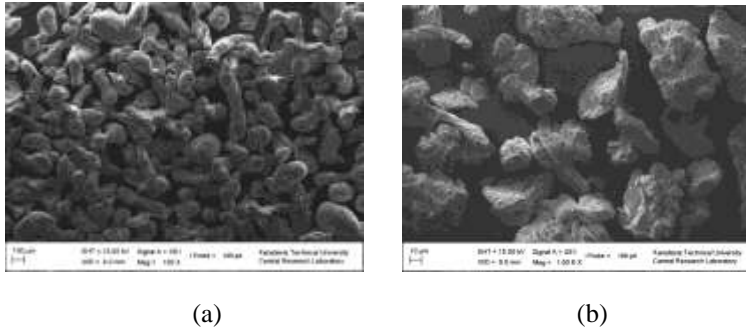
Figure 3. Morphology of as-received a) Al and b) Cu powders.

Table 1. Type, particle size and purity of as-received powders used for ball-milling experiments.

Type of powder	Particle size (microns)	Purity (%)
Al	max. 125 µm	99.7%
Cu	max. 44 µm	99%

Table 2. Chemical compositions of the prepared powder specimens.

No	Al (wt.%)	Cu (wt.%)	PCA (methanol, wt.%)
P1	50 %	50 %	2 %
P2	50 %	50 %	6 %

Table 3. Milling parameters used to synthesize Al-Cu composite powders.

Chemical composition	Al-Cu
Type and amount of process control agent (PCA)	Methanol, 2 wt.% and 6 wt.%
Ball-to-powder weight ratio (BPR)	5:1
Milling speed	400 rpm
Grinding mode	2 min grinding, 1 min pause cycles / reverse mode active
Diameter and material of the grinding balls	10 mm, Tungsten carbide (WC)
Type of ball-mill	Retsch PM 200 / 125 ml vials
Milling duration	2, 4 and 6 hours

3. RESULTS AND DISCUSSION

Considering SEM pictures shown in Fig. 1, both Al (Fig. 1a) and Cu (Fig. 1b) powder particles have an irregularly shaped. The APS results of powder samples obtained after

64

milling runs were presented in Table 4. The curves showing the relationship between particle size and milling duration were plotted and shown in Fig. 2.

Table 4. Average particle size values of Al-Cu powder mixtures as a function of milling duration.

Chemical composition	Milling time (h) and average particle size (APS, μm)			
	0	2	4	6
Al-Cu 2 % methanol	125	82.246	30.287	15.645
Al-Cu 6 % methanol	125	89.364	72.981	75.394

It can be seen from Fig. 2 that both specimens exhibit decreasing values of particle size except for the later periods of ball milling for P2 specimen. Accordingly, a slight increase in APS was detected and APS was increased from 72.981 to 75.694 microns after ball milling for 6 hours.
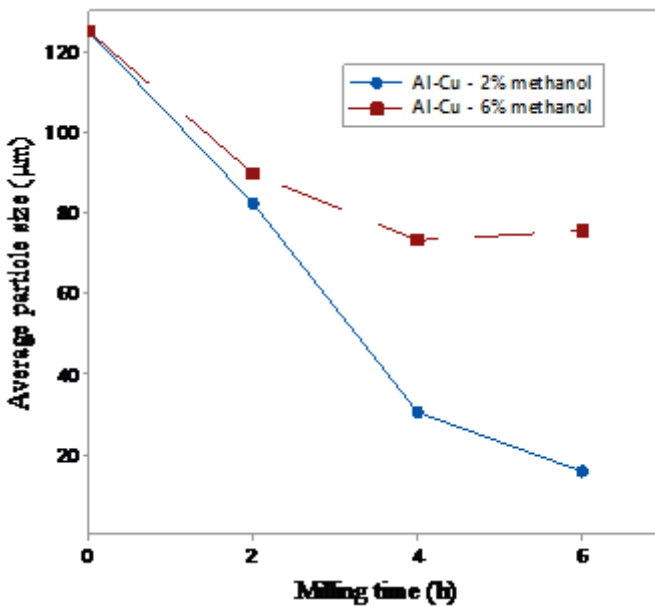
Figure 2. Particle size variation of Al-Cu powder mixtures as a function of milling duration.

65

Fig. 3 shows the morphological evolution of Al-Cu composite powders obtained after milling for 2, 4 and 6 h with PCA contents of 2 and 6% methanol. Accordingly, the effects of cold welding are apparently seen in the first 2 hours of milling (Figs. 3a and d). With further milling, the trails of fracturing are only observed in P1 specimen (Fig. b) and APS is reduced to 30.287 μm (Table 4). On the other hand, the yield in P2 specimen is much lower than that of P1 specimen. It should also be emphasized that, this trend comprises the whole milling process, and consequently APS fluctuates between 4 to 6 hours (Figs. 3e and f) for P2 specimen. On contrary, powder particles of P1 specimen get continuously fractured and are more refined in size. As a consequence of this effort, APS is reduced to 15.645 μm after completion of milling runs.

Considering powder morphologies and APS values throughout the milling process, it was found that the amount of methanol addition significantly affected the final size and shape of powder particles. Accordingly, 6 % of methanol was found detrimental to achieve a composite powder in shorter milling times. Milling duration shortens depending on the optimum amount of PCA content. Therefore, the optimum amount of methanol content was found to be 2 %.

2h   4h   6h

(a)   (b)   (c)

(d)   (e)   (f)
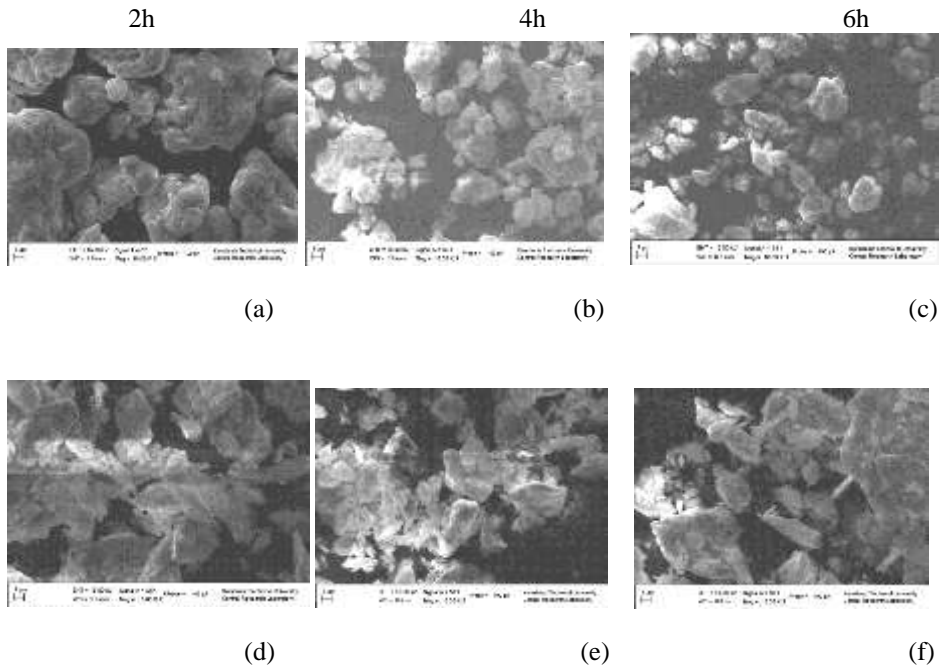
Figure 3. Morphology of the Al-Cu having 2 % methanol after milled for a) 2 h, b) 4 h and c) 6 h; and Al-Cu having 6 % methanol after milled for d) 2 h, e) 4 h and f) 6 h.

66

4. CONCLUSIONS

In this study, the synthesis of Al-Cu composite powders was carried out by ball-milling technique. Considering the SEM pictures and particle size values obtained after milling, it was found that excessive amounts of methanol content was adversely affected the grinding behavior of the powder mixtures. Cold welding was dominant phenomenon for the specimens having higher amounts of methanol (6 wt.%), even after milling for 6 hours. On the other hand, the reduction in average particle size was apparently seen in the powder mixture having 2 wt.% of methanol. Hence, the specimen having 2 wt.% of methanol was found to ensure better milling behaviour owing to the enhanced fracturing effect.

REFERENCES

[27] ASM Handbook, Vol. 7, Powder Metal Technologies and Applications, ASM International Materials Park, Ohio, 1998.

[28] S. Biyik, F. Arslan, M. Aydin, Arc-erosion behavior of boric oxide-reinforced silver-based electrical contact materials produced by mechanical alloying, Journal of Electronic Materials 44 (2015) 457-466. *DOI:10.1007/s11664-014-3399-4*

[29] A. Canakci, T. Varol, H. Cuvalci, F. Erdemir, S. Ozkaya, Development and characterization of bronze-Cr-Ni composites produced by powder metallurgy, Sci. Eng. Compos. Mater. 22 (2015) 425-432. *DOI:10.1515/secm-2013-0262*

[30] F. Erdemir, T. Varol, A. Canakci, Synthesis of SiC nanoparticles by central composite design response surface methodology directed mechanical milling, Micro Nano Lett. 15 (2020) 187-190. *DOI:10.1049/mnl.2019.0468*

[31] S. Biyik, Characterization of nanocrystalline Cu25Mo electrical contact material synthesized via ball milling, Acta Phys. Pol. A 132 (2017) 886-888. *DOI:10.12693/APhysPolA.132.886*

[32] O. Guler, M. Celebi, R. Dalmis, A. Canakci, H. Cuvalci, Novel ZA27/B$_4$C/Graphite hybrid nanocomposite-bearing materials with enhanced wear and corrosion resistance, Metall. Mater. Trans. A 51(2020) 4632-4646. *DOI:10.1007/s11661-020-05863-5*

[33] G. ALMisned, K. Günoğlu, H. V. Özkavak, D. Sen Baykal, H. Tekin, N. Karpuz, İ. Akkurt, An investigation on gamma-ray and neutron attenuation properties of multi-layered Al/B$_4$C composite, Mater. Today Commun. 36 (2023) 106813. *DOI:10.1016/j.mtcomm.2023.106813*

[34] S. X. Zhu, Y. Liu, B. H. Tian, Y. Zhang, K. X. Song, Arc erosion behavior and mechanism of Cu/Cr20 electrical contact material, Vacuum. 143 (2017) 129-137. *DOI:10.1016/j.vacuum.2017.06.002*

[35] C. Suryanarayana, A. A. Al-Joubori, Z. Wang, Nanostructured materials and nanocomposites by mechanical alloying: an overview, Met. Mater. Int. 28 (2022) 41-53.   *DOI:10.1007/s12540-021-00998-5*

[36] S. Biyik, Effect of reinforcement ratio on physical and mechanical properties of Cu-W composites synthesized by ball milling, Mater. Focus 7 (2018) 535-541. *DOI:10.1166/mat.2018.1513*

[37] S. Mimouche, M. Azzaz, Study of nanostructured Cu Al Ni alloy produced by high energy mechanical milling, J. Nano Res. 56 (2019) 109-118. *DOI:10.4028/www.scientific.net/JNanoR.56.109*

[38] S. Biyik, M. Aydin, Optimization of mechanical alloying parameters of Cu25W electrical contact material, Acta Phys. Pol. A 132 (2017) 909-912. *DOI:10.12693/APhysPolA.132.909*

[39] S. A. Tunc, A. Canakci, A. H. Karabacak, M. Celebi, M. Turkmen, Effect of different PCA types on morphology, physical, thermal and mechanical properties of AA2024-B$_4$C composites, Powder Technology 434 (2024) 119373. *DOI:10.1016/j.powtec.2024.119373*

[40] S. Biyik, Effect of polyethylene glycol on the mechanical alloying behavior of Cu-W electrical contact material, Acta Phys. Pol. A 134 (2018) 208-212. *DOI:10.12693/APhysPolA.134.208*

68

Influence of Gradual Process Control Agent Technique on the Ball-Milling Behavior of Cu Powder

Serkan BIYIK[1]*, Aykut ÇANAKÇI[2]

[1]Karadeniz Technical University, Abdullah Kanca Vocational School, Department of Machinery and Metal Technologies, Trabzon, Turkey
[2]Karadeniz Technical University, Department of Metallurgical and Materials Engineering, Trabzon, Turkey

*serkanbiyik@ktu.edu.tr

ABSTRACT

This study investigated the effect of gradual process control agent (PCA) technique on particle size and morphology of copper (Cu) powder. For this aim, copper powders having various types of PCAs were milled in a high-energy planetary type ball-mill. Two different types of PCAs, namely stearic acid and methanol were chosen to observe the evolution of powder morphology and to determine change in average particle size (APS). Scanning electron microscopy (SEM) and laser diffraction analysis (Mastersizer) techniques were used to characterize both starting and milled powders. It was found that the effect of gradual PCA remarkably changed powder morphologies. Moreover, APS values were significantly affected depending on the type of PCA.

KEYWORDS- *Ball-milling, copper, methanol, powder technology, stearic acid.*

1. INTRODUCTION

Ball-milling is a powder processing technique which involves cold-welding and fracturing of a specified powder mixture using several types of grinding vials and balls [1-4]. Among these, tungsten carbide (WC) is advantageous to grind hard and brittle materials. Apart from this, there are many parameters in ball-milling method. The most important milling parameters may be classified as type and amount of process control agent (PCA), ball-to-powder weight ratio (BPR), milling speed and milling duration [5-7]. Meanwhile, powder preparation techniques have a considerable effect on milling process.

Optimization of ball-milling parameters for a given composition is mandatory to increase milling efficiency, and thereby shortening milling times to synthesize very-fine grained materials including nanocomposite powders. Besides, the type of milling equipment also affects the milling process. Accordingly, planetary type ball-mills are favorable to synthesize composite powders due to the created centrifugal force originating from the relative rotating motion between the disc and milling vials [8-11]. Therefore, a planetary type ball-mill is selected to be used in this study to grind starting powder mixtures. In

addition, two different types of PCAs, namely stearic acid and methanol are chosen to investigate their effects on grinding behavior of copper (Cu) powder including size and shape of powder particles with increasing milling time. It is important to reduce particle sizes without sacrificing compositional homogeneity for improving physical and mechanical properties of conventional materials.

2.   EXPERIMENTAL PROCEDURES

Elemental Cu (max. 44 µm) powder was used for ball-milling experiments. Scanning electron microscopy (SEM) picture showing the morphology of starting powder was presented in Fig. 1. Table 1 lists the characteristics of as-received or starting Cu powder. Morphology of as-received powder was investigated by means of SEM on a Zeiss Evo LS 10 model. Two different powder mixtures were prepared with the appropriate amounts of PCAs (wt.%) as described in Table 2. Accordingly, these prepared powder mixtures were milled up to 15 hours in a two stationary planetary-type ball mill (Fritsch Pulverisette 7). Milling parameters were selected as a milling speed of 300 rpm and a BPR of 10:1. Stearic acid and methanol were gradually added to milling vials as PCAs at specified milling time intervals. All milling parameters were listed in Table 3. To control heat fluctuations that occur during milling, grinding process was paused at specified milling time intervals, and then was resumed to complete each milling cycle. Particle size distribution of the powders after milling process was analyzed using a laser diffractometer (Malvern Instruments Mastersizer 2000). Besides, the interaction between average particle size (APS, (d_{50})) and milling duration was investigated using SEM.

Figure 4. Morphology of as-received Cu powder.

Table 1. Type, particle size and purity of as-received powder used for ball-milling experiments.

Type of powder	Particle size (microns)	Purity (%)
Cu	max. 44 µm	99%

70

Table 2. Chemical compositions of the prepared powder specimens.

No	Cu (wt.%)	PCA (wt.%)
P1	100%	6% stearic acid
P2	100%	6% methanol

Table 3. Milling parameters used to investigate the effect of different PCAs on milling behavior of Cu powder.

Chemical composition	Cu
Type and amount of process control agent (PCA)	6% stearic acid; 6% methanol
Ball-to-powder weight ratio (BPR)	10:1
Milling speed	300 rpm
Grinding mode	2 min grinding, 1 min pause cycles / reverse mode active
Diameter and material of the grinding balls	10 mm, Tungsten carbide (WC)
Type of ball-mill	Fritsch Pulverisette 7 / 80 ml vials
Milling duration	3, 6, 9, 12 and 15 hours

3. RESULTS AND DISCUSSION

Considering SEM picture shown in Fig. 1, Cu powder particles have an irregularly shaped. Table 4 lists the APS results of powder samples as functions of PCA and milling time. Fig. 2 shows the curves reflecting the relationship between particle size and milling duration.

71

Table 4. Average particle size values of Cu powder as functions of PCA and milling duration.

Chemical composition	Milling time (h) and average particle size (APS, µm)					
	0	3	6	9	12	15
Cu - 6% stearic acid	28.895	26.846	23.829	16.905	16.373	10.746
Cu - 6% methanol	28.895	42.212	36.135	22.298	13.374	6.559
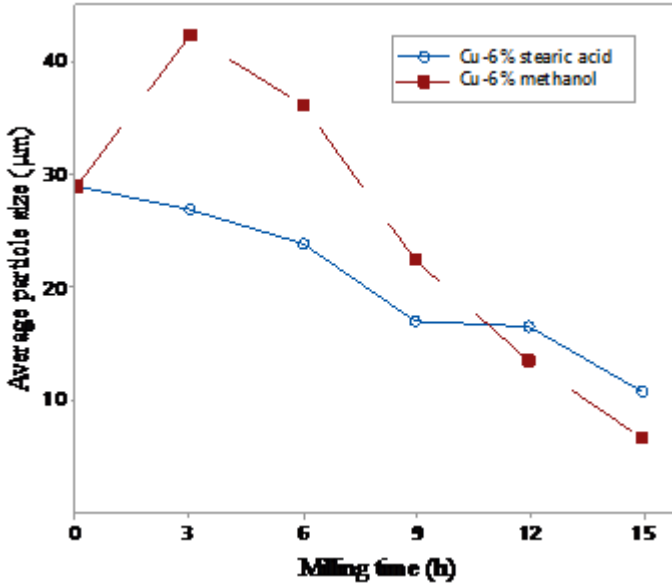
Figure 2. Particle size variation of Cu powder as functions of PCA and milling duration. It can be seen from Table 4 that, an increase in APS occurs for the specimen milled with methanol. Accordingly, APS fluctuates between 28.895 and 42.212 µm for 3 hours of milling. After this point, both curves tend to decrease with increasing milling time (Fig. 2).

Fig. 3 shows the morphological evolution of milled Cu powders obtained after grinding for 3, 6 and 9 h with PCA contents of 6% stearic acid and 6% methanol, respectively. The fluctuation and increase in APS in the earlier stages of milling may be attributed to the formation of flaky particles (Figs. 3a and d). With further milling cycles, constant decrease in APS occurs up to 9 hours of grinding (Figs. 3e and f). However, this decrease in APS is more apparent for the specimen milled with stearic acid addition (Figs. 3b and c). As a result of this effort, APS is reduced to 16.905 and 22.298 µm for stearic acid and methanol additions, respectively.

3h   6h   9h

(a)   (b)   (c)

(d)   (e)   (f)
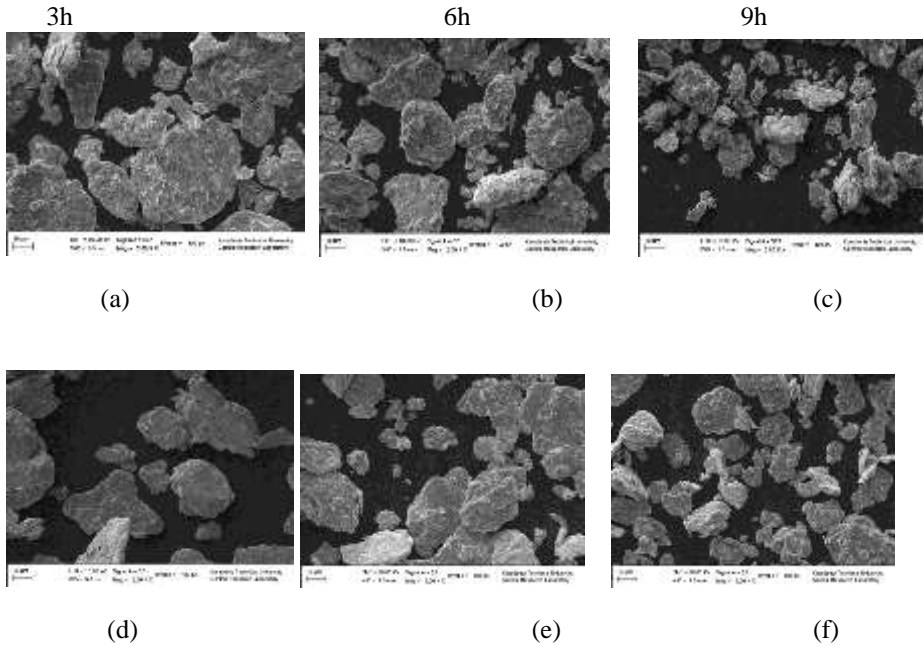
Figure 3. Morphology of the Cu having 6% stearic acid after milled for a) 3 h, b) 6 h and c) 9 h; and Cu having 6% methanol after milled for d) 3 h, e) 6 h and f) 9 h.

Fig. 4 shows the later stages of milling process for Cu powders obtained after grinding for 12 and 15 h with PCA contents of 6% stearic acid and 6% methanol, respectively. The fracturing efficiency is much higher for the powders milled with methanol (Figs. 4c and d) rather than stearic acid (Fig. 4a and b) at milling durations corresponding to 12 and 15 hours of milling. Final APS value were recorded to be 10.746 and 6.559 µm for stearic acid and methanol additions, respectively.

12h   15h

(a)   (b)

73

(c)   (d)
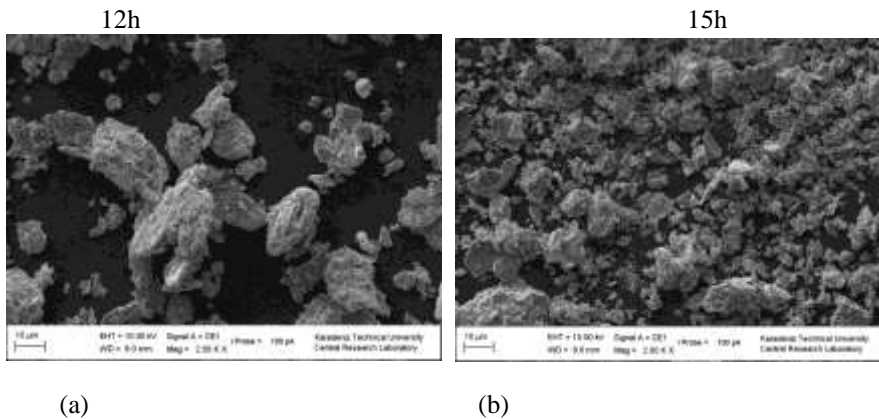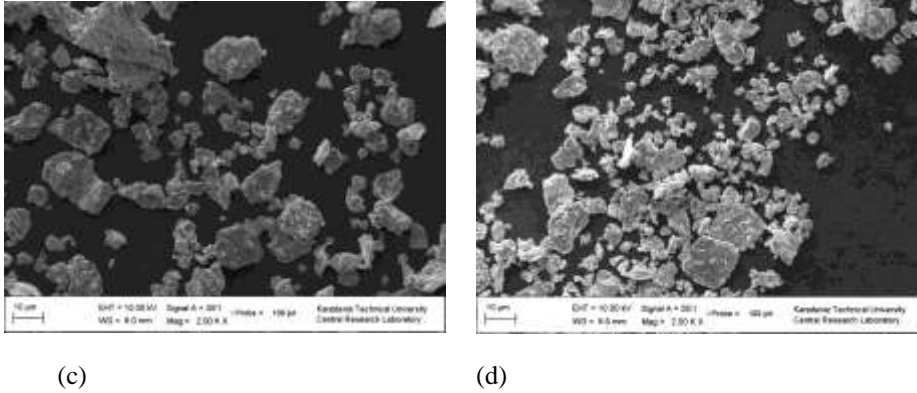
Figure 4. Morphology of the Cu having 6% stearic acid after milled for a) 12 h and b) 15 h; and Cu having 6% methanol after milled for c) 12 h and d) 15 h.

Considering SEM pictures and particle size values obtained after milling, it was found that 6% of methanol content was determined to be optimum condition. The effect of gradual process control addition was found beneficial to reduce particle size values of powders in a reasonable milling time.

4. CONCLUSIONS

In this study, the effects of different types of PCAs were comparatively studied to mill copper (Cu) powder. For this aim, stearic acid and methanol were gradually added to milling vials at specified milling time intervals. Accordingly, stearic acid was exhibited better milling behavior as compared to methanol for milling durations up to 9 hours. Particle size values were shown decreasing trends for both composition, although some fluctuations were observed at first 3 hours of milling process for the specimen milled with methanol addition. On the other hand, methanol addition was found beneficial for milling durations corresponding to 9 to 15 hours. Accordingly, average particles size values at the end of milling cycles were recorded to be 10.746 and 6.559 µm for stearic acid and methanol usages, respectively. Considering SEM pictures and particle size values obtained after milling, it was found that 6% of methanol content was determined to be optimum condition.

REFERENCES

[41] C. Suryanarayana, A. A. Al-Joubori, Z. Wang, Nanostructured materials and nanocomposites by mechanical alloying: an overview, Met. Mater. Int. 28 (2022) 41-53. https://doi.org/10.1007/s12540-021-00998-5

[42] S. Biyik, F. Arslan, M. Aydin, Arc-erosion behavior of boric oxide-reinforced silver-based electrical contact materials produced by mechanical alloying, Journal of Electronic Materials 44 (2015) 457-466. *DOI:10.1007/s11664-014-3399-4*

[43] A. Canakci, T. Varol, H. Cuvalci, F. Erdemir, S. Ozkaya, Development and characterization of bronze-Cr-Ni composites produced by powder metallurgy, Sci. Eng. Compos. Mater. 22 (2015) 425-432. https://doi.org/10.1515/secm-2013-0262

[44] F. Erdemir, T. Varol, A. Canakci, Synthesis of SiC nanoparticles by central composite design response surface methodology directed mechanical milling, Micro Nano Lett. 15 (2020) 187-190. https://doi.org/10.1049/mnl.2019.0468

[45] S. Biyik, M. Aydin, Optimization of mechanical alloying parameters of Cu25W electrical contact material, Acta Phys. Pol. A 132 (2017) 909-912. https://doi.org/10.12693/APhysPolA.132.909

[46] S. A. Tunc, A. Canakci, A. H. Karabacak, M. Celebi, M. Turkmen, Effect of different PCA types on morphology, physical, thermal and mechanical properties of AA2024-B4C composites, Powder Technology 434 (2024) 119373. DOI:10.1016/j.powtec.2024.119373.

[47] S. Biyik, Effect of polyethylene glycol on the mechanical alloying behavior of Cu-W electrical contact material, Acta Phys. Pol. A 134 (2018) 208-212. https://doi.org/10.12693/APhysPolA.134.208

[48] S. Biyik, Characterization of nanocrystalline Cu25Mo electrical contact material synthesized via ball milling, Acta Phys. Pol. A 132 (2017) 886-888. https://doi.org/10.12693/APhysPolA.132.886

[49] S. Biyik, Effect of reinforcement ratio on physical and mechanical properties of Cu-W composites synthesized by ball milling, Mater. Focus 7 (2018) 535-541. https://doi.org/10.1166/mat.2018.1513

[50] O. Guler, M. Celebi, R. Dalmis, A. Canakci, H. Cuvalci, Novel ZA27/B4C/Graphite hybrid nanocomposite-bearing materials with enhanced wear and corrosion resistance, Metall. Mater. Trans. A 51(2020) 4632-4646. https://doi.org/10.1007/s11661-020-05863-5

[51] S. Mimouche, M. Azzaz, Study of nanostructured Cu Al Ni alloy produced by high energy mechanical milling, J. Nano Res. 56 (2019) 109-118. https://doi.org/10.4028/www.scientific.net/JNanoR.56.109

75

Evaluation of Effective Electron Density in Aluminum-Enhanced Glass Compositions

Kadir GÜNOĞLU[1*] Osman GÜNAY[2], Fatih Ekrem ONAT [2] ,İskender AKKURT[3]

[1]Isparta University of Applied Sciences, Technical Vocational School, Isparta-TURKEY*

[2]Yıldız Technical University, Faculty of Electrical and Electronics Engineering, Department of Biomedical Engineering, Istanbul, TURKEY
[3]Suleyman Demirel University, Science Faculty,Physics Department, Isparta-TURKEY

ABSTRACT

The utilization of glass in environments exposed to radiation, such as medical imaging facilities and nuclear power plants, serves a fundamental purpose in safeguarding human health and operational integrity. These environments emit ionizing radiation, which poses significant health risks to individuals and equipment if not properly managed. Radiation shielding glasses are specifically engineered to mitigate these risks by incorporating materials that effectively absorb or deflect ionizing radiation. These glasses are manufactured using advanced techniques that optimize their ability to attenuate radiation while preserving optical clarity, crucial for accurate visual monitoring and efficient equipment operation within high-risk radiation environments. By reducing radiation exposure, these glasses play a crucial role in maintaining a safe working environment and minimizing health hazards associated with prolonged exposure to ionizing radiation. The development of radiation shielding glasses involves a synthesis of materials science, engineering, and optics. Specialized glass formulations and coatings are tailored to enhance radiation attenuation properties without compromising transparency or structural integrity. Advanced manufacturing processes such as ion implantation and chemical vapor deposition are employed to fortify the glass against radiation-induced damage and ensure long-term performance in demanding operational conditions. These glasses are indispensable for protecting personnel and critical equipment in industries where radiation exposure is a constant concern. Through continuous innovation and stringent quality control measures, radiation shielding glasses uphold safety standards and mitigate health risks associated with ionizing radiation in diverse industrial and medical applications. In this research, the effective electron density of aluminum-enhanced glass compositions has been evaluated across various energy levels.

Keywords: Glass, Electron Density, Aluminum

✉ *Corresponding Author Email   : kadirgunoglu@isparta.edu.tr*

1   INTRODUCTION

The implementation of specialized glass in radiation-prone environments, such as medical imaging centers and nuclear power facilities, is essential for ensuring both human safety and operational stability. Ionizing radiation emitted in these settings poses significant risks, including biological harm to individuals and potential degradation of sensitive equipment. To address these challenges, radiation shielding glasses are developed with materials that can efficiently absorb or scatter ionizing radiation, thereby reducing exposure levels.

These shielding glasses are produced using state-of-the-art manufacturing technologies that enhance their radiation attenuation capabilities while retaining high optical transparency. This transparency is critical for enabling precise visual observation and the accurate operation of equipment within radiation-intensive environments. By minimizing radiation penetration, these glasses contribute to creating safer workspaces and reducing the long-term health effects associated with extended radiation exposure.

The design and development of radiation shielding glasses involve a multidisciplinary approach, incorporating principles from materials science, optics, and engineering. Unique glass compositions, often augmented with specialized coatings and heavy metal oxides, are formulated to achieve optimal shielding performance. Advanced fabrication methods, such as ion implantation and vapor-based deposition techniques, are utilized to enhance the glass's resistance to radiation damage, ensuring durability and reliability under extreme conditions. Various parameters associated with radiation shielding have been examined extensively in the literatüre [1-8].

This study evaluates the effective electron density of aluminum-enhanced glass systems across a range of photon energy levels, aiming to better understand their radiation attenuation properties and potential applications in shielding technologies.

2   MATERIALS AND METHODS

The aluminum-enhanced glass samples investigated in this study were prepared by integrating varying concentrations of aluminum oxide (Al_2O_3) into a borate glass matrix.

To evaluate the effective electron density of the aluminum-enhanced glass systems, simulations were performed across a range of photon energy levels using the phy-X/PSD[9] software. This program is widely recognized for its accuracy in calculating radiation interaction parameters for shielding materials. The chemical composition, density, and thickness of the glass samples were entered into the simulation software. Photon energies ranging from 0.01 MeV to 10 MeV were selected to analyze the glass performance under varying radiation conditions. The software provided key parameter,is effective electron density (Neff)

77

icsusat.net/icsusat-2024   *icsusat2024@gmail.com*

3   RESULTS

The effective electron density as a function of photon energy is presented in Table 1. The effective electron density exhibits significant variations with energy. Starting from 1 keV, it shows an increase, followed by a slight decrease around 50 keV, and reaches its maximum value near 100 keV. Beyond approximately 100 keV, it undergoes a sharp decline, reaching its minimum level around 1 MeV. After 1 MeV, the effective electron density begins to rise again, stabilizing at a constant value near 100 MeV. Beyond 100 MeV, it remains stable. Figure 1 illustrates the variation of effective electron density over time.

Table 1. Effective Electron Density

Energy (MeV)	Neff (electrons/g)
1,00E-03	3,99E+23
1,50E-03	4,62E+23
2,00E-03	4,82E+23
3,00E-03	5,17E+23
4,00E-03	5,44E+23
5,00E-03	5,71E+23
6,00E-03	1,04E+24
8,00E-03	1,09E+24
4,00E-02	1,43E+24
5,00E-02	1,34E+24
6,00E-02	1,23E+24
8,00E-02	1,00E+24
1,00E-01	8,13E+23
1,50E-01	5,39E+23
2,00E-01	4,23E+23

78

3,00E-01	3,40E+23
4,00E+00	3,05E+23
1,20E+01	3,70E+23
1,30E+01	3,76E+23
1,40E+01	3,82E+23
1,50E+01	3,87E+23
1,60E+01	3,92E+23
1,80E+01	4,01E+23
1,00E+02	4,83E+23
1,50E+02	4,88E+23
2,00E+02	4,91E+23
3,00E+02	4,92E+23
4,00E+02	4,93E+23
5,00E+02	4,93E+23
6,00E+02	4,93E+23
8,00E+02	4,93E+23
1,00E+03	4,93E+23
8,00E+03	4,92E+23
1,00E+04	4,92E+23
1,00E+05	4,91E+23
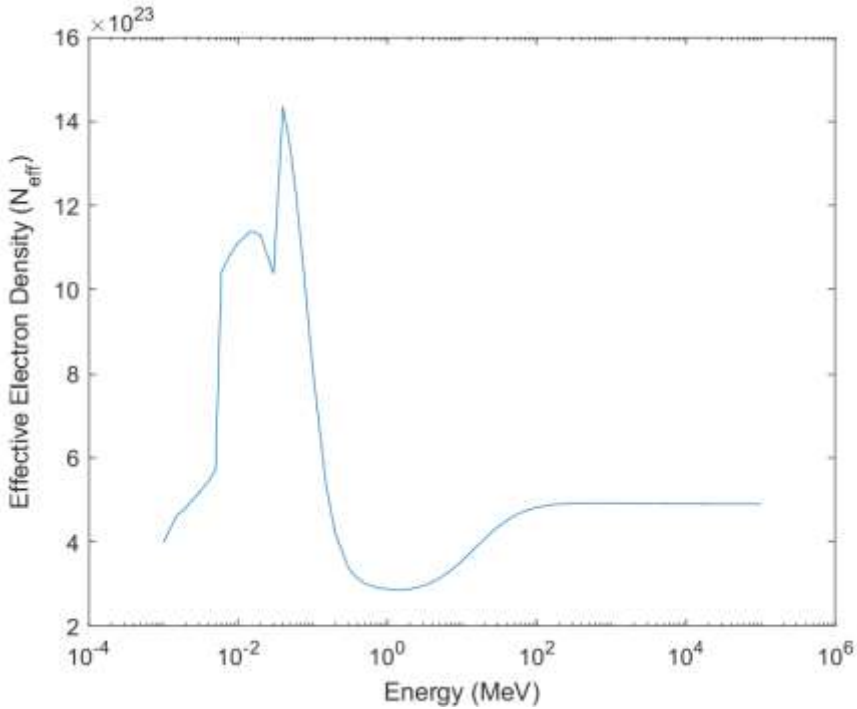
Figure 1. The variation of effective electron density with respect to energy.

4   CONSLUSION

This study examined the effective electron density of aluminum-enhanced glass systems across a range of photon energy levels. The results indicate that the effective electron density increases with energy up to 100 keV, after which it decreases and reaches its minimum around 1 MeV. Beyond this point, it starts to rise again and stabilizes near 100 MeV. These findings provide valuable insights into the radiation attenuation properties of aluminum-enhanced glasses, demonstrating their potential effectiveness in shielding applications. The stable electron density at higher photon energies suggests that these materials could offer reliable performance in radiation-prone environments, such as medical imaging centers and nuclear facilities.

REFERENCES

[1] A.A. Alfuraih Simulation of Gamma-Ray Transmission Buildup Factors forStratified Spherical Layers Dose Response 20 1 2022 Feb 17 1559325582110686251 0.1177/15593258211070911.

[2] H.O. Tekin, Ghada ALMisned, Y.S. Rammah, Emad M. Ahmed, Fatema T. Ali, Duygu Sen Baykal, Wiam Elshami, Hesham M.H. Zakaly, Shams A.M. Issa, G. Kilic,Antoaneta Ene, Transmission factors, mechanical, and gamma ray attenuationproperties of barium-phosphate-tungsten glasses: Incorporation impact of WO3,Optik, Volume 267, 2022, 169643. doi: 10.1016/j.ijleo.2022.169643.

[3] Al Huwayz M, Albarkaty KS, Alrowaili ZA, Olarinoye IO, Elqahtani ZM, Al-Buriahi M S (2023) Gamma, neutron, and charged particle shielding performance of ABKT glass system. J. Radiat, Res. Appl. Sci. 16:100742

[4] H. O. Tekin, Fatema T. Ali, Ghada Almisned, Gulfem Susoy, Shams A. M. Issa,Antoaneta Ene, Wiam Elshami, Hesham M. H. Zakaly, Kai Xu, Multiple Assessmentson the Gamma-Ray Protection Properties of Niobium-Doped Borotellurite Glasses:A Wide Range Investigation Using Monte Carlo Simulations, Science and Technologyof Nuclear Installations, 2022. 1-17, (2022).

[5] Shams A. M. Issa, Hesham M. H. Zakaly, Ali Badawi, Reda Elsaman, H. O. Tekin, A.A. Showahy, P. S. Anjana, Devika R. Nath, N. Gopakumar, Yasser B. Saddeek, Anexperimental investigation on structural, mechanical and physical properties ofStrontium–Silicon Borate glass system through Bismuth-Aluminum substitution,Optical Materials, 117. 111124, (2021).

[6] Park, P.E., Park, J.M., Kang, J.E., Cho, J.H., Cho, S.J., Kim, J.H., Sim, W.S., Kim, Y.C., 2012. Radiation safety and education in the applicants of the final test for the expert of pain medicine. Kor. J. Pain 25, 16–21.

[7] Sakar, E., Ozpolat, O.F., Alim, B., Sayyed, M.I., Kurudirek, M., 2020. Phy-X/PSD: development of a user-friendly online software for calculation of parameters relevant to radiation shielding and dosimetry. Radiat. Phys. Chem. 166, 108496.

[8] Sariyer, D., 2020. Investigation of neutron attenuation through FeB, Fe2B and concrete. Acta Phys. Pol., A 137, 539–541.[9]Akkurt, I., Malidarre, R.B., 2021. Gamma photon-neutron attenuation parameters of marble concrete by MCNPX code. Radiat. Eff. Defect 176 (9–10), 906–918

[9] Şakar, E., Özpolat, Ö. F., Alım, B., Sayyed, M. I., & Kurudirek, M. (2020). Phy-X/PSD: development of a user friendly online software for calculation of parameters relevant to radiation shielding and dosimetry. Radiation Physics and Chemistry, 166, 108496.

Exploring the effective conductivity (Ceff) in a Borate Glass System Doped with Sodium

İskender AKKURT[1] , Kadir GÜNOĞLU[2] Osman GÜNAY[3],

[1]Suleyman Demirel University, Science Faculty,Physics Department, Isparta-TURKEY
[2]Isparta University of Applied Sciences, Technical Vocational School, Isparta-TURKEY*
[3]Yıldız Technical University, Faculty of Electrical and Electronics Engineering, Department of Biomedical Engineering, Istanbul, TURKEY

✉ *Corresponding Author Email　　: iskender.akkurt@sdu.edu.tr*

ABSTRACT

In facilities exposed to high-energy radiation sources like X-rays and gamma rays, such as nuclear reactors and medical imaging centers, the use of radiation shielding glasses is indispensable for minimizing health risks and ensuring operational safety. These glasses are designed to effectively attenuate ionizing radiation, which can otherwise pose significant dangers to human health and sensitive electronic equipment. The composition of radiation shielding glasses typically involves specialized materials like leaded glass or borosilicate compositions infused with heavy metals, selected for their high radiation absorption capabilities. These materials are carefully integrated into glass formulations through advanced manufacturing processes aimed at optimizing radiation shielding performance. The deployment of radiation shielding glasses involves rigorous testing and validation to ensure their effectiveness in real-world radiation environments. These glasses are engineered to maintain optical clarity and mechanical strength while effectively reducing the penetration of ionizing radiation. Their use is crucial for protecting personnel from radiation exposure and safeguarding critical infrastructure against potential damage. By implementing radiation shielding glasses, industries adhere to strict safety regulations and standards, promoting safe operational practices that prioritize both human welfare and environmental stewardship. In this research, the effective electrical conductivity (Ceff) of a borate glass system doped with sodium has been investigated across various energy levels.

Keywords: Glass, effective conductivity, Sodium

1. INTRODUCTION

In environments where high-energy radiation sources, such as X-rays and gamma rays, are prevalent—including nuclear reactors and medical imaging facilities—the use of radiation shielding glasses is critical for minimizing health risks and ensuring operational safety. Ionizing radiation, if not adequately controlled, can cause serious

biological harm to individuals and degrade sensitive electronic equipment. To address this, radiation shielding glasses are specifically designed to attenuate ionizing radiation effectively, reducing its penetration while maintaining essential optical clarity and mechanical strength.

Radiation shielding glasses are typically composed of specialized materials, such as leaded glass or borosilicate glass systems infused with heavy metals, which are known for their superior radiation absorption properties. These materials are incorporated into glass formulations using advanced manufacturing techniques to optimize their performance under varying radiation intensities. Furthermore, extensive testing and validation procedures are conducted to ensure these glasses meet the rigorous standards required for real-world radiation shielding applications. Different parameters relevant to radiation shielding have been studied across multiple research Works[1-8].

The adoption of radiation shielding glasses is vital for protecting personnel and critical infrastructure from the harmful effects of ionizing radiation. Their use not only supports adherence to strict safety regulations but also promotes sustainable operational practices that prioritize human health and environmental protection. In this study, the effective electrical conductivity (Ceff) of a borate glass system doped with sodium has been evaluated across various photon energy levels to analyze its potential performance in radiation shielding applications.

2.   MATERIALS AND METHODS

The borate glass samples analyzed in this study were prepared by incorporating sodium oxide (Na_2O) into a boron oxide (B_2O_3)-based glass matrix. The samples were synthesized using the conventional melt-quenching technique.

To evaluate the effective electrical conductivity (Ceff) of the sodium-doped borate glass system, simulations and experimental measurements were performed across a range of photon energy levels. The simulation data were generated using the phy-X/PSD[9] software, a reliable tool for analyzing photon interactions and radiation shielding parameters. Input parameters, such as the glass composition, density, and photon energy range, were provided to the software to calculate the effective electrical conductivity values. The energy range analyzed extended from 0.01 MeV to 10 MeV to cover low, medium, and high photon energies relevant to radiation shielding applications.

3.   RESULTS

The changes in effective conductivity over time are presented in Table 1. Starting at 8.8×10^8 at 1 keV, the effective conductivity increases, reaching 2.49×10^9 at 20 keV. It then decreases to 2.29×10^9 at 30 MeV. After this, it begins to increase again, reaching its maximum value of 3.16×10^9 at 40 keV. Following 40 keV, a rapid decrease is observed, reaching its minimum value at 1.5 MeV. After 1.5 MeV, the effective conductivity begins to rise again, gradually increasing until 200 MeV, after which no significant changes occur.

83

Table 1. Effective Conductivity

Energy (MeV)	Ceff (S/m)
1,00E-03	8,80E+08
1,50E-03	1,02E+09
2,00E-03	1,06E+09
3,00E-03	1,14E+09
4,00E-03	1,20E+09
5,00E-03	1,26E+09
6,00E-03	2,30E+09
8,00E-03	2,39E+09
1,00E-02	2,45E+09
1,50E-02	2,51E+09
2,00E-02	2,49E+09
3,00E-02	2,29E+09
4,00E-02	3,16E+09
5,00E-02	2,95E+09
6,00E-02	2,70E+09
8,00E-02	2,21E+09
1,00E-01	1,79E+09
1,50E-01	1,19E+09
2,00E-01	9,31E+08
3,00E-01	7,50E+08
4,00E-01	6,91E+08
5,00E-01	6,66E+08
6,00E-01	6,53E+08

84

8,00E-01	6,41E+08
1,00E+00	6,35E+08
1,50E+00	6,32E+08
2,00E+00	6,36E+08
3,00E+00	6,53E+08
4,00E+00	6,73E+08
5,00E+00	6,93E+08
6,00E+00	7,13E+08
7,00E+00	7,33E+08
8,00E+00	7,51E+08
9,00E+00	7,68E+08
1,00E+01	7,85E+08
1,10E+01	8,00E+08
1,20E+01	8,15E+08
1,30E+01	8,28E+08
1,40E+01	8,41E+08
1,50E+01	8,53E+08
1,60E+01	8,63E+08
1,80E+01	8,83E+08
2,00E+01	9,00E+08
2,20E+01	9,15E+08
2,40E+01	9,29E+08
2,60E+01	9,41E+08
2,80E+01	9,51E+08
3,00E+01	9,60E+08
4,00E+01	9,96E+08

5,00E+01	1,02E+09
6,00E+01	1,03E+09
8,00E+01	1,05E+09
1,00E+02	1,06E+09
1,50E+02	1,08E+09
2,00E+02	1,08E+09
3,00E+02	1,09E+09
4,00E+02	1,09E+09
5,00E+02	1,09E+09
6,00E+02	1,09E+09
8,00E+02	1,09E+09
1,00E+03	1,09E+09
1,50E+03	1,09E+09
2,00E+03	1,09E+09
3,00E+03	1,08E+09
4,00E+03	1,08E+09
5,00E+03	1,08E+09
6,00E+03	1,08E+09
8,00E+03	1,08E+09
1,00E+04	1,08E+09
1,50E+04	1,08E+09
2,00E+04	1,08E+09
3,00E+04	1,08E+09
4,00E+04	1,08E+09
5,00E+04	1,08E+09
6,00E+04	1,08E+09

| 8,00E+04 | 1,08E+09 |
| 1,00E+05 | 1,08E+09 |

4. CONSLUSION

The study of the effective electrical conductivity (Ceff) of sodium-doped borate glass systems reveals significant variations across a range of photon energy levels, which are crucial for their performance in radiation shielding applications. Initially, the effective conductivity increases with photon energy, reaching a peak at 40 keV, before exhibiting a rapid decrease and stabilizing at higher photon energies (above 1.5 MeV). This behavior suggests that the sodium-doped borate glass system is more effective in shielding at intermediate photon energy levels, with a relatively constant performance observed at energies exceeding 200 MeV.

The ability of these glasses to attenuate ionizing radiation efficiently, coupled with their conductivity properties, underscores their potential for use in environments where radiation exposure is a concern. These findings contribute to the understanding of the material's behavior in radiation shielding applications, emphasizing the importance of selecting appropriate materials based on energy-specific requirements to enhance safety and operational efficiency in radiation-prone environments.

REFERENCES

[1] ALMisned G, Bilal G, Baykal DS, Ali FT, Kilic G, Tekin HO (2023) Bismuth (III) Oxide and Boron (III) Oxide Substitution in Bismuth-Boro-Zinc Glasses: A Focusing in Nuclear Radiation Shielding Properties. Optik 272:170214

[2] Juhim F, Chee FP, Awang A, Duinong M, Rasmidi R, Rumaling MI (2022) Radiation Shielding Properties of Tellurite and Silicate Glass. ECS J. Solid State Sci. Techol. 11:076006

[3] El-Sayed, A.W., Fusco, M.A., Bourham, M.A., 2016. Gamma-ray mass attenuation coefficient and half value layer factor of some oxide glass shielding materials. Ann. Nucl. Energy 96, 26–30.

[4] Elazaka, A.I., Zakaly, H.M., Issa, S.A.M., Rashad, M., Tekin, H.O., Saudi, H.A., Gillette, H., Erguzel, T.T., Mostafa, A.G., 2021. New approach to removal of hazardous Bypass Cement Dust (BCD) from the environment: 20Na2O-20BaCl2-(60-x)B2O3-(x) BCD glass system and optical, mechanical, structural and nuclear radiation shielding competences. J. Hazard Mater. 403, 123738.

87

[5]Singh, G., Gupta, M.K., Dhaliwal, A.S., Kahlon, K.S., 2015. Measurement ofattenuation coefficient, effective atomic number and electron density of oxides of lanthanides by using simplified ATM-method. J. Alloys Compd. 619, 356–360.

[6]Tekin, H.O., Cavli, B., Altunsoy Guclu, E.E., Manici, T., Ozturk, C., Karakas, H.M., 2018. An investigation on radiation protection and shielding properties of 16 slice computed tomography (CT) facilities. Int. J. Comput. Exp. Sci. Eng. 4, 37–40.

[7] Huda F. Khalil, Roya Boudaghi Malidarreh, Mahmoud T. Alabsy, Ahmed M. Hassan, Ahmed M. El-Khatib, Shams A. M. Issa, Hesham M. H. Zakaly, Structural, Morphological, and γ-ray Attenuation properties of m-type hexaferrite BaFe12O19 doped with V2O5, Ce2O3 and Bi2O3 for Radiation Shielding applications, Ceramics International, (2024).

[8] ALMisned, G., Elshami, W., Issa, S.A.M., Susoy, G., Zakaly, H.M.H., Algetha mi, M.,Rammah, Y.S., Ene, A., Al-Ghamdi, S.A., Ibraheem, A.A., Tekin, H.O. Enhancement of gamma-ray shielding properties in cobalt-doped heavy metal borate glasses: the role of lanthanum oxide reinforcement. Materials 2021;14 (2021):7703. https://doi.org/10.3390/MA14247703. Page 7703 14.

[9] Şakar, E., Özpolat, Ö. F., Alım, B., Sayyed, M. I., & Kurudirek, M. (2020). Phy-X/PSD: development of a user friendly online software for calculation of parameters relevant to radiation shielding and dosimetry. Radiation Physics and Chemistry, 166, 108496.

The Impact of the AI Revolution on the Future Labor Market: A Panel Data Analysis of Selected Developed Countries

Bilgehan Yildiz[1]*, Murat Ustaoglu[2]

[1] *University of San Francisco/School of Management, San Francisco, USA*
[2] *Istanbul University/Faculty of Economics, Istanbul University, USA*

*byildiz@usfca.edu

ABSTRACT

This study explores the potential consequences of the AI revolution on the labor market, emphasizing its potential to reshape the labor market and the employment dynamics. Historical evidence demonstrates how technical advancements have affected the job market significantly. Over time, there have been profound transformations in the labor market, spanning from the industrial revolutions to the ongoing digital technology revolution. The study begins by elucidating the concept of AI, its historical context, classifications, and potential applications. Employing a panel data analysis approach, the study evaluates the correlation between AI patent applications and unemployment rates, revealing a statistically significant relationship that suggests AI adoption could initially decrease unemployment in the short term. However, the long-term effects of AI on employment are still uncertain and require proactive measures to address skill mismatches and socio-economic inequalities, as noted in numerous studies in the literature. Accordingly, the study recommends policy interventions prioritizing education and workforce development to facilitate a seamless transition to an AI-driven economy.

Keywords – Artificial Intelligence, Unemployment, Panel Data Analysis.

1. INTRODUCTION

The capacity to utilize and adjust to technological advancements at an institutional level is equally crucial as fundamental factors like education level, legislation, pay level, and market laws in influencing productivity in the labor market. Artificial intelligence applications (AI), which are now emblematic of technological progress, epitomize this transformation process. Stephen Hawking sheds light on the impact of AI, tracing its origins back to the 1950s when research began on algorithms imitating human intelligence, and anticipate its imminent impact on human life: "Artificial Intelligence will be the greatest revolution in the history of mankind." He summarizes it well with the words "Unfortunately, it will also be the last, unless we learn how to avoid it." Various studies in the literature demonstrate that the extent of active utilization of AI in the labor market has a direct impact on productivity and overall production. Although there are few encouraging examples in the labor market, negative prospects for the near future largely

89

shape the current agenda. The illustration on the cover of the New Yorker magazine in October 2017, depicting humanoid robots giving alms to a beggar while heading to work, effectively captures the issues that occupy human thoughts on this matter. The magazine's latest issue features an in-depth investigation of the interaction between human workers and modern industrial machinery. The article scrutinizes the repercussions of using modern automation technologies in production and assesses the potential effects of technological advancements on the labor market [8]. These evaluations, conducted t prior to the rise of AI as a technological revolution, express concerns about how technology advancements will affect the job market in the coming years.

This study examines the correlation between artificial intelligence (AI) and the job market in eight developed countries: the United Kingdom, the United States, Canada, France, Germany, Israel, Japan, and the Netherlands. Despite being relatively recent, AI revolution technologies are impacting all aspects of economic life. The literature extensively employs patent applications as a means to monitor technological advancements, with numerous examples specifically focused on AI. This research analyzes the number of patents associated with the AI revolution at a country level and examines its impact on the labor market using the unemployment rate. The study aims to assess the effects of AI advancement on employment trends through panel data analysis, therefore clarify how AI advancement impacts labor market trends in developed economies. The impacts of AI technology on new job prospects, labor demographics, and economic stability in industrialized nations can be examined.

Today, AI systems outperform human capabilities in certain economically significant occupations. These include high-paying professions like radiologists, as well as low-paying occupations such as farm workers. In modern nations, rising inequality represents a significant social and political concern. The rapid advancement of AI is expected to render several occupational categories obsolete, spanning from farm labor to professionals such as attorneys and doctors. It is anticipated that economic disparity will exacerbate in this scenario [16]. Technological advancements impact the workforce in terms of both skill level and compensation. Skill-Biased Technical Change refers to a shift in production technology that favors skilled labor over unskilled labor, leading to a higher demand for skilled workers due to their increased productivity and quality compared to unskilled workers [15]. AI's effect on salaries exacerbates the increasing wage inequality trend that began in the 1980s. Gender and nationality become less significant in employment, particularly in modern cultures, yet salary disparities persist among workers in the labor market, highlighting the importance of education for all age groups.

The increased utilization of technology in the skilled labor market positively impacts productivity, leading to a higher need for a highly skilled and educated workforce, as anticipated. Consequently, incomes for highly educated individuals proficient in technology have increased in comparison to those that are unskilled. AI technology results in Routine Biased Technical Change, which alters the connection between technology, skills, and vocations. Technologies lead to employment polarization by boosting the need for highly trained, well-paid positions that include cognitive abilities while decreasing the demand for low-skilled jobs that rely on physical tasks that are not routine [11].

90

Developed nations, characterized by mature industries and service-oriented economies, have a higher proportion of occupations in sectors that usually demand intricate cognitive skills, as stated in the IMF report. Hence, these economies are more vulnerable to AI advancements and are well positioned to benefit from them. Developed economies use AI to gain a competitive edge, but it is expected to exacerbate current economic disparities. Some literature research investigating the effects of advancements in AI technology on the workforce are grounded in Acemoglu and Restrepo's task-based model [1]. The model quantifies the extent to which patent applications in a specific technology are directed towards the performance of particular professions, through the correlation between patent applications and job descriptions within the workforce. Predictions can be made regarding the effectiveness of AI technology in transforming professional areas in the near future. The swift advancement of AI-driven technology can lead to discrepancies in capabilities within the work market. Workers with outdated skills may face challenges securing employment in industries with a significant demand for new talents, resulting in underemployment and societal unrest. AI-induced layoffs may result in reduced wages, particularly for people with lower skill levels. Wage stagnation exacerbates income inequality and hinders economic mobility in society. As AI technologies advance, layoffs across several sectors are unavoidable [4]. The IMF predicts that artificial intelligence would likely replace a substantial number of current jobs, potentially impacting up to 40% of global employment [7].

The literature highlights a concern that the quick implementation of AI could lead to an increase in structural unemployment and a decrease in middle-skilled occupations, causing polarization in the labor market [9]. Human employment is expected to decline, particularly in routine-based jobs, due to the widespread adoption of AI in manufacturing. This will lead to a decline in medium-skilled jobs and may result in issues such as structural unemployment and stagnant wage growth, particularly impacting low-skilled workers. Routine-based occupations are clearly at risk of experiencing job cuts.

2. WHEN PATHS CROSS: THE AI REVOLUTION AND THE LABOR MARKET

Concerns over the adverse impacts of technological advancements on the job market are longstanding. Keynes [12] discusses the issue of technological unemployment in his theory before the Second World War, which also tackles difficulties related to overcoming the Great Depression. Technological change is theoretically associated with job displacement. Throughout different stages of the industrial revolution, scholars have examined the correlation between the labor market and technological advancement from diverse angles. The stages are typically categorized in literature as the First Industrial Revolution, characterized by mechanical innovations like steam engines and railways, the Second Industrial Revolution, representing mass production, and the Third Industrial Revolution, marked by the introduction of computer and internet technologies to economies. Next, digital technologies like informatics, cloud infrastructures, big data technologies, wireless networks, internet of things, AI-powered robots, smart factories, and cyber-physical systems integrate into economic activities, marking the onset of the Fourth Industrial Revolution in our society [10], [13-14]. The final stage, typically analyzed as automation, is viewed as the apex of utilizing AI technology in production

91

and employment sectors. In contemporary economies, AI applications are regarded as the pinnacle of technological advancement in economic activities. AI encompasses several technologies that aim to allow robots to see, interpret, act, and learn in order to mimic human cognitive functions. An advanced technology comprising systems like sophisticated large language models (LLM) that generate new material, including text and images, through learning from extensive training data. Specialized AI models exhibit capabilities such as pattern recognition. Also, GenAI's emergence is leading to rapid evolution in the potential applications of AI. Researchers suggest that this indicates AI's influence will continue to expand in the future, reshaping corporate operations and workforce distribution [7]. Zarifhonarvar [17] explores the influence of ChatGPT on labor market dynamics, utilizing a text-mining approach to analyze the International Standard Occupation Classification. The study finds that 32.8% of occupations could be fully impacted by ChatGPT, while 36.5% might experience a partial impact. These assessments raise concerns about the future of the labor economy. AI is expected to decrease the necessity for labor to a minimum level, leading to lower error margins and manufacturing costs, while simultaneously enhancing production quality and efficiency. Upon full implementation of the Fourth Industrial Revolution, a reorganization process is expected to initiate across several sectors, including industry, informatics, education, and communication [3].

2.1 AI's Impact on Unemployment in Selected Developed Countries: Panel Data Analysis

AI's impact on the job market is typically analyzed on a sectoral basis. Historically, technological advancements have usually enhanced human work rather than entirely displacing it, leading to shifts in job roles rather than extensive job loss. The impact of AI on the labor market is influenced by various aspects such as the type of duties, the flexibility of workers, and the speed of technical advancements. Policymakers and stakeholders focus on building skills and supporting workforce transitions to help people effectively adjust to the evolving demands of the AI-driven economy [4]. In this study, the United Kingdom, the United States, Canada, France, Germany, Israel, Japan, and the Netherlands were identified as the top 8 developed countries with comparable numbers of artificial intelligence patents. There are many examples from the literature studying AI's impact on labor markets in these developed countries. Acemoglu & Restrepo [2] employed US data and showed theoretically that robots may reduce employment and wages and that their local impacts. Data from the period spanning 2005 to 2017 were utilized as the time frame. The model assessed the unemployment rate as the dependent variable and AI-based technological patents as the independent variable. Data from the OECD database included patents related to AI-based technology and unemployment rates.

Model used for developed countries:

$$\Upsilon_{it} = \alpha_{it} + \beta_1 X_{1_{it}} + u_{it}$$
$$(1)$$

92

Ɣ: Unemployment rate; X_1: AI Patents

Panel data analysis is considered to be more effective and advantageous in handling variation among individuals, countries, or enterprises. Also, panel data analysis outperforms time series and cross-sectional analysis in managing heterogeneity. Panel data is desirable due to reduced multicollinearity, increased degrees of freedom, and improved efficiency [5]. Therefore, panel data approaches were employed in the model based on these criteria.

The model was initially assessed? for time impact and unit effect, with the panel data group showing a significant statistical value for the unit effect. The time effect was defined and tested using the fixed effects test, random effects test, and the Breusch and Pagan test. The Breusch-Pagan test, introduced by Breusch and Pagan [6] within the framework of the Lagrangian multiplier test, addresses heteroscedasticity issues in linear regression models. This test yields pertinent findings within the realm of academic research. The unit effect was activated to conduct the same experiments, resulting in specific outcomes. Upon examination of the results, tests where the unit effect was effective indicated substantial statistical significance. Tests were conducted by triggering the unit effect in our model.

Prior to testing our model, we conducted a fixed effects test under the assumption that the unit effect exerts a significant impact. LR and Breusch-Pagan tests were conducted prior to the Hausman test to examine whether the model was influenced by fixed effects or random effects. The Hausman test was conducted and upon analysis of the data, the null hypothesis was rejected, indicating that the model adhered to the random effects assumption.

Table 1. *Fixed Effects Results*

unprate	Coeff.	Std. Err.	P>IzI
aipatents	-0.002	0.001	0.033
cons	7.270	0.354	0.000

Table 2. *Random Effects Results*

unprate	Coeff.	Std. Err.	P>IzI
aipatents	-0.002	0.000	0.003
cons	7.224	0.472	0.000

***Table 3.** Hausman Results*

	Coeff. - Fixed	**Coeff. - Random**
aipatents	-0.0027	-0.0025

***Table 4.** Deviations From Assumption*

	Prob.	**Results**
Frees	$0.660 > 0.31$	Inter-Unit Correlation
Heteroscedasticity	$0.000 < 0.05$	There is heteroscedasticity
Durbin Watson	$0.339 < 2$	There is autocorrelation
Baltagi-Wu LBI	$0.627 < 2$	There is autocorrelation

***Table 5:** Random Effects GLS Regression Estimation*

unprate	**Coeff.**	**Std. Err.**	**P>IzI**
aipatents	-0.0025	0.000	0.000
cons	7.2242	0.416	0.000

The model's deviation tests for developed countries reveal the presence of autocorrelation, heteroscedasticity, and inter-unit correlation when compared to the assumption. The model will be estimated and tested using the Random Effects GLS Regression estimator.

3. CONCLUSION

This study aims to assess the potential impacts of the AI revolution on the labor market in developed countries. The initial stage of the project involved analyzing the definition of AI, its historical context, and its applications. The discussion focuses on assessing the potential impact of AI on the labor market and its effects on the existing workforce in developed countries. Authors observed that the growing adoption of AI technology is resulting in shifts in job characteristics and required skills. The study employed panel data analysis to assess the prospective impacts of the AI revolution on the workforce. The

research findings indicate a statistically significant link at the 5% level between the variable 'unemployment rate' and 'the number of artificial intelligence-based technology patents' in the quantitative model for industrialized countries. A rise of one unit in AI-based technology patents results in a 0.0025 decrease in the unemployment rate variable. The economic potential of technology is now uncertain, akin to the initial phases of the industrial revolution. AI technologies are expected to have a positive impact on the labor market by increasing the demand for professions related to AI, given they have not yet been widely adopted in the production sector throughout the research period. The continuous advancement of AI technologies is anticipated to have a negative impact on the labor market in the near future. Education and skills need to be enhanced to tackle the challenges arising in the labor market due to technological advancements. New policies should prioritize adjusting social policies to keep pace with industrial improvements.

References

[52] D. Acemoglu, P. Restrepo, Artificial intelligence, automation, and work, The Economics of Artificial Intelligence: An Agenda (2018) 197-236. *DOI:10.3386/w24196*.

[53] D. Acemoglu, P. Restrepo, Robots and jobs: Evidence from US labor markets, Journal of Political Economy 128(6) (2020) 2188-2244. DOI:10.1086/705716.

[54] B. Akgül, Z. Ayer, Change in the Staff Structure of Media Institutions in Industry 4.0 Process, Route Educational and Social Science Journal 6(8) (2019) 126-134.

[55] D. H. Autor, Why are there still so many jobs? The history and future of workplace automation, Journal of Economic Perspectives, 29(3) (2015) 3-30. DOI: 10.1257/jep.29.3.3.

[56] B.H. Baltagi, Econometric Analysis of Panel Data, John Wiley & Sons, Chichester, 2005. *DOI:10.1002/9781118522154*

[57] T. S. Breusch, A. R. Pagan, A simple test for heteroscedasticity and random coefficient variation, Econometrica, 47(5) (1979) 1287-1294. *DOI: 10.2307/1911963*.

[58] M. Cazzaniga, F. Jaumotte, L. Li, G. Melina, A. J. Panton, C. Pizzinelli, . . . M. M. Tavares, Gen-AI: Artificial Intelligence and the Future of Work, Staff Discussion Notes, 2024(001) (2024). *DOI: 10.5089/9781513593543.006*.

[59] V. De Stefano, 'Negotiating the algorithm': Automation, artificial intelligence and labour protection, Artificial Intelligence and Labour Protection (May 16, 2018), Comparative Labor Law & Policy Journal, 41(1) (2019). *DOI: 10.2139/ssrn.3178233*.

95

[60] C. B. Frey, M. A. Osborne, The future of employment: How susceptible are jobs to computerisation?, Technological Forecasting and Social Change, 114 (2017) 254-280. *DOI: 10.1016/j.techfore.2016.08.019.*

[61] C. E. Hepaktan, D. Şimşek, Industry 4.0 and the Future of the Labor Market, İzmir Sosyal Bilimler Dergisi, 4(2) (2022) 80-88.

[62] H. B. İrhan, Yapay Zeka ve İstihdam: Covid-19 Sürecinde OECD Ülkeleri İstihdam Değerlendirmesi, Dumlupınar Üniversitesi İİBF Dergisi, 4(8) (2021) 25-34.

[63] J. M. Keynes, The general theory of employment, The Quarterly Journal of Economics, 51(2) (1937) 209-223. *DOI: 10.2307/1882087.*

[64] F. Othman, M. Bahrin, N. Azli, Industry 4.0: A review on industrial automation and robotic, J Teknol, 78(6-13) (2016) 137-143.

[65] L. Thames, D. Schaefer, Cybersecurity for Industry 4.0 and advanced manufacturing environments with ensemble intelligence, Cybersecurity for Industry 4.0: Analysis for Design and Manufacturing (2017) 243-265. *DOI: 10.1007/978-3-319-50660-9_10*

[66] G. L. Violante, Skill-Biased Technical Change, In The New Palgrave Dictionary of Economics, London: Palgrave Macmillan UK (2016) 1-6. *DOI: 10.1057/978-1-349-95121-5_1941-2*

[67] M. Webb, The impact of artificial intelligence on the labor market, Available at SSRN 3482150 (2019). *DOI: 10.2139/ssrn.3482150.*

[68] A. Zarifhonarvar, Economics of chatgpt: A labor market view on the occupational impact of artificial intelligence, Journal of Electronic Business & Digital Economics (2023).

96

Quantitative Analysis of equivalent atomic number (Zeq) in Barium-Infused Glass Systems

Hilal ÖZTÜRK[1✉], Osman GÜNAY[2] , Didem AVCI KARAKURT[3]

[1] Karadeniz Technical University, Faculty of Medicine, Department of Biophysics, Trabzon, Turkey
[2] Yıldız Technical University, Faculty of Electrical and Electronics Engineering, Department of Biomedical Engineering, Istanbul, TURKEY
[3] Department of Medical Imaging Techniques, Istanbul Arel University, 34010 Istanbul, Turkey

ABSTRACT

The incorporation of glass in radiation-intensive environments, such as medical imaging facilities and industrial applications involving radioactive materials, plays a pivotal role in ensuring safety and mitigating health risks. These environments emit ionizing radiation, which necessitates effective shielding to protect personnel and equipment from potential harm. Radiation shielding glasses are specially designed to attenuate ionizing radiation by incorporating materials that absorb or scatter radiation particles. These glasses undergo stringent manufacturing processes that enhance their ability to block radiation while maintaining optical transparency, essential for clear visibility and precise operation in radiation-rich settings. By reducing radiation exposure, these glasses contribute significantly to creating a secure working environment and minimizing health hazards associated with prolonged exposure to ionizing radiation.

The development of radiation shielding glasses involves a multidisciplinary approach that integrates materials science, optics, and engineering principles. Advanced glass formulations and specialized coatings are engineered to optimize radiation attenuation properties without compromising the glass's mechanical integrity or visual clarity. Techniques such as heavy metal doping and controlled crystallization are employed during manufacturing to enhance the glass's ability to withstand radiation-induced damage and ensure long-term reliability in challenging operational conditions. These glasses are indispensable in industries where radiation exposure is prevalent, safeguarding both human health and operational efficiency. By continually advancing technological innovations and adhering to stringent safety standards, radiation shielding glasses uphold crucial safety protocols and minimize the risks associated with ionizing radiation exposure.

In this study, the equivalent atomic number (Zeq) of Barium-Infused Glass Systems, varying with different energies, has been determined.

Keywords: Atomic number, Barium, Glass

✉ *Corresponding Author Email   :* hilal.ozturk@ktu.edu.tr

1. INTRODUCTION

The use of specialized glass in environments with significant radiation exposure, such as medical imaging facilities and industrial sectors handling radioactive materials, is critical for ensuring both safety and operational efficiency. These settings emit ionizing radiation, which poses serious health hazards to individuals and potential risks to sensitive equipment if not properly managed. Radiation shielding glasses are specifically engineered to mitigate these risks by attenuating ionizing radiation through the integration of radiation-absorbing materials into their composition.

To balance radiation protection with functional performance, these glasses are produced using advanced manufacturing methods that optimize their shielding capacity while preserving optical transparency and structural durability. Clear visibility is essential for accurate monitoring and safe operation of equipment in radiation-intense conditions. By reducing radiation exposure, shielding glasses help maintain safe working environments and prevent long-term health complications caused by cumulative radiation exposure.

The design and development of radiation shielding glasses rely on an interdisciplinary approach that combines expertise in materials science, optical engineering, and manufacturing processes. Enhanced formulations, often incorporating heavy metals like barium, are carefully optimized to improve radiation attenuation without compromising mechanical strength or transparency. Manufacturing techniques, such as heavy metal doping and crystallization control, are utilized to improve durability and ensure resistance to radiation-induced degradation over time. These advancements make radiation shielding glasses indispensable in radiation-sensitive industries, supporting the safety of personnel and the reliability of operations.

In this study, the equivalent atomic number (Zeq) of barium-infused glass systems has been evaluated across a range of photon energy levels to assess their effectiveness as radiation shielding materials.

2. MATERIALS AND METHODS

In this research, barium-infused glass systems were prepared and analyzed to determine their equivalent atomic number (Zeq) at varying photon energy levels.

The equivalent atomic number (Zeq) of the barium-infused glass systems was calculated across a photon energy range of 0.01 MeV to 10 MeV. The **phy-X/PSD** software, a reliable computational tool for radiation shielding analysis, was employed to determine Zeq values. Input parameters included the glass composition, density, and photon energy levels. The software computed the effective atomic number by analyzing photon interaction processes, such as photoelectric absorption, Compton scattering, and pair production, as a function of energy.The examination of various factors influencing radiation shielding has been a common theme in numerous studies[1-7].

Through this integrated approach, the equivalent atomic number of barium-infused glass systems was comprehensively evaluated, providing insights into their radiation shielding efficiency across different energy levels.

3. RESULTS

The equivalent atomic number as a function of photon energy is presented in Table 1. Starting from 1 keV, the equivalent atomic number gradually increases. After 30 keV, a sharp rise is observed, with the equivalent atomic number reaching up to 15. Subsequently, the increase in the equivalent atomic number slows down in accordance with the rising energy. The equivalent atomic number reaches its maximum value of 36.55 at 1 MeV. Following this, as photon energy increases beyond 1 MeV, the equivalent atomic number begins to decrease. This decrease continues until approximately 10 MeV, after which the equivalent atomic number stabilizes.

Table 1. Equivalent Atomic Number

Energy (MeV)	Zeq
1,00E-03	7,76
1,50E-03	8,52
2,00E-03	8,93
3,00E-03	9,37
4,00E-03	9,70
5,00E-03	10,36
6,00E-03	15,44
8,00E-03	15,82
1,00E-02	16,14
1,50E-02	16,77
2,00E-02	17,19
3,00E-02	17,76
4,00E-02	30,73

99

5,00E-02	31,58
6,00E-02	32,18
8,00E-02	33,03
1,00E-01	33,61
1,50E-01	34,51
2,00E-01	35,05
3,00E-01	35,66
4,00E-01	36,01
5,00E-01	36,23
6,00E-01	36,37
8,00E-01	36,51
1,00E+00	36,55
1,50E+00	33,02
2,00E+00	25,55
3,00E+00	20,73
4,00E+00	19,48
5,00E+00	18,92
6,00E+00	18,57
7,00E+00	18,35
8,00E+00	18,19
9,00E+00	18,09
1,00E+01	18,02
1,10E+01	17,98
1,20E+01	17,96

1,30E+01	17,95
1,40E+01	17,93
1,50E+01	17,91
1,60E+01	17,89
1,80E+01	17,86
2,00E+01	17,83
2,20E+01	17,82
2,40E+01	17,80
2,60E+01	17,80
2,80E+01	17,78
3,00E+01	17,76

4. CONSLUSION

The results of this study demonstrate the significant variation in the equivalent atomic number (Zeq) of barium-infused glass systems across different photon energy levels. Initially, from 1 keV, the equivalent atomic number gradually increases, reflecting the increased shielding capacity as energy rises. A sharp increase is observed at 30 keV, reaching a peak value of 36.55 at 1 MeV. This increase in Zeq is consistent with the enhanced radiation attenuation capabilities of the material at these energy levels.

However, beyond 1 MeV, as the photon energy continues to rise, the equivalent atomic number begins to decrease, indicating a reduction in the material's effectiveness in shielding against higher-energy radiation. This decrease continues up to approximately 10 MeV, after which the equivalent atomic number stabilizes, suggesting a leveling off in the material's ability to absorb or scatter radiation at very high energies.

These findings highlight the energy-dependent behavior of barium-infused glass in radiation shielding applications. The material exhibits optimal shielding performance at photon energies near 1 MeV, making it particularly effective for shielding in this energy range. However, at higher photon energies, alternative materials or modifications may be necessary to maintain high levels of radiation protection. This research contributes to understanding the radiation shielding characteristics of barium-infused glass systems, emphasizing their potential for use in environments exposed to ionizing radiation, such as medical imaging and nuclear industries

REFERENCES

[1] Kurudirek M. Heavy metal borate glasses: potential use for radiation shield ing.J Alloys Compd 2017;727:1227–36. https://doi.org/10.1016/j. jallcom.2017.08.237.

[2] Tekin HO, Rainey C, Ghada ALMisned, Shams A.M. Issa, Baki Akkus, Hesham M.H.Zakaly,. Heavy metal oxide added glassy portable containers for nuclear waste management applications: In comparison with reinforced concrete containers. Radiat Phys Chem 2022;201:110449. https://doi.org/10.1016/j. radphyschem.2022.110449.

[3] Sen Baykal, D., Tekin, H.O., Cakirli Mutlu, R., 2021. An investigation on radiation shielding properties of borosilicate glass systems. Int. J. Comput. Exp. Sci. Eng. 7, 99–108.

[4] Singh, N., Singh, K.J., Singh, K., Singh, H., 2004. Comparative study of lead borate and bismuth lead borate glass systems as gamma-radiation shielding materials. Nucl. Instrum. Methods Phys. Res. Sect. B Beam Interact. Mater. Atoms 225, 305–309.

[5] Ahmed MR, Hanafy T, Issa S (2020) Structural, Electrical and Radiation Shielding Properties of Polyvinyl Alcohol Doped with Different Nanoparticles. J. Mater Sci Mater Electron. 31:15192–7

[6] Dogra M, Singh KJ, Kaur K, Anand V, Kaur P (2017) Gamma Ray Shielding and Structural Properties of Bi2O3-B2O3-Na2WO4 Glass System. Universal Journal of Physics and Application 11(5):190-195

[7] Şakar, E., Özpolat, Ö. F., Alım, B., Sayyed, M. I., & Kurudirek, M. (2020). Phy-X/PSD: development of a user friendly online software for calculation of parameters relevant to radiation shielding and dosimetry. Radiation Physics and Chemistry, 166, 108496.

LAC for Calcium Molybdate

Nurdan KARPUZ[✉]

[✉]Amasya University, Sabuncuoğlu Şerefeddin Vocational School of Health Services, Amasya, Turkey

ABSTRACT

Radiation is important for technological development and thus it has been used in different fields. In order to protect hazardous effect of radiation, the shielding is used and thus shielding parameters should be obtained for materials. In this paper we obtained linear attenuation coefficients (LAC) for calcium molybdate and the results were discussed.

Keywords: LAC, radiation, Calcium Molybdate

[✉] *Corresponding Author Email　　: nurdankarpuz@amasya.edu.tr*

1 INTRODUCTION

Radiation, which is used in medical applications, industrial applications, energy production, research and scientific investigation, can cause serious harm to humans and the environment if it is not used with due care and safety. Protection from ionising radiation, which is defined as energetic particles or electromagnetic waves that split atoms or molecules into ions, produced by both artificial and natural sources and used in various fields, particularly in the health sector, is of greater importance. Appropriate protective measures should be taken to minimise the effects of ionising radiation because it has sufficient energy. Radiation shielding materials are special materials designed to reduce the effects of radiation or to protect people and the environment from the harmful effects of radiation.

When selecting shielding materials, low cost and availability are important, as well as some well-known criteria such as high density and high atomic number (Z) [1-4]. Lead has been the most widely used material for shielding against X-rays and γ-rays in the past, but due to its toxicity, weight, hardness and poor portability, researchers have been working on new alternative materials for radiation shielding. Many different types of materials have been tested for this purpose [5-11].

Glass is one of the most important alternative materials, attracting attention due to its high transparency, non-toxicity, anti-corrosion and environmental friendliness [12]. In addition, glass occupies an important place among the materials used for radiological protection purposes, as it can be made into samples of various thicknesses and shapes [13-16].

Glass materials, which can be the best substitutes for traditional materials for radiation protection, have recently been studied on experimental or simulation codes [17- 26].

In order to evaluate the radiation shielding properties of new types of glasses, it is necessary to obtain the linear attenuation coefficient (LAC), the mean free path (mfp), the half-value length (HVL), the effective atomic number (Z_{eff}) and the effective electron density (N_{eff}). These parameters can be obtained in experimental studies, but in most cases it is not possible to carry out experimental research due to the lack of sufficient resources, including the lack of radioactive sources. Therefore, the theoretical approach is a good choice for evaluating the radiation shielding properties of glass materials. In line with this knowledge, this study is an attempt to use glass to develop alternative and environmentally friendly materials for gamma radiation protection applications.

The main objective of this study is to obtain the linear attenuation coefficient (LAC) parameter for calcium molybdate and to investigate the effect of its radiation shielding properties.

2 MATERIALS AND METHODS

The gamma-ray absorption properties of the calcium molybdate used in this study were investigated using the Phy-X/PSD code [27].

The absorption of gamma rays depends on the thickness and density of the material. A thick and dense material can absorb more gamma rays because the gamma rays are more likely to interact with atoms in the material.

Very high energy gamma rays can pass through many materials. However, as it passes through a material, the intensity of the gamma ray decreases as it interacts with the atoms of the material. As a result of these interactions, the intensity of the radiation decreases exponentially as a function of the thickness of the absorbing material, as described by equation (1) [28-31].

$$I=I_0e^{-\mu x}$$

(1)

where I_0 and I are the incident and transmitted γ-ray intensities respectively. x is the thickness of the absorbing medium. And again, μ (cm^{-1}) in the exponential expression is called the linear attenuation coefficient (LAC). μ is one of the most important shielding parameters, depending on the γ-ray energy and the composition of the absorber.

The LAC value calculated in the study was calculated according to the formula in equation 2 [32;33].

$$LAC = \frac{1}{x} ln \frac{I_0}{I} \qquad (2)$$

3 RESULTS AND DISCUSSIONS

The 'LAC' parameter evaluated in the study and shown in Figure 1 is an abbreviation of the concept of 'Linear Attenuation Coefficient'. It is an important parameter in radiation armour testing. It is an important measure of how well a material attenuates radiation and is also referred to as the linear attenuation coefficient. It varies with the thickness of the material, the composition of the material and the energy of the radiation. A higher LAC

104

value means that the measured material attenuates more radiation. LAC values are used to determine which of the measured materials will provide better armour.
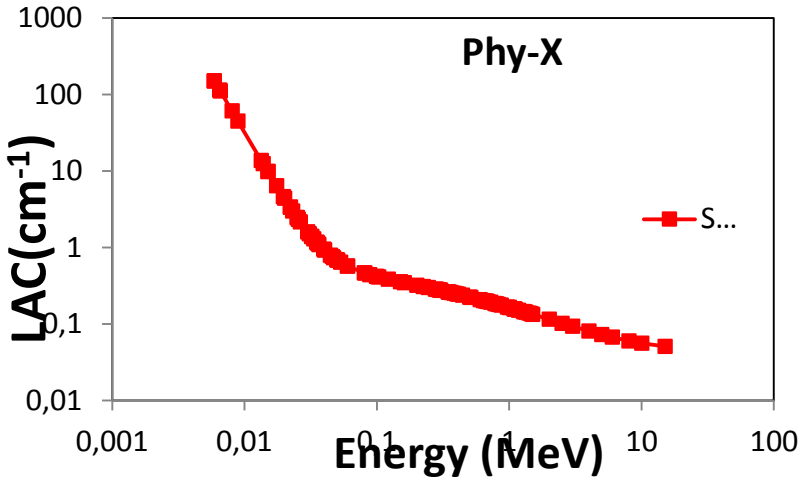
Figure 1. Variation of LAC value obtained for calcium molybdate with gamma energy

In this study, LAC values were evaluated at gamma ray energies ranging from 0 to 15 MeV. The calculated results are shown in Figure 1, where it can be seen that the LAC values for the proposed sample depend on the incident gamma-ray energy. A rapid decrease is observed up to 0,1 MeV. A slower decrease is observed for subsequent energy values. This indicates that the interaction of gamma rays with matter is energy dependent. However, the decrease in the LAC value with increasing incident photon energy can be attributed to three main interactions of gamma rays with matter: Photoelectric effect, Compton scattering and pair formation. The photoelectric effect is the dominant interaction at low photon energies, so the LAC is expected to decrease rapidly with increasing photon energy.

4 CONCLUSION
Due to its high density, lead is widely used as a shielding material against gamma radiation, but it is environmentally toxic and expensive for large-scale applications. As radiation shielding is important for human health and safety, alternative materials are being investigated for use in this field. To this end, this study calculated the LAC radiation shielding parameter of flexible, lightweight and low-cost composites based on calcium molybdate glass sample that is not toxic to humans or the environment.

REFERENCES

[1] Akkurt, I., Boodaghi Malidarre, R. (2022). Physical, structural, and mechanical properties of the concrete by FLUKA code and phy-X/PSD software. Radiation Physics and Chemistry, 193, Article 109958. https://doi.org/10.1016/j.radphyschem.2021.109958

[2] Akkurt, I., Akyıldırım, H., Karipçin, F., Mavi, B. (2012). Chemical corrosion on gamma- ray attenuation properties of barite concrete. Journal of Saudi Chemical Society, 16–2, 199–202. https://doi.org/10.1016/j.jscs.2011.01.003

[3] Altunsoy, E. E., Tekin, H. O., Mesbahi, A., Akkurt, I. (2020). MCNPX simulation for radiation dose absorption of anatomical regions and some organs. Acta Physica Polonica A, 137–4, 561. https://doi.org/10.12693/APhysPolA.137.561

[4] Boodaghi Malidarre, R., Akkurt, I., Gunoglu, K., Akyıldırım, H. (2021). Fast neutrons shielding properties for HAP-Fe2O3 composite materials. International Journal of Computational and Experimental Science and Engineering, 7(3), 143–145. https://doi.org/10.22399/ijcesen.1012039

[5] Boodaghi Malidarre, R., Akkurt, I. (2022). Evaluation of bioactive borosilicate added Ag glasses in terms of radiation shielding, structural, optical, and electrical properties. Silicon. https://doi.org/10.1007/s12633-022-01925-y

[6] Demir, N., Tarim, U. A., Popovici, M. A., Demirci, Z. N., Gurler, O., Akkurt, I. (2013). Investigation of mass attenuation coefficients of water, concrete and bakelite at different energies using the FLUKA Monte Carlo code. Journal of Radioanalytical and Nuclear Chemistry, 298, 1303–1307. https://doi.org/10.1007/s10967-013-2494-y

[7] Waheed, F., Imamoglu, M., Karpuz, N., Ovalıoglu, H. (2022). Simulation of neutrons shielding properties for some medical materials. International Journal of Computational and Experimental Science and Engineering, 8(1), 5–8. https://doi.org/10.22399/ijcesen.1032359

[8] Karpuz, N. (2024). Effect of La_2O_3 on Magnesium Borosilicate glasses glass for radiation shielding materials in nuclear application. Radiation Physics and Chemistry, 214. https://doi.org/10.1016/j.radphyschem.2023.111305

[9] Akkurt, I., Basyigit, C., Kilincarslan, S., Mavi, B. (2005). The shielding of g-rays by concrete produced with barite. Prog. Nucl. Energy 46 (1), 1–11.

[10] Akkurt, I., Basyigit, C., Kilincarslan, S., Mavi, B., Akkurt, A. (2006). Radiation shielding of concretes containing different aggregates. Cement Concr. Compos. 28 (2), 153–157. https://doi.org/10.1016/j.cemconcomp.2005.09.006

[11] Tekin, H.O., Cavli, B., Altunsoy, E.E., Manici, T., Ozturk, C., Karakas, H.M. (2018). An investigation on radiation protection and shielding properties of 16 slice computed tomography (CT) facilities. International Journal of Computational and Experimental Science and Engineering 4–2, 37–40. https://doi.org/10.22399/ijcesen.408231

[12] Sarihan, M. (2022). Simulation of gamma-ray shielding properties for materials of medical interest. Open Chem. 20 (1), 81–87. https://doi.org/10.1515/chem-2021-0118

[13] Akkurt, I., Boodaghi Malidarre, R. (2022). Physical, structural, and mechanical properties of the concrete by FLUKA code and phy-X/PSD software. Radiat. Phys. Chem. 193, 109958 https://doi.org/10.1016/j.radphyschem.2021.109958

[14] Biswas, R., Sahadath, H., Mollah, A.S., Huq, Md F. (2016). Calculation of gamma-ray attenuation parameters for locally developed shielding material: Polyboron. Journal of Radiation Research and Applied Sciences 9, 26–34. https://doi.org/10.1016/j.jrras.2015.08.005

[15] Afaneh, F., Khattari, Z. Y., Al-Buriahi, M. S. (2022). Monte Carlo simulations and phy-X/PSD study of radiation shielding and elastic effects of molybdenum and tungsten in phosphate glasses. Journal of Materials Research and Technology 19, 3788-3802. https://doi.org/10.1016/j.jmrt.2022.06.125

[16] Almisned, G., Sen Baykal, D., Susoy, G., Kilic, G., Zakaly H, M.H., Ene, A., Tekin, H.O. (2022). "Determination of gamma-ray transmission factors of WO3–TeO2–B2O3 glasses using MCPX Monte Carlo code for shielding and protection purposes". Appl. Rheol. 32 (1).

[17] Akkurt, I., Tekin, H. O. (2020). Radiological Parameters for bismuth oxide Glasses using Phy-X/PSD software. Emerg. Mater. Res. 9–3, 1020–1027. https://doi. org/10.1680/jemmr.20.00098

[18] Issa, Shams A.M., Saddeek, Y.B., Sayyed, M.I., Tekin, H.O., Kilicoglu, O. (2019). Radiation shielding features using MCNPX code and mechanical properties of the PbO Na2O B2O3 CaO Al2O3 SiO2 glass systems. Composites, Part B 167, 231–240. https://doi. org/10.1016/j.compositesb.2018.12.029

[19] Akkurt, I., El-Khayatt, A.M. (2013). The effect of barite proportion on neutron and gamma-ray shielding. Ann. Nucl. Energy 51, 5–9. https://doi.org/10.1016/j. anucene.2012.08.026

[20] ALMisned, G., Sen Baykal, D., Susoy, G., Kilic, G., Zakaly H, M. H., Ene, A., Tekin, H. O. (2022). Determination of gamma-ray transmission factors of WO3–TeO2–B2O3 glasses using MCPX Monte Carlo code for shielding and protection purposes. Applied Rheology, 32(1).

[21] ALMisned, G., Sen Baykal, D., Kilic, G., Susoy, G., Zakaly H, M. H., Ene, A., Tekin, H. O. (2022). Assessment of the usability conditions of Sb2O3-PbO-B2O3 glasses for shielding purposes in some medical radioisotope and a wide gamma-ray energy spectrum. Applied Rheology, 32(1).

[22] Hanfi, M. Y., Sayyed, M. I., Lacomme, E. K., Mahmoud, K. A., Akkurt, I. (2020). The influence of MgO on the radiation protection and mechanical roperties of tellurite Glasses. Nucl. Eng. Technol., oi.org/. https://doi.org/10.1016/j.net.2020.12.012

[23] Issa, S. A. M., Saddeek, Y. B., Sayyed, M. I., Tekin, H. O., Kilicoglu, O. (2019). Radiation shielding features using MCNPX code and mechanical properties of the PbO Na2O B2O3 CaO Al2O3 SiO2 glass systems. Composites, Part B: Engineering, 167, 231–240. https://doi.org/10.1016/j.compositesb.2018.12.029

[24] Oruncak, B. (2022). Gamma-ray shielding properties of Nd2O3 added iron-boron- phosphate based composites. Open Chemistry, 20(1). https://doi.org/10.1515/chem- 2022-0143

[25] Sarihan, M., Boodaghi Malidarre, R., Akkurt, I. (2021). An extensive study on the neutron-gamma shielding and mass stopping power of (70-x) CRT–30K2O–xBaO glass system for 252Cf neutron source. Environmental Technology. https://doi.org/10.1080/ 09593330.2021.1987529

107

[26] Karpuz, N. (2023). Radiation shielding properties of glass composition. Journal of Radiation Research and Applied Sciences 16. https://doi.org/10.1016/j.jrras.2023.100689

[27] Şakar, E., Fırat Ozpolat, O., Alım, B., Sayyed, M. I., Kurudirek, M. (2020). Phy-X/PSD: Development of a user friendly online software for calculation of parameters relevant to radiation shielding and dosimetry. Radiation Physics and Chemistry, 166, Article 108496.

[28] Akkurt, I., Malidarre, R. B., Kavas, T. (2021). Monte Carlo simulation of radiation shielding properties of the glass system containing Bi2O3. European Physical Journal E: Soft Matter, 136, 264. https://doi.org/10.1140/epjp/s13360-021-01260-y

[29] El-bashir, B. O., Sayyed, M. I., Zaid, M. H. M., Matori, K. A. (2017). Comprehensive study on physical, elastic and shielding properties of ternary BaO-Bi2O3-P2O5 glasses as a potent radiation shielding material. Journal of Non-Crystalline Solids, 468, 92–99

[30] Rammah, Y. S., Olarinoye, I. O., El-Agawany, F. I., Mahmoud, K. A., Akkurt, I., Yousef, E. S. (2021). Evaluation of radiation shielding capacity of vanadium–tellurite–antimonite semiconducting glasses. Optical Materials, 114, Article 110897. https://doi.org/10.1016/j.optmat.2021.110897

[31] Tekin, H. O., Abouhaswa, A. S., Kilicoglu, O., Issa, S. A. M., Akkurt, I., Rammah, Y. S. (2020). Fabrication, physical characteristic, and gamma-photon attenuation parameters of newly developed molybdenum reinforced bismuth borate glasses. Physica Scripta, 95 (12pp), Article 115703. https://doi.org/10.1088/1402-4896/abbf6e

[32] Akkurt, I. (2009). Effective atomic and electron numbers of some steels at different energies. *Annals of Nuclear Energy, 36–11*(12), 1702–1705. https://doi.org/10.1016/j.anucene.2009.09.005

[33] Boodaghi Malidarre, R., Akkurt, I. (2021). Monte Carlo simulation study on TeO_2–Bi_2O–PbO–MgO–B_2O_3 glass for neutron-gamma ^{252}Cf source. *Journal of Materials Science: Materials in Electronics, 32*, 11666–11682. https://doi.org/10.1007/s10854-021-05776-y

Analysis of equivalent atomic number (Z$_{eq}$) of Calcium Molybdate

Nurdan KARPUZ$^{\boxtimes}$

$^{\boxtimes}$Amasya University, Sabuncuoğlu Şerefeddin Vocational School of Health Services, Amasya, Turkey

$^{\boxtimes}$ *Corresponding Author Email   : nurdankarpuz@amasya.edu.tr*

ABSTRACT

There are many different types of parameters for radiation shielding properties of any materials. Besides other parameters the equivalent atomic number (Z$_{eq}$) is one of the important one and it is used to test shielding properties. In this work equivalent atomic number (Z$_{eq}$) have been obtained and presented for calcium molybdate..

Keywords: Z$_{eq}$, radiation, Calcium Molybdate

1 INTRODUCTION

Radiation, which is used in medical applications, industrial applications, energy production, research and scientific investigation, can cause serious harm to humans and the environment if it is not used with due care and safety. Protection from ionising radiation, which is defined as energetic particles or electromagnetic waves that split atoms or molecules into ions, produced by both artificial and natural sources and used in various fields, particularly in the health sector, is of greater importance. Appropriate protective measures should be taken to minimise the effects of ionising radiation because it has sufficient energy. Radiation shielding materials are special materials designed to reduce the effects of radiation or to protect people and the environment from the harmful effects of radiation.

When selecting shielding materials, low cost and availability are important, as well as some well-known criteria such as high density and high atomic number (Z) [1-4]. Lead has been the most widely used material for shielding against X-rays and γ-rays in the past, but due to its toxicity, weight, hardness and poor portability, researchers have been working on new alternative materials for radiation shielding. Many different types of materials have been tested for this purpose [5-11].

Glass is one of the most important alternative materials, attracting attention due to its high transparency, non-toxicity, anti-corrosion and environmental friendliness [12]. In addition, glass occupies an important place among the materials used for radiological protection purposes, as it can be made into samples of various thicknesses and shapes [13-16].

109

Glass materials, which can be the best substitutes for traditional materials for radiation protection, have recently been studied on experimental or simulation codes [17- 26].

In order to evaluate the radiation shielding properties of new types of glasses, it is necessary to obtain the linear attenuation coefficient (LAC), the mean free path (mfp), the half-value length (HVL), the effective atomic number (Z_{eff}) and the effective electron density (N_{eff}). These parameters can be obtained in experimental studies, but in most cases it is not possible to carry out experimental research due to the lack of sufficient resources, including the lack of radioactive sources. Therefore, the theoretical approach is a good choice for evaluating the radiation shielding properties of glass materials. In line with this knowledge, this study is an attempt to use glass to develop alternative and environmentally friendly materials for gamma radiation protection applications.

The main objective of this study is to obtain the equivalent atomic number (Z_{eq}) parameter for calcium molybdate and to investigate the effect of its radiation shielding properties.

2 MATERIALS AND METHODS

The gamma-ray absorption properties, Z_{eq} parameter, of the calcium molybdate used in this study were investigated using the Phy-X/PSD code [27].

Equivalent atomic number (Z_{eq}) is a significant parameter that provides an effective measure of a material's shielding capability against nuclear radiation. It generally refers to the effect of a material's atomic number on the attenuation or absorption of radiation. Z_{eq} plays an important role in the selection and design of shielding materials. The Z_{eq} parameter is used to compare the shielding capacities of different materials.

The absorption of gamma rays depends on the thickness, density, and Z_{eq} of the material. A material with a high Z_{eq}, along with sufficient thickness and density, can absorb more gamma rays because the gamma rays are more likely to interact with the atoms in the material.

3 RESULTS AND DISCUSSIONS

In the graph in Figure 1, Z_{eq} represents the shielding capacity of calcium molybdate against nuclear radiation in this study. A higher Z_{eq} value in the graph indicates that the material absorbs or attenuates radiation more effectively. This is because the Z_{eq} value depends on the atomic number, density, and thickness of the material.

110
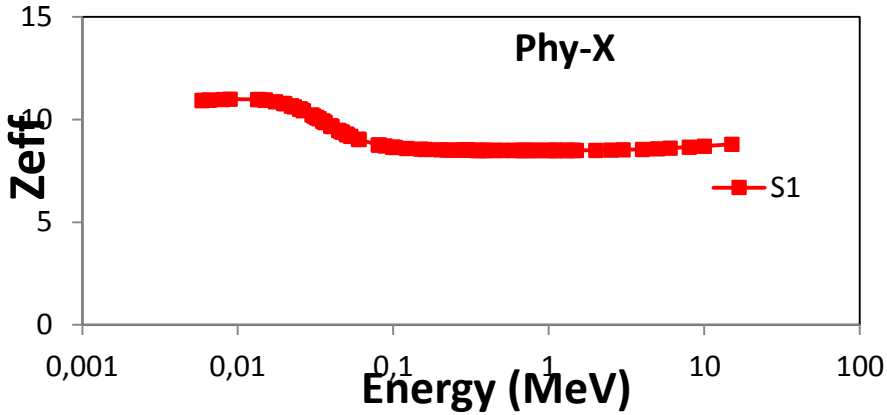
Figure 1. Variation of Zeq value obtained for calcium molybdate with gamma energy

In this study, Z_{eq} values were evaluated at gamma ray energies ranging from 0,015 to 15 MeV. The calculated results are shown in Figure 1, where it can be seen that the Z_{eq} values for the proposed sample depend on the incident gamma-ray energy. The effect of high-energy radiation on Z_{eq} is generally observed to be more significant. Additionally, an increase in density also leads to a rise in the Z_{eq} value.

4 CONCLUSION
Due to its high density, lead is widely used as a shielding material against gamma radiation, but it is environmentally toxic and expensive for large-scale applications. As radiation shielding is important for human health and safety, alternative materials are being investigated for use in this field. To this end, this study calculated the Z_{eq} radiation shielding parameter of flexible, lightweight and low-cost composites based on calcium molybdate glass sample that is not toxic to humans or the environment.

REFERENCES
[1] Akkurt, I., Boodaghi Malidarre, R. (2022). Physical, structural, and mechanical properties of the concrete by FLUKA code and phy-X/PSD software. Radiation Physics and Chemistry, 193, Article 109958. https://doi.org/10.1016/j.radphyschem.2021.109958

[2] Akkurt, I., Akyıldırım, H., Karipçin, F., Mavi, B. (2012). Chemical corrosion on gamma- ray attenuation properties of barite concrete. Journal of Saudi Chemical Society, 16–2, 199–202. https://doi.org/10.1016/j.jscs.2011.01.003

[3] Altunsoy, E. E., Tekin, H. O., Mesbahi, A., Akkurt, I. (2020). MCNPX simulation for radiation dose absorption of anatomical regions and some organs. Acta Physica Polonica A, 137–4, 561. https://doi.org/10.12693/APhysPolA.137.561

[4] Boodaghi Malidarre, R., Akkurt, I., Gunoglu, K., Akyıldırım, H. (2021). Fast neutrons shielding properties for HAP-Fe2O3 composite materials. International Journal of Computational and Experimental Science and Engineering, 7(3), 143–145. https://doi.org/10.22399/ijcesen.1012039

[5] Boodaghi Malidarre, R., Akkurt, I. (2022). Evaluation of bioactive borosilicate added Ag glasses in terms of radiation shielding, structural, optical, and electrical properties. Silicon. https://doi.org/10.1007/s12633-022-01925-y

[6] Demir, N., Tarim, U. A., Popovici, M. A., Demirci, Z. N., Gurler, O., Akkurt, I. (2013). Investigation of mass attenuation coefficients of water, concrete and bakelite at different energies using the FLUKA Monte Carlo code. Journal of Radioanalytical and Nuclear Chemistry, 298, 1303–1307. https://doi.org/10.1007/s10967-013-2494-y

[7] Waheed, F., Imamoglu, M., Karpuz, N., Ovalıoglu, H. (2022). Simulation of neutrons shielding properties for some medical materials. International Journal of Computational and Experimental Science and Engineering, 8(1), 5–8. https://doi.org/10.22399/ijcesen.1032359

[8] Karpuz, N. (2024). Effect of La_2O_3 on Magnesium Borosilicate glasses glass for radiation shielding materials in nuclear application. Radiation Physics and Chemistry, 214. https://doi.org/10.1016/j.radphyschem.2023.111305

[9] Akkurt, I., Basyigit, C., Kilincarslan, S., Mavi, B. (2005). The shielding of g-rays by concrete produced with barite. Prog. Nucl. Energy 46 (1), 1–11.

[10] Akkurt, I., Basyigit, C., Kilincarslan, S., Mavi, B., Akkurt, A. (2006). Radiation shielding of concretes containing different aggregates. Cement Concr. Compos. 28 (2), 153–157. https://doi.org/10.1016/j.cemconcomp.2005.09.006

[11] Tekin, H.O., Cavli, B., Altunsoy, E.E., Manici, T., Ozturk, C., Karakas, H.M. (2018). An investigation on radiation protection and shielding properties of 16 slice computed tomography (CT) facilities. International Journal of Computational and Experimental Science and Engineering 4–2, 37–40. https://doi.org/10.22399/ijcesen.408231

[12] Sarihan, M. (2022). Simulation of gamma-ray shielding properties for materials of medical interest. Open Chem. 20 (1), 81–87. https://doi.org/10.1515/chem-2021-0118

[13] Akkurt, I., Boodaghi Malidarre, R. (2022). Physical, structural, and mechanical properties of the concrete by FLUKA code and phy-X/PSD software. Radiat. Phys. Chem. 193, 109958 https://doi.org/10.1016/j.radphyschem.2021.109958

[14] Biswas, R., Sahadath, H., Mollah, A.S., Huq, Md F. (2016). Calculation of gamma-ray attenuation parameters for locally developed shielding material: Polyboron. Journal of Radiation Research and Applied Sciences 9, 26–34. https://doi.org/10.1016/j.jrras.2015.08.005

[15] Afaneh, F., Khattari, Z. Y., Al-Buriahi, M. S. (2022). Monte Carlo simulations and phy-X/PSD study of radiation shielding and elastic effects of molybdenum and tungsten in phosphate glasses. Journal of Materials Research and Technology 19, 3788-3802. https://doi.org/10.1016/j.jmrt.2022.06.125

[16] Almisned, G., Sen Baykal, D., Susoy, G., Kilic, G., Zakaly H, M.H., Ene, A., Tekin, H.O. (2022). "Determination of gamma-ray transmission factors of WO3–TeO2–B2O3 glasses using MCPX Monte Carlo code for shielding and protection purposes". Appl. Rheol. 32 (1).

[17] Akkurt, I., Tekin, H. O. (2020). Radiological Parameters for bismuth oxide Glasses using Phy-X/PSD software. Emerg. Mater. Res. 9–3, 1020–1027. https://doi.org/10.1680/jemmr.20.00098

[18] Issa, Shams A.M., Saddeek, Y.B., Sayyed, M.I., Tekin, H.O., Kilicoglu, O. (2019). Radiation shielding features using MCNPX code and mechanical properties of the PbO Na2O B2O3 CaO Al2O3 SiO2 glass systems. Composites, Part B 167, 231–240. https://doi. org/10.1016/j.compositesb.2018.12.029

[19] Akkurt, I., El-Khayatt, A.M. (2013). The effect of barite proportion on neutron and gamma-ray shielding. Ann. Nucl. Energy 51, 5–9. https://doi.org/10.1016/j.anucene.2012.08.026

[20] ALMisned, G., Sen Baykal, D., Susoy, G., Kilic, G., Zakaly H, M. H., Ene, A., Tekin, H. O. (2022). Determination of gamma-ray transmission factors of WO3–TeO2–B2O3 glasses using MCPX Monte Carlo code for shielding and protection purposes. Applied Rheology, 32(1).

[21] ALMisned, G., Sen Baykal, D., Kilic, G., Susoy, G., Zakaly H, M. H., Ene, A., Tekin, H. O. (2022). Assessment of the usability conditions of Sb2O3-PbO-B2O3 glasses for shielding purposes in some medical radioisotope and a wide gamma-ray energy spectrum. Applied Rheology, 32(1).

[22] Hanfi, M. Y., Sayyed, M. I., Lacomme, E. K., Mahmoud, K. A., Akkurt, I. (2020). The influence of MgO on the radiation protection and mechanical roperties of tellurite Glasses. Nucl. Eng. Technol., oi.org/. https://doi.org/10.1016/j.net.2020.12.012

[23] Issa, S. A. M., Saddeek, Y. B., Sayyed, M. I., Tekin, H. O., Kilicoglu, O. (2019). Radiation shielding features using MCNPX code and mechanical properties of the PbO Na2O B2O3 CaO Al2O3 SiO2 glass systems. Composites, Part B: Engineering, 167, 231–240. https://doi.org/10.1016/j.compositesb.2018.12.029

[24] Oruncak, B. (2022). Gamma-ray shielding properties of Nd2O3 added iron-boron- phosphate based composites. Open Chemistry, 20(1). https://doi.org/10.1515/chem- 2022-0143

[25] Sarihan, M., Boodaghi Malidarre, R., Akkurt, I. (2021). An extensive study on the neutron-gamma shielding and mass stopping power of (70-x) CRT–30K2O–xBaO glass system for 252Cf neutron source. Environmental Technology. https://doi.org/10.1080/ 09593330.2021.1987529

[26] Karpuz, N. (2023). Radiation shielding properties of glass composition. Journal of Radiation Research and Applied Sciences 16. https://doi.org/10.1016/j.jrras.2023.100689

[27] Şakar, E., Fırat Ozpolat, O., Alım, B., Sayyed, M. I., Kurudirek, M. (2020). Phy-X/PSD: Development of a user friendly online software for calculation of parameters relevant to radiation shielding and dosimetry. Radiation Physics and Chemistry, 166, Article 108496.

Investigation of the Role and Selection Criteria of Green PLM in New Product Development Strategies in Companies

Enes ÖNDEN [1*], Coşkun HARMANŞAH [2]

[1] *Ege University, Graduate School of Natural and Applied Sciences, Product Lifecycle Management Master Programme, İzmir,TURKEY*

[2] *Ege University, Product Lifecycle Management Research and Application Excellence Center, İzmir, TURKEY*

*enesonden@gmail.com

ABSTRACT

Product Lifecycle Management (PLM) is a strategic business approach that uses a consistent set of business solutions to support the creation, management, dissemination, and use of product information within enterprises, bringing together people, processes, business systems, and information from concept to end-of-life.

As sustainability becomes more important today, PLM systems that aim to manage a product's whole commercial life must likewise be sustainable. Life cycle assessment (LCA) is a systematic framework for monitoring and assessing the environmental consequences of products throughout their life cycle. Eco Design, on the other hand, builds a Green PLM approach that incorporates green themes such as sustainable production, logistics, and energy efficiency. While LCA assesses the product's environmental impact, Green PLM manages the environmental impact throughout the entire life cycle of the product. In this regard, LCA may be viewed as a methodological tool for Green PLM.

According to the survey results, 50% of SMEs (Small and Medium Enterprise) employed in various industries are familiar with PLM software, and the majority uses PDM (Product Data Management) and comparable systems. It was observed that many PLM-using companies have integrated modules like 'Configuration Management,' 'Design,' 'Project Management,' and 'Change Management' into their operations. On the other hand, it was observed that 47% of the companies are environmentally conscious and prioritize Green Engineering ideas such as "preventing waste generation" and "protecting the environment and human health". In the survey, "Management" and "Time" were evaluated as "High" risks, while "Personnel" and "Integration Difficulties" were evaluated as "Critical" and "High" risks in the transition to Green PLM. The research evaluated organizations' present sustainability status and provided a roadmap for incorporating sustainability indicators into PLM modules throughout the transition to green products.

Keywords - *Green PLM, Green Product, Sustainability*

114

1. INTRODUCTION

Environmental issues have grown in importance in recent years, making it necessary for manufactured products to have the green label. The problem of environmental pollution has revealed the necessity of using not only quality and economic criteria in production, but also sustainable methods [1] . In this context, sustainability has become an engineering objective and necessity along with the prevention of environmental pollution. The increase in the number of environmentally conscious consumers has also increased the interest of companies in sustainable production and has led them to focus on this issue. In this regard, the European Commission has shared the sustainable product initiative protocol [2]. Eco-friendly raw material procurement and subsequent proof of energy efficiency are among the requirements of sustainability [3]. For this purpose, smart and artificial intelligence-based systems are being created today for quality, innovative and sustainable design and production. Therefore, the use of PLM systems, which utilize innovative business technologies that enable the development of a company's product content and the integration of production stages into the entire operation of the company, in sustainable production gains importance in terms of facilitating the follow-up of the process.

In recent years, the rapid consumption of natural resources, increasing population and the use of limited resources, as well as the inevitable necessity of globalization, have led many companies to use sustainable production methods and to make transformations and improvements in line with their business strategy. It has become important to consider process and product benefits together with their environmental and social impacts [4]. In this context, production industries and all product-related data plays an important role in the environmental dimension of sustainability. It has become the goal of manufacturers to promote production processes and suitable products for this purpose in order to minimize environmental impacts while maintaining social and economic benefits. At this point, the manufacturing industry has faced new challenges due to the consuming of energy and natural resources, economic stagnation and increasing human needs. Therefore, low-carbon green growth, cleaner production and environmentally friendly products are the main topics and sustainable production is emerging as a driving force in the manufacturing industry of the future [5]. Here, the vision of the manufacturing company should be to supply products that meet customer needs, taking into account all life cycle impacts and to move forward the company's innovation, quality and sustainable production systems. The most significant issue in this regard is the difficulty in incorporating this strategy into private-sector organizations. As a result, a new model for the factory of the future should be built from present industrial networks, with existing organizational structures not completely discarded. According to this concept, firms that have made sustainability a priority need to start by being conscious of challenges related to green manufacturing. Thus, processes from the idea stage of a product to its recycling phases can be integrated with the work and understanding of businesses on sustainability issues. In our research, we proposed an approach to assist identify the design, development, and manufacturing processes, tasks, criteria, or indicators of the Green product, which is a new strategy for businesses. In the 1985 report, the Brundtland Commission defined sustainable development as "development that meets the needs of the present without compromising future generations' capacity to meet their own needs" [6].

115

The goal of this study is to provide various suggestions on how to integrate environmental indicators into PLM modules while adhering to the environment sustainable development goals and keeping in mind that PLM software should be in line with environmental policies in companies' new product development studies. In this regard, a survey was sent to the firms in order to examine the situation and reveal the plan of action for the work to be completed later. The survey results are analyzed and proposals for Green PLM systems are presented.

2. PLM SYSTEMS AND GREEN PLM

PLM is a collection of systems that handle a company's product information from concept to end-of-life. Its goals are to accelerate innovation, shorten product development time, minimize costs, maximize quality, visualize product information, and eliminate communication gaps among collaborating parties [7]. From a different perspective, PLM is regarded as a strategic business approach that brings together people, processes, business systems and information to provide a coherent set of business solutions that support the creation, management, dissemination and utilization of a business's product information from concept to end-of-life [8].

In terms of sustainability, PLM systems consist of product design, production tracking with real-time data processing, product maintenance and recycling. At this moment, the processes in product life cycles are intimately linked to three essential phases: BOL (beginning of life), MOL (middle of life) and EOL (end of life) [9]. Different modules within PLM have been developed for the management and implementation of all these phases. The most frequently used modules are document, design, supply chain, configuration and change management modules.

The concept of Green PLM differs from the standard PLM methodology that it involves the incorporation and use of sustainability concerns at all stages of product-related activities. In their study, Vila et al. [10] present this concept in four stages; *(i)* Defining the Green PLM strategy with operational actions (processes, methodologies, tools, etc.), *(ii)* Outlining collaborative methodologies and tools for the globalized market, defining all necessary methodologies, evaluation procedures and selection guidelines (green product and process design, manufacturing, logistics, etc.), *(iii)* Research on the development of green manufacturing technologies and plant design, analyzing existing technologies and improvements for alternative solutions, *(iv)* Establishment of green factory, defining and launching pilot projects.

PLM systems that include these activities are consistent with the Green PLM philosophy. In recent years, PLM software has begun to adopt this paradigm. This understanding may be controlled using PLM-specific modules. In this environment, several PLM firms have started to provide solutions for integrating Green PLM techniques that support sustainability goals due to their flexible and adaptable structure. This program allows you to analyze and optimize elements like material selection, energy consumption, and waste management. It also allows for the assessment of environmental implications over the product's life cycle. PLM systems provide complete capabilities for ensuring that products meet environmental legislation and requirements. It can help to design products that

116

comply with European Union rules such as European Union regulations such as RoHS (Restriction of Hazardous Substances Directive) and REACH (Registration, Evaluation, Authorization and Restriction of Chemicals). It may monitor and handle such regulatory requirements, easing the introduction of environmentally friendly items to the market [11].

2.1 LCA METODOLOGY FOR GREEN PLM

LCA is a method for the quantitative analysis of the environmental impacts of a product over its entire life cycle. It is a systematic tool for analyzing the environmental burdens of a product throughout its life cycle and assessing its potential impacts on the environment. In this context, LCA can include both products and services. Environmental burdens are emissions to air, water and land, such as CO_2, solid waste and resource consumption. In the context of LCA, environmental impacts refer to negative impacts on the ecosystem, human health and the use of natural resources. An LCA review consists of four stages: target and scope definition, life cycle inventory analysis, life cycle impact assessment and life cycle interpretation [12].

The life cycle assessment research generated by this study can serve as an example of how LCA can be applied to all processes for products that go through the current design and modeling, manufacturing, distribution and maintenance phases. The traceability and utilization of each of these phases in PLM-specific modules will enable the use of long evaluation methods such as LCA in PLM. On the other hand, the integration of sustainability indicators into PLM, which is one of the objectives of our study, will increase the sensitivity and maturity of the Green PLM concept in the sector. The identification of the modules commonly used in PLM platforms and the appropriate sustainability parameters and their integration into the software will shed light on the process and reveal a roadmap.

3. MATERIAL AND METHOD

Within the purpose of this study, a questionnaire was prepared and sent to firm employees in various industries in order to conduct a scenario analysis of companies' transition procedures from their current organizations to Green PLM and establish a plan of action. The research's goal is to reveal current patterns by gathering information on the present situation of PLM usage in enterprises as well as their perspectives on Green PLM, and so establish an action plan for incorporating sustainability standards into their current organizations.

In the study, a survey was given out to 30 firms from different sectors. Regarding Creswell's guidance that a sample of 5 to 20 may be sufficient in qualitative research [13], this survey, which is the first phase in our study, was carried out with the involvement of workers from the appropriate organizations. Academics and professionals who are experts

117

in their fields were consulted throughout the preparation of the research questions to ensure the study's validity and reliability. After the survey questions were produced, they were made available online and sent to relevant sector employees. The survey included 22 questions of various forms, such as short answer, multiple choice, 5-point Likert scale, multiple choice tables, yes/no, and check boxes.

The survey questions were divided into four categories: personal experience and general corporate information, the firm's usage of PLM, degree of understanding regarding Green PLM, and environmental viewpoints. The identities of the participating firms were not disclosed in accordance with the research and PDPA's (Personal Data Protection Authority Law No. 6698 in Turkey) ethical norms. Our survey has 30 participants, including 29 workers from Adana, Ankara, Bursa, Eskişehir, İstanbul, İzmir, Manisa, and Sakarya, as well as one firm employee from abroad. The survey questions were disseminated at random to individuals, and the fact that the data acquired spans many cities throughout Turkey demonstrates the survey's uniqueness.

4. RESULTS AND RESULT

The majority of participants work in large companies. 43.3% of those who participated are from the machinery manufacturing, automotive, and electrical-electronics industries, while the remaining 56.7% are from companies servicing several industries (Figure 1).
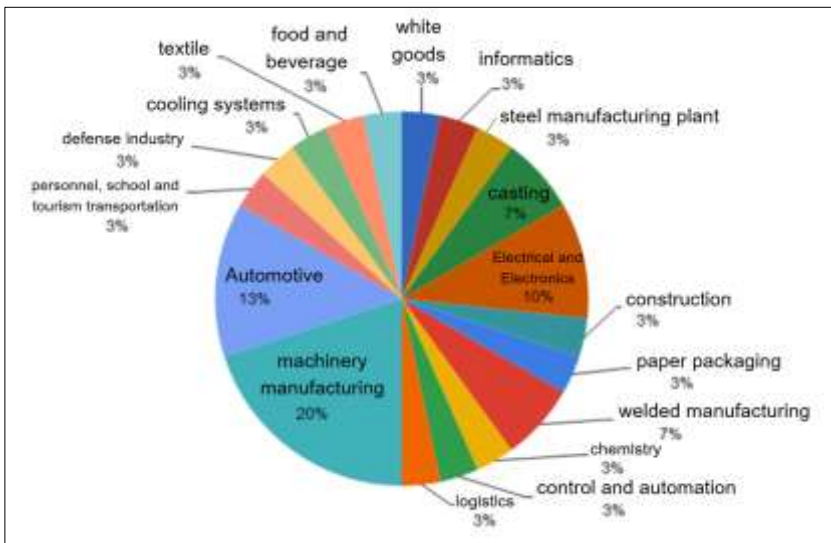
Figure 1. *Sectors of the surveyed companies*

The questions and answers given to the participants within the scope of the survey study are given below in detail. In the question regarding the level of education, it was seen that 83.3% of the participants had "bachelor's degree" and 6.7% had "master's degree". It is foreseen that the fact that majority of the respondents' education level is bachelor's degree and above may contribute positively to the transition from the existing organizations of the companies to Green PLM and the integration of sustainability parameters and facilitate these processes. As can be seen in Figure 2, it is seen that the majority of the participants work as responsible engineers or expert engineers in the companies, and 26.6% of them work as managers or senior managers in the companies. This shows that the answers to the questions in our survey include the perspectives of managers and it is thought that the transformation to Green PLM and the adoption of sustainability parameters will contribute positively to the adaptation of companies.
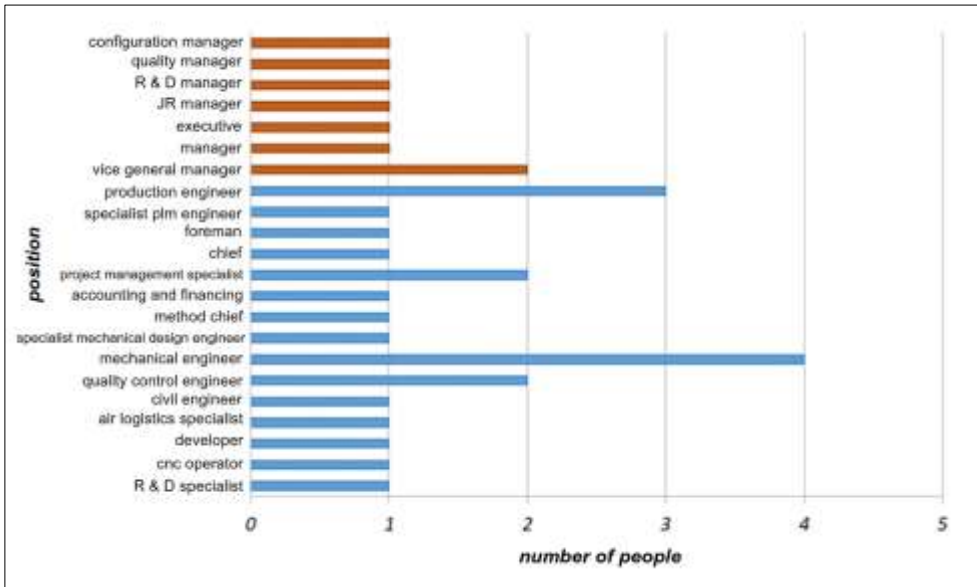
Figure 2. *Positions of employees in companies*

The participants answered the question about the activity that they think "poses a threat to the world in terms of pollution and is the biggest cause" as "Solid waste" with 26.7% and "Industrial activities" with 23.3%. At this point, since the participants are conscious of the industry and know the polluting effects of industrial activities, these answers were highly emphasized in the survey. This situation emphasizes the necessity of integrating sustainability activities into the PLM software.

Regarding the question "The level of sensitivity of the company to the environment in terms of sustainability", 63.3% of the respondents answered that their companies are sensitive at the "High" and "Very high" level. When the answers given by the participants

119

on company basis are evaluated, it is seen that a high majority of them have environmental sensitivity. This means that companies can facilitate the addition of environmental indicators to their existing organizations.

In response to the question on the sensitivity of companies on "Environmental impacts and sustainability", the respondents answered "Very high" on "Disposal of waste oil and hazardous substances" and "Energy saving in supply chain and management". And they answered "Medium level" on "Environmentally friendly material selection in raw material procurement", "Energy efficiency in production" and "Energy saving in social areas" as sensitive. Another issue that stands out in this question is that the companies are "Less sensitive" and "Partially sensitive" in terms of "Use of renewable energy sources".

In the answers given to the questions on "Recognition and use of PLM systems", it was observed that 50% of the participants had knowledge and the majority of the companies used PDM or similar systems.

In response to the question on "Product design and development software", 46.7% of the participants used AutoCAD and 33.3% used SolidWorks. This situation can be a guide to which software the sustainability parameters should be widespread, starting from which software. In the answers given to the question regarding the "green engineering concept", it is revealed that 46.7% of the participants have heard of the concept of green engineering before.

In the question on "Green engineering practices", 46.7% of the participants ranked "Environment and human health" and "Prevention of waste generation" in first place, while they ranked "Energy consumption" and "Product and process" in second place.

In the survey question regarding the process of "Transition from the existing PLM software to Green PLM software", 46.7% of the participants rated the risk level as "High" in terms of "Time", "Cost" and "Labor" (Figure 3).
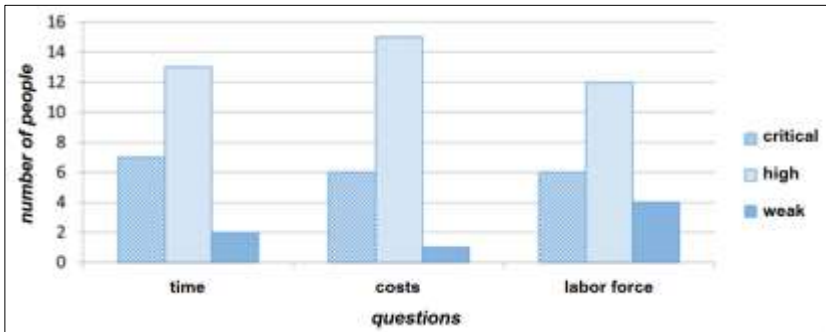
Figure 3. Evaluation of the transition process from the existing PLM software to Green PLM software

120

The responses to this survey question indicate that companies will not experience a high level of hesitation in transitioning to and operating Green PLM. In response to the question on "Risks of transition to Green PLM", the respondents rated "Cost", "Personnel" and "Integration difficulties" as "Critical" risks, while "Time", "Management" and "Cost" as "High" risks (Figure 4).
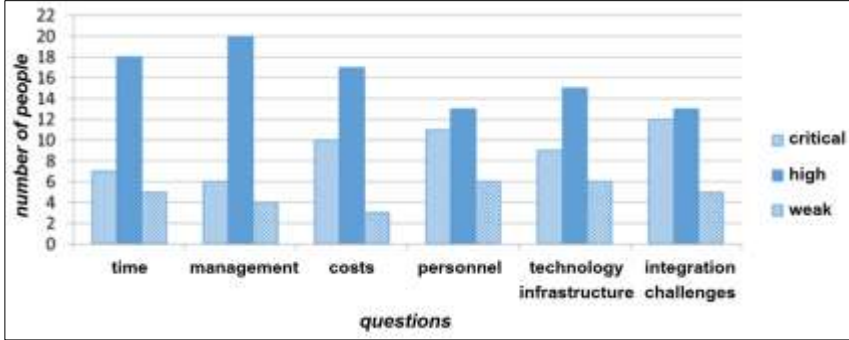
Figure 4. *Risks of transition to Green PLM*

In response to the question "Current sustainability infrastructure process" (Figure 5), respondents ranked "Personnel" first (66.7%), followed by "Environmental policies" and "Digitalization of core business processes" in second place. This shows that companies should always prioritize personnel training on sustainability infrastructure processes.
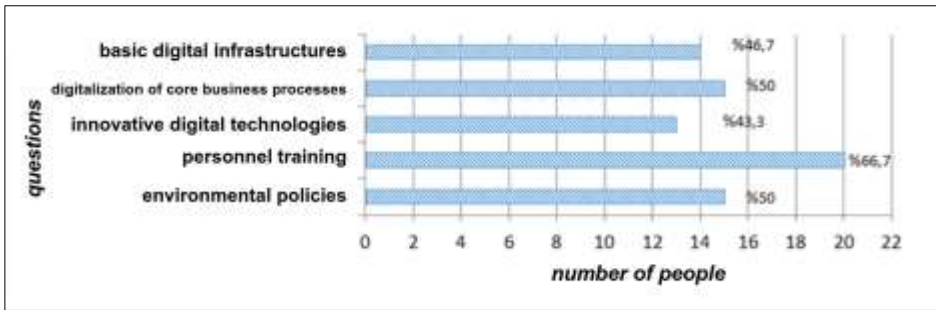
Figure 5. *Existing sustainability infrastructure processes of companies*

The survey aimed to collect datas that could contribute the evaluation of maturity levels of PLM systems implemented by companies, as well as the specific modules utilized across the industry. One of the important objectives of the survey study is to determine

121

the activities carried out for green engineering in companies and to obtain findings on a sectoral basis in this context. The results showed that companies use modules such as design, supply chain management and configuration management in PLM systems. Additioanally, they carry out studies on "Waste prevention" and "Environment and human health" and "Waste disposal" in the field of sustainability and that their level of sensitivity to the environment.

5. DISCUSSION AND SUGGESTION

The findings provide valuable insights for guiding companies in terms of which parameters that should be incorporated into existing systems to enhance sustainability. Based on the results of the survey, it is recommended to integrate the determined sustainability parameters into PLM, including design, supply chain management, and configuration management. Example of selected parameters for recommendation are listed below;

i) The integration of eco-friendly materials into CAD software used in design modules is essential for promoting sustainability in companies. These materials, including bio-plastics and cross-laminated wood, along with data on their production and environmental impacts, should be incorporated into the software. Additionally, the inclusion of specific metrics such as global warming potential (CO_2 -eq), Ecosystem Toxicity Potential Impact (CTUe-Comparative Toxic Units), energy use (kWh), and recycled water use (m³) would facilitate the pursuit of sustainability aims at the design and conceptualization phases.

ii) For the supply chain module, qualitative metrics play a more significant role. Here, a control mechanism within the PLM system could be established to monitor the environmental impact of the supply chain through targeted questions. For instance, tracking the renewable resource utilization rates of transportation vehicles used during the supply phase would provide valuable insights. Furthermore, incorporating tools into PLM software to support the selection of environmentally appropriate packaging materials, powered by artificial intelligence to suggest recycled materials, and creating smart routing systems that minimize fuel consumption would be crucial for environmental protection.

iii) In configuration management systems, the integration of data such as CO_2 emission rates during product usage (kg/kWh), life cycle analysis options on product-based selection screens, maintenance cost estimation for selected products (price/year), and total water usage (TWU) for water-powered products is critical issues. These features would not only support acheiving sustainability goals for PLM users but also benefit end-users by promoting informed and environmentally responsible choices.

6. CONCLUSIONS

Considering that companies evaluate "Personnel integration difficulty" and "Cost" at a "Critical" level during the transition to Green PLM, it is essential to follow an action plan that addresses or mitigates these critical factors. Goverment institutions such as SME

122

Development Organization, Scientific and Technological Research Council, and the Ministry of Industry and Technology should play a supportive and encouraging role in this transition by introducing new funding calls and initiatives. Such measures can have a significant positive impact and are strongly recommended from a global perspective [1,6]. The survey results indicate that 26.6% of the participants are managers or senior managers, which is a promising factor for achieving Green PLM targets, as decision-makers' perspectives are crucial in integrating sustainability parameters into company strategies. Additionally, it was observed that 66.7% of companies allocate their existing infrastructure development efforts related to sustainability integration toward personnel training and education. This finding reveals the importance companies place on environmental activities by investing in employee training and development programs. To further advance these efforts, companies should closely monitor environmental regulations and provide continuous environmental training to their staff. Another notable finding from the survey is the gender distribution among participants, with the majority being male. Despite the low number of female professionals in the sector, it is noteworthy that half of the six female participants hold senior management positions. This highlights the significant potential of female leadership in fostering a positive outlook on environmental and social initiatives within organizations. Encouraging greater gender diversity, particularly at the management level, can contribute to a more holistic approach to sustainability and social responsibility.

REFERENCES

[1] V. A. Yavuz, Sürdürülebilirlik kavramı ve işletmeler açısından sürdürülebilir üretim stratejileri, Mustafa Kemal University Journal of the Institute of Social Sciences, 7(14), (2010), 63-86.

[2] European Commission Sustainable Products Initiative, (2022), https://ec.europa.eu/info/law/better-regulation/have-your-say/initiatives/12567-Sustainable-products-initiative_en , (accessed on 8 August 2024).

[3] M. F. Ashby, Materials and the environment: eco-informed material choice, Elsevier, (2012), 49-65.

[4] M. Düzer Sürdürülebilirlik performans göstergelerine ilişkin açıklamaların finansal performans üzerine etkisi, Doktora Tezi, Anadolu Üniversitesi, (2018), Türkiye, 13-21. *DOI: 10.29067/muvu.372882*

[5] B. Esin, Avrupa Birliği döngüsel ekonomi politikası: Çok düzeyli yönetişim açısından bir analiz, Master's thesis, Marmara University, (2019), Turkey, 54-58.

[6] G. H. Brundtland, World commission on environment and development Environmental policy and law, 14(1), (1985), 26-30. *DOI: 10.1016/S0378-777X(85)80040-8*

[7] K. H. Kung, C. F. Ho, W. H. Hung, and C. C. Wu, Organizational adaptation for using PLM systems: Group dynamism and management involvement, Industrial Marketing Management, 44, (2015), 83-97. *DOI: 10.1016/j.indmarman.2014.04.018*

[8] S. B. Sawan, An Introduction and Implementation of PLM in Aviation Industries, MPGI National Multi Conference (MPGINMC2012), 7-8 March, 2012, India.

[9] X. L. Liu, W. M. Wang, H. Guo, A. V. Barenji, Z. Li and G. Q. Huang, Industrial blockchain based framework for product lifecycle management in industry 4.0, Robotics and computer-integrated manufacturing, 63, (2020), 101897, 4-6. *DOI: 10.1016/j.rcim.2019.101897*

[10] C. Vila, J. V. Abellán-Nebot, J. C. Albiñana, and G. Hernández, An Approach to Sustainable Product Lifecycle Management (Green PLM), Procedia Engineering, 132, (2015), 585–592. *DOI: 10.1016/j.proeng.2015.12.608*

[11] Engineering, Siemens Teamcenter And PTC Windchill Top Forrester's New PLM Evaluation, (2023), https://www.engineering.com/siemens-teamcenter-and-ptc-windchill-top-forresters-new-plm-evaluation/ , (accessed on 8 August 2024).

[12] K. M. Lee, A. Inaba, Life cycle assessment: best practices of ISO 14040 series, Center for Ecodesign and LCA (CEL), Committee on Trade and Investment, Ajou University, (2004), February 2004, South Korea, 1-5.

[13] J. W. Creswell, J. D. Creswell, Research design: Qualitative, quantitative, and mixed methods approaches, 5th ed, Sage publications, United Kingdom, 2017.